NILE-SEC
NILE BASIN INITIATIVE
INITIATIVE DU BASSIN DU NIL

NBI Technical Reports: Water Resource Management Series

Flood Frequency Analysis under Climate Change

WRM-2022-10

giz Deutsche Gesellschaft für Internationale Zusammenarbeit (GIZ) GmbH

On behalf of:
Federal Ministry
for the Environment, Nature Conservation
and Nuclear Safety
of the Federal Republic of Germany

Document Sheet

This Technical Report series publishes results of work that has been commissioned by the member states through the three NBI Centers (Secretariat based in Entebbe- Uganda, the Eastern Nile Technical Regional Office based in Addis Ababa - Ethiopia and the Nile Equatorial Lakes Subsidiary Action Program Coordination Unit based in Kigali - Rwanda. The content there-in has been reviewed and validated by the Member States through the Technical Advisory Committee and/or regional expert working groups appointed by the respective Technical Advisory Committees.

The purpose of the technical report series is to support informed stakeholder dialogue and decision making in order to achieve sustainable socio-economic development through equitable utilization of, and benefit from, the shared Nile Basin water resources.

Document	
Citation	NBI Technical Reports - WRM-2022-10
Title	Flood Frequency Analysis under Climate Change
Series Number	Water Resources Management 2022-10
Date	September 2022
Responsible and Review	
Responsible NBI Center	Nile-Secretariat
Responsible NBI	Dr Modathir Zaroug and Dr Michael Kizza
Document Review Process	Climate Services Regional Expert Working Group, May 2022
Final Version endorsed	Climate Services Regional Expert Working Group, May 2022
Author / Consultant	
Consultant Firm	SYDRO Consult GmbH
Author	Nada Abdelwahab
Project	
Funding Source	German Federal Ministry for the Environment and Nuclear Safety (BMU)
Project Name	Enhancing Climate Services for Infrastructure Investments (CSI)
Project Number	16.9025.4

Contents

List of Figures

List of Tables

Climate Services for Infrastructure

1 INTRODUCTION

It is expected and widely acknowledged that climate change brings an increase in extreme events, be it flood or drought. Concerning flood events, the increase occurs in relation to four aspects: i) higher rainfall intensities, ii) higher frequencies of extreme rainfall, iii) longer duration of extreme rainfall events and iv) increase of areal distribution. All components lead to higher and more severe flood peaks and flood volumes. The risk that existing design guidelines underestimate these flood extremes is given and in particularly true for the future.

As a response, the Nile Basin Initiative Secretariat has launched the project "Enhancing Climate Services for Infrastructure Investments (CSI)" funded by the German Federal Ministry for the Environment and Nuclear Safety (BMU). The aim of the CSI is to provide climate data products and develop human capacity to conduct climate risk assessments and to prioritize measures to adapt to the negative consequences of climate change and extreme weather events on water infrastructures. In essence, the focus is on two climate services:

- Products considering climate change for PMF and IDS for floods based on NBI downscaled climate scenarios
- Assessments in terms of the reliability of services

The Nile Basin Initiative undertook climate change assessments and conducted studies related to climate change scenarios. The results are climate change affected time series for temperature and precipitation. The objective of this assignment is to utilize the work already done in combination with the climate change affected time series in order to:

- develop guidelines on how to incorporate climate change in design flood analysis, operation and safety evaluation of water infrastructures in a changing climate, in particular to develop a Nile Basin Reference Guideline for Flood Frequency assisting planners, policy makers, design experts, dam owners, operators, etc. in design flood analysis for new projects and hydrological safety evaluation of existing water infrastructures.
- apply the Nile Basin Reference Guideline for Flood Frequency for the seven prioritized multi-purpose projects resulting from the Nile Equatorial Lakes Investment Programme (NEL-IP),
- support the NELSAP in strengthening the capacity of the NEL countries to respond and adapt to climate change challenges by providing coaching for participants on the methodologies that will be incorporated in the Nile Basin Reference Guideline for Flood Frequency as part of the Climate Services in planning and climate risk assessment for the seven NELIP prioritized multi-purpose projects.

1.1 Background of hydrological safety assessments

This section serves the purpose to provide a full picture of hydrological water infrastructure safety assessments in which this assignment is embedded.

Hydrological safety assessments are necessary to prevent a failure of water infrastructure, in particular dams. The failure of dams can have extreme consequences depending on the size, location and type of

the dam. Results of the hydrological safety assessment are necessary inputs for the geotechnical safety assessments, which consider the stability of the dam against sliding, turning, base failure. All assessments feed into to design of a water infrastructure or help devise rehabilitation measures in case safety standards are not met. In particular, dams require a comprehensive safety assessment. Dam failures can be associated with the following topics:

First impoundment

- 38% of all dam failures occurred during the initial filling of a reservoir (Costa, 1985).

Main reasons of dam failure for concrete dams (Zhang, 2009)

- internal erosion of foundation
- lack of resistance to sliding

Main reasons for dam failure of earthen dams (Zhang, 2009)

- Piping and base failure

Cause of failure related to spillways (Evans, 2000)

- 22% of failures happen due to insufficient spillway capacity

Dam failure mostly happen as a series of incidences creating a failure path. Two examples of failure paths:

1. Debris blocks part of the spillway → water level rise beyond dam crest → overtopping of the dam → erosion of the downstream dam side → dam failure

or

2. Earthquake → landslide into the reservoir → overtopping of the dam → erosion of the downstream dam side → failure

The design of water infrastructure must consider these failure pathways.

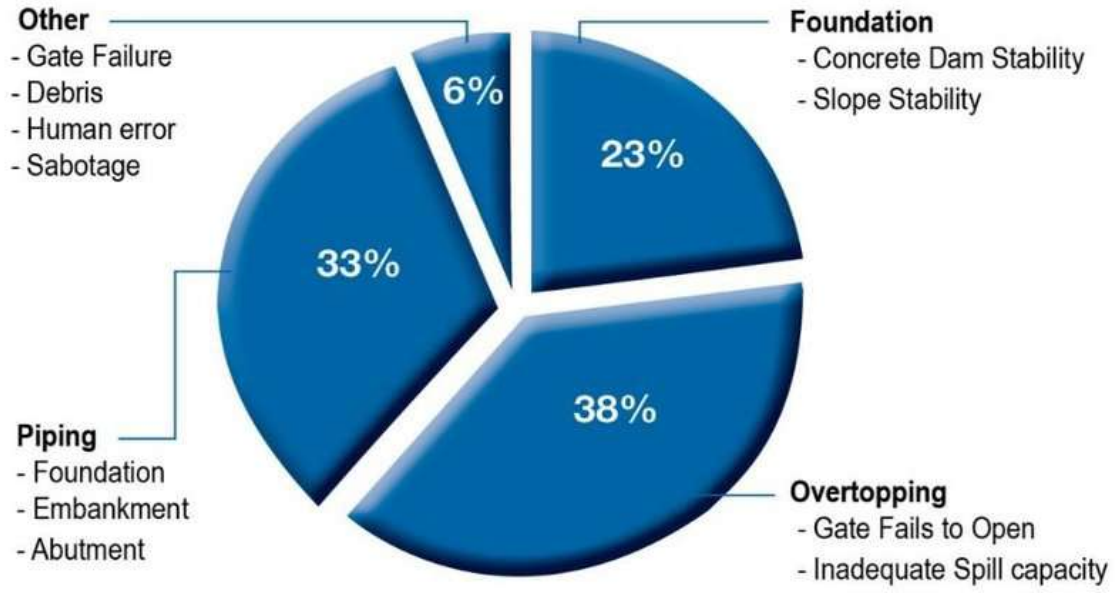

Figure 1: Overview of reasons for dam failure (after: (Donnell, 2015)).

The hydrological dam safety analysis consists of three pillars.

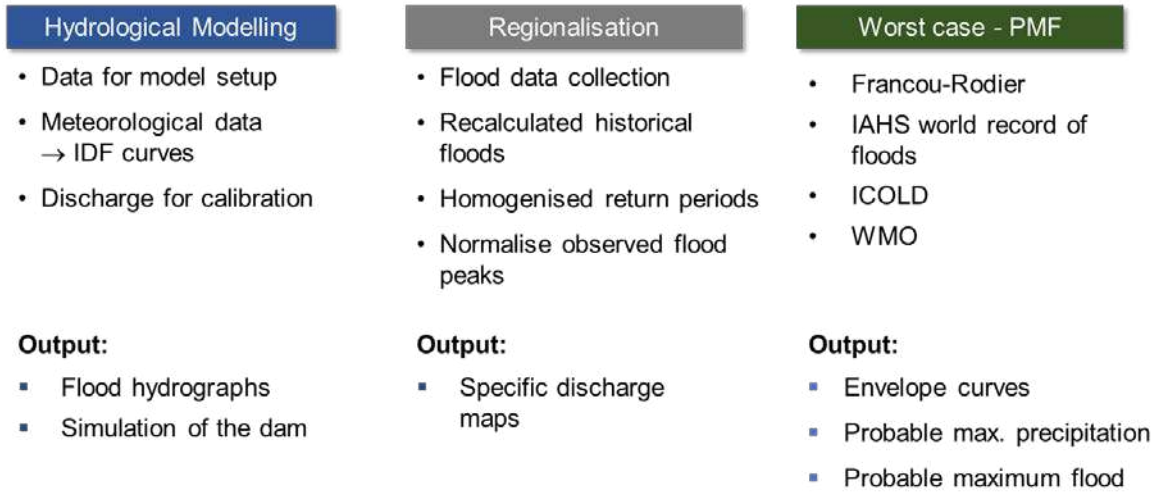

Figure 2: Methodologies to undertake a comprehensive hydrological dam safety analysis

This assignment focuses on input for the hydrological modelling, contributes to the regionalisation and provides input for deriving worst case scenarios.

IDF curves are the means to identify changes due to climate change. They provide the basics for applying a hydrological model. Storm profiles need to be considered on top of the IDF output. Storm profiles with rainfall maximum at the end of an event will always produce worst conditions. The likelihood of such a storm profile needs to be estimated and considered in combination with the selected return period of the rainfall intensity. This is relevant to obtain the overall probability of occurrence of the event.

The regionalisation also allows to create maps for specific discharge, which is the peak runoff per unit of area.

Observed discharges and/or climate change affected time series are used to conduct frequency analyses and to derive specific discharge - area relationships. These relationships show expected peak flows depending on the size of a catchment. Usually, they follow a typical shape: specific discharge increases with smaller catchments and decrease with larger catchments. This approach is also used to derive envelope curves.

A design flood is not a single hydrograph. Different durations and storm profiles must be tested to obtain a set of potential design floods, each of which must be simulated to obtain maximum conditions at the respective dam or water infrastructure.

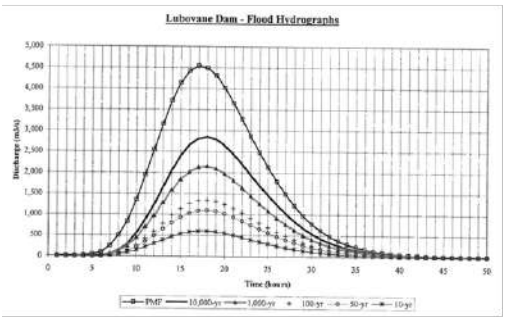

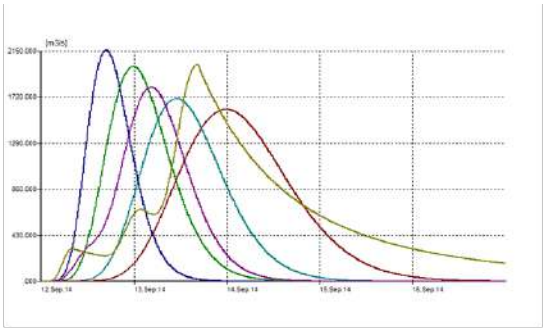

- One rain duration
- One storm profile

- Different rain durations
- Different storm profiles

Figure 3: Example of inappropriate (left) and sufficient (right) design floods

2 OBJECTIVE AND APPROACH

2.1 Objective and scope of work

The objective of this project was to provide the Nile Basin with the necessary climate data products and capacity building to help the decision-makers to assess the hydrological water infrastructure safety. Hydrological water infrastructure safety plays an essential role in reducing the risk of water infrastructure failure in particular dams.

This project was split into 2 main packages as mentioned in the ToR:

Work package-1 (WP1) – Technical Analysis:

1- Review and collect the available CORDEX climate data and bring them into a coherent time series format, for example CSV for each 50x50 grid cell for the Eastern Nile Region. These CORDEX data are already bias corrected.
2- Selection of the time period that will be used to calculate the Intensity-Duration-Frequency matrices (IDF). It is most likely the time period between 2010 up to 2100.
3- There are different climate scenarios as drivers of the CORDEX data, namely the RCP 4.5 and 8.5. Four scenarios should be selected from all available CORDEX representations which cover the minimum and maximum signal changes of climate in terms of temperature and precipitation. The four selected scenarios will be used to derive the Intensity-Duration-Frequency matrices (IDF), PMP, and PMF.
4- Calculation of the Intensity-Duration-Frequency matrices (IDF) based on the daily time series for each 50x50 grid cell and harmonize them over the regions. The best way to do this is to derive contour lines for the return periods of 2, 5, 10, 20, 50, 100, 200, 500 and 1000.
5- The climate change affected IDFs will be compared with selected time series of rainfall representing the current climate in order to estimate the factors how to change observed precipitation time series to adopt them to climate change conditions. The climate change signal is not consistent, meaning that no increase or decrease of precipitation on an annual basis is clearly visible. However, it is more likely that intensities will increase, meaning that higher daily precipitation will occur rather than an increase of the annual mean.
6- Development of a standard approach to derive PMP and PMF based on the available and selected CORDEX time series. The recommendations of the WMO will be used. The approach could be a deterministic, physically based approach or a statistical approach depending on the information that can be derived from the CORDEX data source.
7- The PMP and PMF will be made consistent with the IDF curves in order to avoid any inconsistencies.
8- Report generation.

Scope of work

Work package 1 covers the entire Nile Basin and its deliverables which consist of climate products such as IDF curves and PMP values derived from the CORDEX climate projections were embedded into a web database. A manual to get hold of the data and apply it is available.

2.2 Approach and Methodology

2.2.1 Inception phase

Meetings were held directly to collect the data, exchange the information, and discuss the project work plan. The main information and discussions in the inception phase were related to the CORDEX data, observed data, bias correction methods and work plan.

2.2.2 WP 1 - Technical Analysis

The main purpose of this work package is to generate climate products such as Climate datasets, Intensity Duration Frequency (IDF) curves and Probable Maximum Precipitation (PMP) taking climate change into consideration.

After acquiring the CORDEX climate datasets and the observed precipitation time series from the NBI-SEC a GIS environment collecting different geographic geodatabase layers was created. The extent of the CORDEX cells could then be overlayed with the map of the Nile Basin and the point shapefile of observed rainfall gauge stations. The climate datasets were processed, analysed and filtered. Furthermore, the 13 CORDEX datasets provided by the NBI were compared to select the ones with the maximum signal changes with regards to precipitation and temperature.

The IDF curves for the different climate scenarios were calculated according to the German Weather Service (DWD) approach. The results were represented using graphs, tables, and maps. A comparison between IDF curves generated from projected climate scenarios and the baseline scenario were conducted taking into consideration the following states: rainfall intensity, duration, frequency, and spatial extent of the extreme rainfall. The comparison results were visualized using radar diagrams for defined sub-basins.

To calculate the PMP, the series of maximum annual precipitation was derived for all CORDEX datasets. Then, the PMP was calculated for each CORDEX cell according to the statistical WMO approach. The results were represented in grid maps.

A web based database containing all climate services has been prepared for the NBI. The database facilitates looking up climate services for each CORDEX cell that lies within the Nile Basin.

3 DATA MANAGEMENT

3.1 Available Datasets

3.1.1 CORDEX Data

CORDEX is the Coordinated Regional Downscaling Experiment developed by the World Climate Research Program (https://www.wcrp-climate.org/). CORDEX datasets are obtained by running Global Climate Models (GCM), which are set-up by different meteorological research institutes all over the world. The model output can then be downscaled using Regional Climate Models (RCM). The 17 CORDEX datasets provided by the NBI have additionally been corrected by applying the quantile mapping bias correction approach using NCEP/NCAR reanalysis (https://rda.ucar.edu/datasets/ds314.0/). The datasets include daily values of precipitation, maximum temperature, and minimum temperature. Table 1 demonstrates an overview of the acquired bias corrected CORDEX datasets received from Nile-SEC as NetCDF files.

Table 1: Overview on the acquired bias corrected CORDEX data acquired from NBI.

Climate variable	Precipitation (mm/sec), maximum temperature (°C), Minimum Temperature (°C)
Spatial resolution	0.44°
Temporal resolution	Daily
Bottom left coordinates	Longitude = 22.44 °, Latitude = -4.84 °
Upper right coordinates	Longitude = 40.04 °, Latitude = 32.56 °
Periods	• 1971-2000 (historical) • 2006-2035 (near projeciton) • 2036-2065 (mid century projection) • 2066-2095 (far projection)
Meteorological Research Institute	BCCR, CLMcom, DMI, KNMI, SMHI, MPI
Global Climate Model (GCM)	CNRM, ICHEC, IPSL, MIROC, MOHC, MPI, NCC, NOAA
Regional Climate Model (RCM)	CCLM4817, HIRHAM5, RACMO22T, RCA4, REMO2009, WRF331
Representative Concentration Pathway (RCP)	RCP 4.5, RCP 8.5

CORDEX datasets was stored in netCDF files. NetCDF is a file format that can be utilized to store the array-oriented scientific data. The files are spatially distributed and require programming scripts to extract the data at a certain longitude and latitude for a climatic variable. Hence, Python scripts were used to extract the required time-series data to TXT files ZRX files prior to being processed or to calculate the IDF and PMP. The CORDEX datasets were also visualized in maps by importing the NetCDF files directly into ArcGIS. Figure *4* shows a precipitation time series sample for a chosen grid cell.

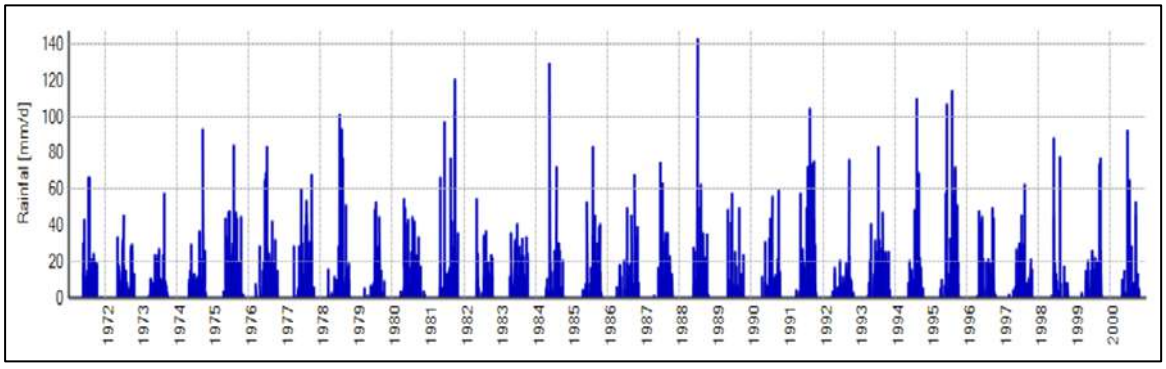

Figure 4: A time series data sample representing the rainfall values for a chosen grid (Cell Number = 739).

The received CORDEX datasets cover a large area beyond the Nile Basin. Grid cells that are located outside the basin boundary could, therefore, be eliminated by clipping the datasets to a grid raster representing the boundary of the Nile basin to avoid the processing of insignificant data. To facilitate the CORDEX data processing, an ID value has been assigned to each grid of the layer. Figure *5* shows the grid raster layer and the CORDEX dataset domain.

3.1.2 Observed Monthly Rainfall Data

Observed monthly rainfall data was acquired from the interactive knowledge portal (IKP) developed by NBI (http://ikp.nilebasin.org/en/hydromet-component), where hundreds of meteorological stations that are spatially distributed over the entire basin can be found. The rainfall data available on the IKP has a monthly resolution and is collected from different sources such as DST, NBE, FAO, GHCN, ETH_MP, and MWE. Monthly rainfall data obtained from the IKP was used to attempt to verify the bias corrected historical CORDEX dataset.

Since the IKP provides data from multiple meteorological stations and different sources, it was necessary to make a small selection of stations that can be used for a preliminary comparison with the CORDEX data. Those meteorological stations have been selected taking into account the following criteria:

- The stations should be located in different climate zones.
- The stations should be well distributed along the entire Nile Basin.
- The stations should be located in different countries.
- The time series should cover the period from 1-1-1971 to 1-1-2000 as much as possible.
- The time series should have as few gaps as possible.

After applying the adopted criteria, six meteorological stations were chosen: Khartoum, Bahar Dar, Juba, Kampala, Kakamega forest, Rulindo. Figure *5* shows the location of the selected meteorological stations, whereas Table 2 demonstrates brief information on the stations.

3.1.3 Observed Daily rainfall data (DST-FAO)

Even though the IKP web-based monitoring system comprises abundant meteorological data, the data is only represented on a monthly time step. To achieve a proper data evaluation of the CORDEX precipitation dataset daily meteorological data is necessary. Daily data was provided by the Nile SEC and is a product of the Nile Decision Support Tool Project lead by the FAO. The stations have been divided by country and the data covers periods between 1901 and 2000 as shown in Table *3*.

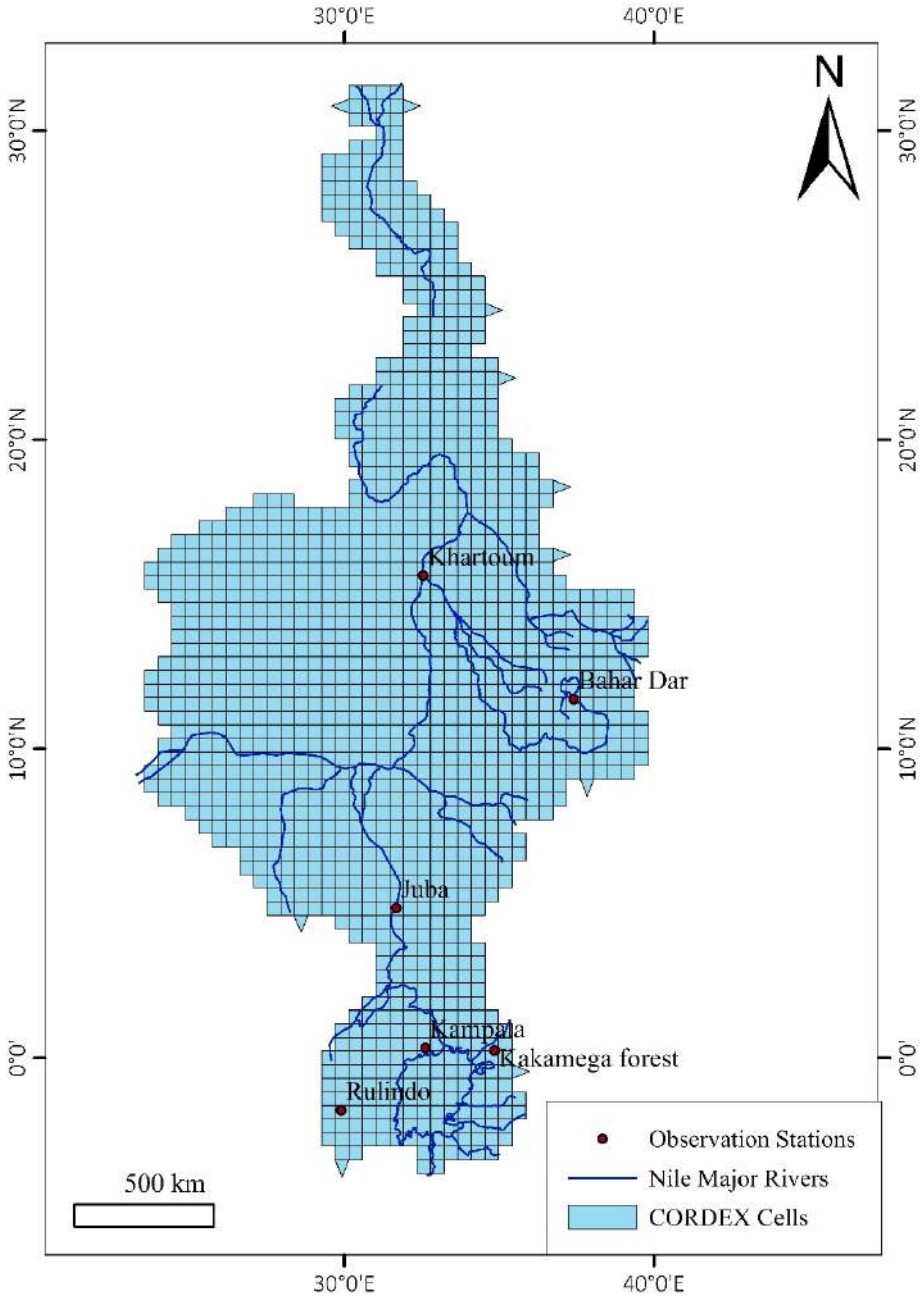

Figure 5: Location of the observation stations within the CORDEX domain.

Table 2: Selected meteorological stations required for the project.

Station	Start Date	End Date	Country	Data Source
Khartoum	01.01.1951	01.12.2005	Sudan	GCHN
Bahar Dar	01.02.1961	01.04.2000	Ethiopia	GCHN
Juba	01.01.1901	01.05.2004	South Sudan	GCHN
Kampala	01.01.1931	01.11.2003	Uganda	MWE
Kakamega Forest	01.01.1951	01.12.1996	Kenya	GCHN
Rulindo	01.01.1951	01.12.1993	Rwanda	GCHN

Table 3: FAO data summary

Country	Number of stations	Start year	End year

Burundi	107	1927	1999
DR Congo	10	1944	1998
Egypt	7	1988	2000
Ethiopia	15	1952	1999
Kenya	131	1926	1999
Rwanda	73	1930	2000
Sudan	331	1901	2000
Tanzania	176	1970	1998
Uganda	598	1902	2001

The 1448 FAO time series contain many data gaps, some of which are marked as 0 values. There is therefore no way of knowing if 0 values refer to a gap or a day without precipitation. To use the time series for the bias correction it could be assumed that all 0 values represent gaps and conduct the bias correction only on days with precipitation. This approach must be verified as it might lead to an inaccuracy in results.

If the observed timeseries collected by the FAO were to be used to correct the CORDEX data for bias, the period between 1950 and 2000 would be relevant, as it is the period covered by the historical CORDEX dataset. There are two possible approaches for the bias correction:

1. Conduct bias correction using time series that cover a defined period where there are no long gaps. (the definition of long gaps must be defined here)
2. Conduct the bias correction for the whole period but using different lengths for different stations.

3.2 Data Analysis

3.2.1 Mean Absolute Error

The CORDEX datasets were the chosen source of climate change data achieve the objectives of this project. The datasets had been bias-corrected using NCEP/NCAR reanalysis (https://rda.ucar.edu/datasets/ds314.0/) due to the lack of daily observed rainfall. Usually, the global observational and reanalysis datasets need to be bias-corrected before they deliver accurate results. However, in this case, they were the best available option to carry out the bias correction. To ensure that the bias correction of the CORDEX datasets using NCEP/NCAR reanalysis yields sufficiently accurate results, a comparison of the historical CORDEX dataset with observed rainfall data was necessary.

Daily rainfall values would have been more suitable for the evaluation, however we first proceeded with the monthly IKP data. Since the CORDEX datasets are spatially distributed (gridded format), the six gird cells where the six chosen ground stations lie have been identified and the rainfall time series were extracted from the NetCDF files. Table 4 shows the relevant grids cells for the comparison process.

Table 4: The determined grids for the comparison process.

Station	Longitude (Station)	Latitude (Station)	Grid ID	Longitude (Grid)	Latitude (Grid)
Khartoum	32.55	15.60	416	32.56	15.40
Bahar Dar	37.42	11.60	739	37.40	11.44
Juba	31.60	4.80	1144	31.68	4.84
Kampala	32.62	0.32	1242	32.56	0.44

Kakamega Forest	34.85	0.23	1247	34.76	0.44
Rulindo	29.90	-1.70	1308	29.92	-1.76

To compare the historical CORDEX data with the observed data, statistical goodness of fit tests should be performed. One of the most common goodness of fit tests in the field of hydrology is the Mean Absolute Error (MAE). The smaller the value, the closer the CORDEX rainfall value to the observed rainfall value. This method is calculated using the following equation as described by (Willmott & Matsuura, 2005)

$$MAE = \frac{1}{N}\left(\sum_{i=1}^{N}|P - O|\right)$$

With

N	:	Number of observed records
P	:	Predicted value (CORDEX model)
O	:	Observed value (observed rainfall)

It has been deduced that the temporal resolution of the CORDEX dataset (daily) differs from that of the observed dataset (monthly). Therefore, the CORDEX data was aggregated from daily to monthly values using a python script. In the aggregation process that took place the mean monthly precipitation, as well as the mean annual precipitation, were calculated, to conduct monthly and annual analyses.

Figure 6 shows the comparison between the CORDEX data and the observed data for all the selected meteorological stations. The results show that the sum of the annual and monthly mean absolute errors for the datasets 9, 10, 11, 12, 13, 14, 15, 16 and17 are significantly high. Hence, they were screened out. On the other hand, the mean absolute error for the dataset number 1 and 2 are low.

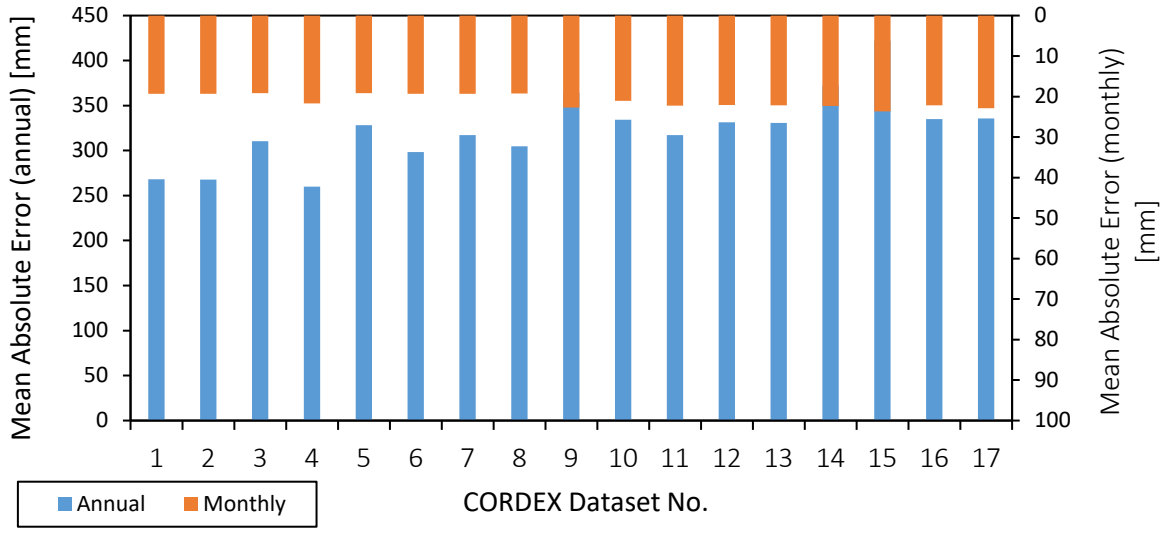

Figure 6: Comparison between CORDEX dataset and observed data.

3.2.2 Signal change

The signal change [SC] related to temperature and precipitation of each CORDEX dataset can be calculated to detect the deviation from the historical observation dataset using this equation:

$$SC\ [-] = \frac{P - O}{O}$$

With

P : Predicted value (CORDEX model)
O : Observed value (observed rainfall)

Due to lack of temperature and precipitation daily observation datasets covering the whole Nile basin, mean precipitation and temperature can represent the signal change instead of the relative change. Figure 7 shows the mean precipitation and temperature results for all CORDEX datasets including historical, rcp4.5 and rcp8.5.

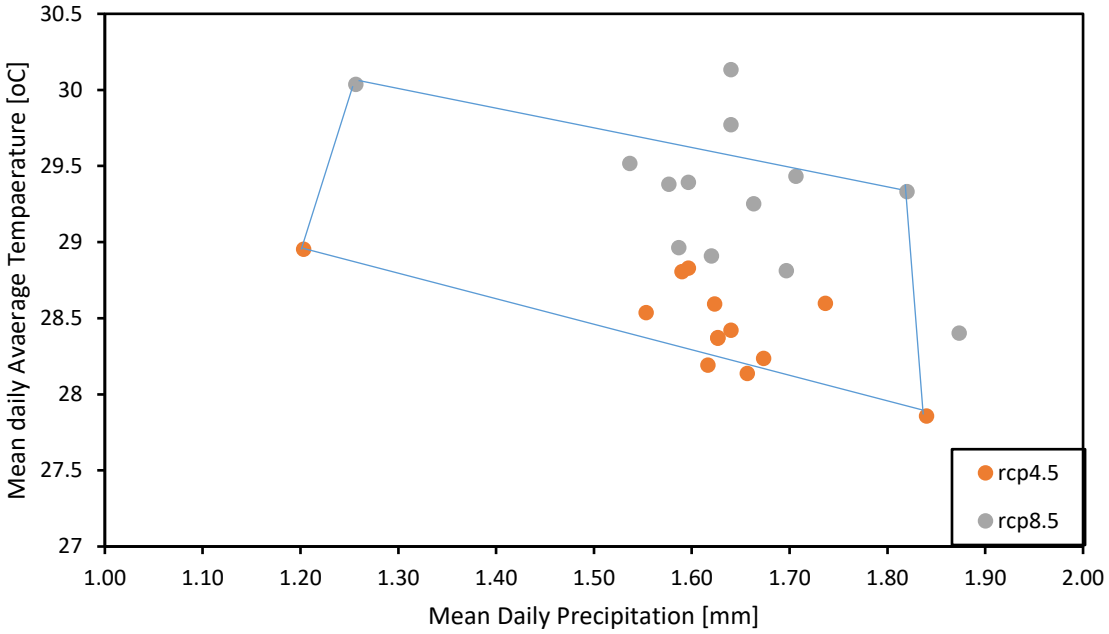

Figure 7: Signal change for selecting CORDEX datasets. Note: the corners of the blue polygon represent the maximum and minimum signal change in terms of precipitation and temperature..

Based on Figure 7, 4 scenarios were determined which cover the minimum and maximum signal changes of climate in terms of temperature and precipitation:

1. rcp45SMHI_RCA4MOHC_HadGEM2 (represents minimum precipitation and minimum temperature)
2. rcp85SMHI_RCA4MOHC_HadGEM2 (represents minimum precipitation and maximum temperature)
3. rcp45BCCR_WRF331NCC_NorESM1_M (represents maximum precipitation and minimum temperature)
4. rcp85BCCR_WRF331NCC_NorESM1_M (represents maximum precipitation and maximum temperature)

3.2.3 Spatial representation of the historical CORDEX dataset

While the chosen grid cells of the CORDEX dataset have been compared with the observed rainfall at the corresponding ground stations, it is also important to check the spatial distribution of the historical CORDEX dataset. Therefore, maps representing the mean annual precipitation for each CORDEX dataset were generated. Figure 8 shows a sample of the results. The maps show that the spatial distribution of the mean annual precipitation values extracted from the CORDEX datasets is very similar. It is noticeable in all datasets that low precipitation values dominate the southwestern side of the basin where Rwanda, Burundi, and part of Uganda are situated. In addition, Null values are present in the upper middle part of the basin in Egypt in all historical CORDEX datasets as shown in the following figure.

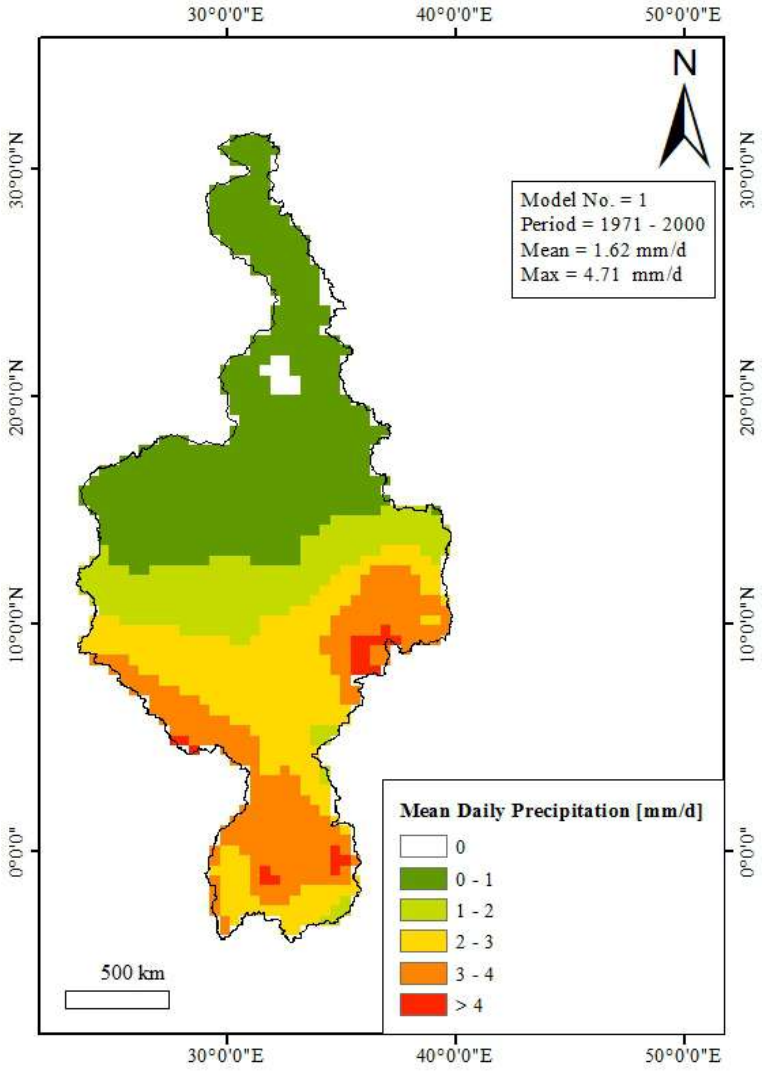

Figure 8: Spatial distribution of the mean daily precipitation for the CORDEX dataset 1.

4 INTENSITY DURATION FREQUENCY CURVES

4.1 Definition and Importance

The failure of dams can have extreme consequences depending on the size, location and type of the dam. One of the main reasons of dam failure is the hydrological design of the infrastructure. To avoid dam failure, IDF curves can be provided for hydrologists to support the process of dam design and dimensioning.

Intensity Duration Frequency (IDF) curves represent rainfall at a certain location taking into consideration the following parameters:

1. Rainfall intensity
2. Duration of rainfall events
3. Frequency of occurrence

According to (IPCC, 2007) until the end of the 21st Century, the global temperature is expected to cause an increase in frequency and amount of rainfall leading to floods, droughts, water shortages, or stresses as well as problems in agricultural productivity. Therefore, the effects of climate change on IDF have to be taken into account in order to prevent future problems in water infrastructures such as dam failure.

IDF curves are means to identify changes due to climate change. They provide the basics for applying a hydrological model. Storm profiles need to be considered on top of the IDF output. Storm profiles rainfall maximum at the end of an event will always produce worst conditions. The likelihood of such a storm profile needs to be estimated and considered in combination with the selected return period of the rainfall intensity. This is relevant to obtain the overall probability of occurrence of the event.

4.2 IDF Calculation Approach

4.2.1 Calculation Approach for Durations > 24 hours

To calculate IDF curves, the widely used German Weather Service (DWD) approach was applied. Daily rainfall time series data are required as input to run the calculations. Hence, time series datasets have been extracted from the selected daily CORDEX datasets for different time periods: historical (1971 - 2000), near projection (2006 - 2035), mid century projection (2036-2066), far projection (2066 – 2095), and different Representative Concentration Pathway scenarios (RCP): RCP4.5, RCP8.5, using python scripts. The input has been saved as BIN files.

4.2.2 Calculation Method for Durations < 24 hours

Since the CORDEX datasets provide daily time series of precipitation, the IDF calculation will produce rainfall durations equal or larger to daily values, e.g. 24 h, 48 h, 72 h, etc. Rainfall durations less than 24h can be derived based on the assumption that rainfall intensities for duration less than 24 h follow a non-linear relationship that turns into a straight line when plotting them with a logarithmic scale. To determine the Precipitation depth at lower duration (less than 24 h), the straight line in the logarithmic function was extrapolated. Table 5 represents an output sample of the IDF calculation tool, whereas Figure 9 shows the IDF curves of a chosen grid cell on a logarithmic scale.

Table 5: IDF table output.
Note: the blue, red and green cells represent intensity [mm], duration [min], and frequency [a] respectively.

0	0.5	1	2	5	10	20	50	100
15	0	12.2	40.8	78.6	107.3	135.9	173.7	202.3
20	0	14.1	43.2	81.8	110.9	140.1	178.6	207.8
30	0	17.1	47.1	86.7	116.7	146.6	186.2	216.2
45	0	20.8	51.6	92.3	123.1	153.9	194.6	225.4
60	0	23.9	55.3	96.8	128.2	159.6	201.1	232.5
90	0	29.2	61.4	104	136.3	168.6	211.2	243.5
120	0.6	33.5	66.4	109.9	142.8	175.6	219.1	252
180	7	40.8	74.6	119.3	153	186.8	231.5	265.3
240	12.5	46.9	81.4	126.9	161.3	195.8	241.3	275.8
360	21.7	57.1	92.5	139.3	174.7	210.1	256.9	292.3
540	33.1	69.5	105.9	154	190.3	226.7	274.8	311.1
720	42.8	79.9	117	166	203.1	240.2	289.2	326.3
1080	59.2	97.3	135.4	185.7	223.8	261.9	312.3	350.4
1440	73	111.8	150.7	202	240.9	279.7	331	369.9
2880	115.8	156.5	197.2	251	291.7	332.3	386.1	426.8
4320	148.7	190.5	232.3	287.6	329.4	371.2	426.5	468.3
5760	176.4	219	261.6	318	360.6	403.2	459.6	502.2
7200	200.7	244	287.3	344.5	387.8	431	488.2	531.5
8640	222.8	266.6	310.4	368.3	412.1	455.9	513.8	557.6

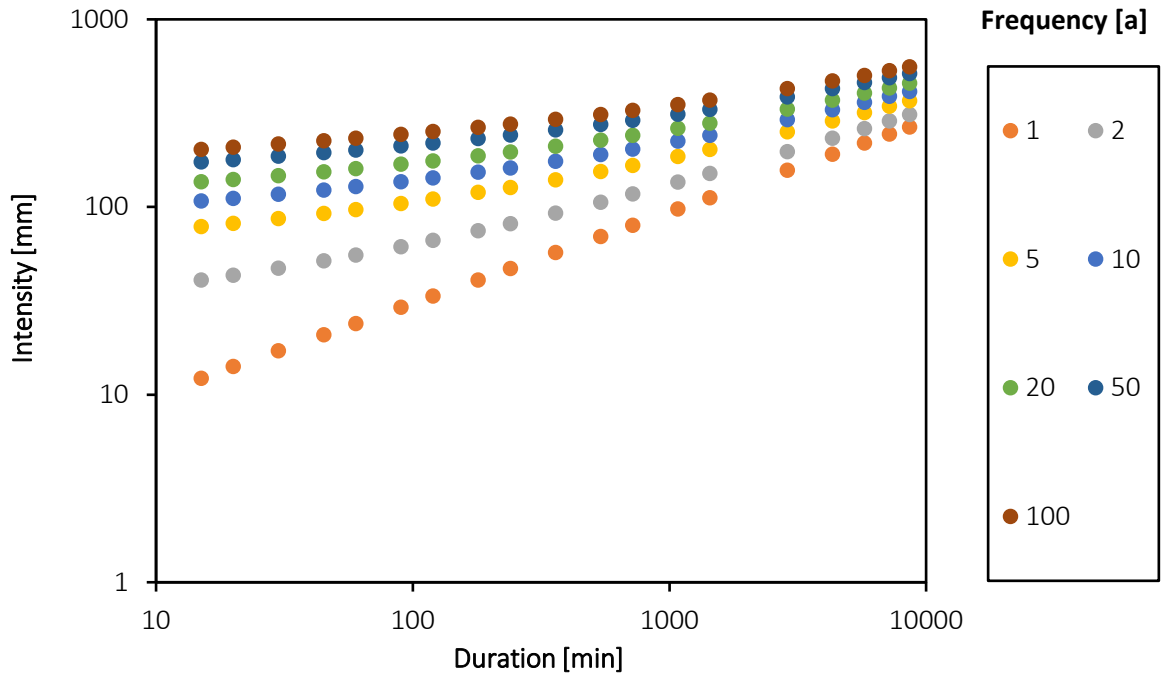

Figure 9: IDF curves for a chosen grid cell.

4.3 Maps

Since the output data of the IDF calculations is very extensive it was important to represent the output taking not only the intensities into consideration, but also the spatial distribution of the output. Therefore, different maps have been generated including grid maps, contour maps, and radar diagram maps.

4.3.1 Grid maps

Grid maps show the results of input data of the same RCP scenario with a chosen frequency of occurrence and duration for different periods of time. They show the IDF results before processing. Figure 10 depicts an IDF grid map sample. The map was generated for all periods including the historical period and demonstrates statistical parameters such as the mean and maximum values as well as the histogram of the grid values (located lower left of the graph). The histogram graph respresents the distribution of the results. It can indicate how the distribution of the values varies from the historical period to the future periods. The spatial variability of the IDF results can be well represented for different future projections using those grid maps.

4.3.2 Contour maps

Since the grid maps are not sufficient enough to be utilized by hydrologists to design the water infrastructure, contour maps could be generated to facilitate the map user to extract the values. To map contour lines from the grid maps, the grid maps were processed in ArcGIS. Figure 11 depicts an example of a generated contour map for a chosen RCP 4.5 scenario, 100 year frequency, and 1 day duration.

4.3.3 Cluster radar diagrams

To evaluate the IDF result datasets, one can look at radar diagrams which represent the change in frequency, duration, intensities and extent of specific extreme events in the future compared to the historical results. By comparing the historical and future IDF results one can draw conclusions about the severity of extreme events for different locations.

To create the cluster radar diagrams, 2 steps were performed. The first step includes defining the clusters, whereas the latter step is developing a radar diagram visualizing the comparison of data for each cluster.

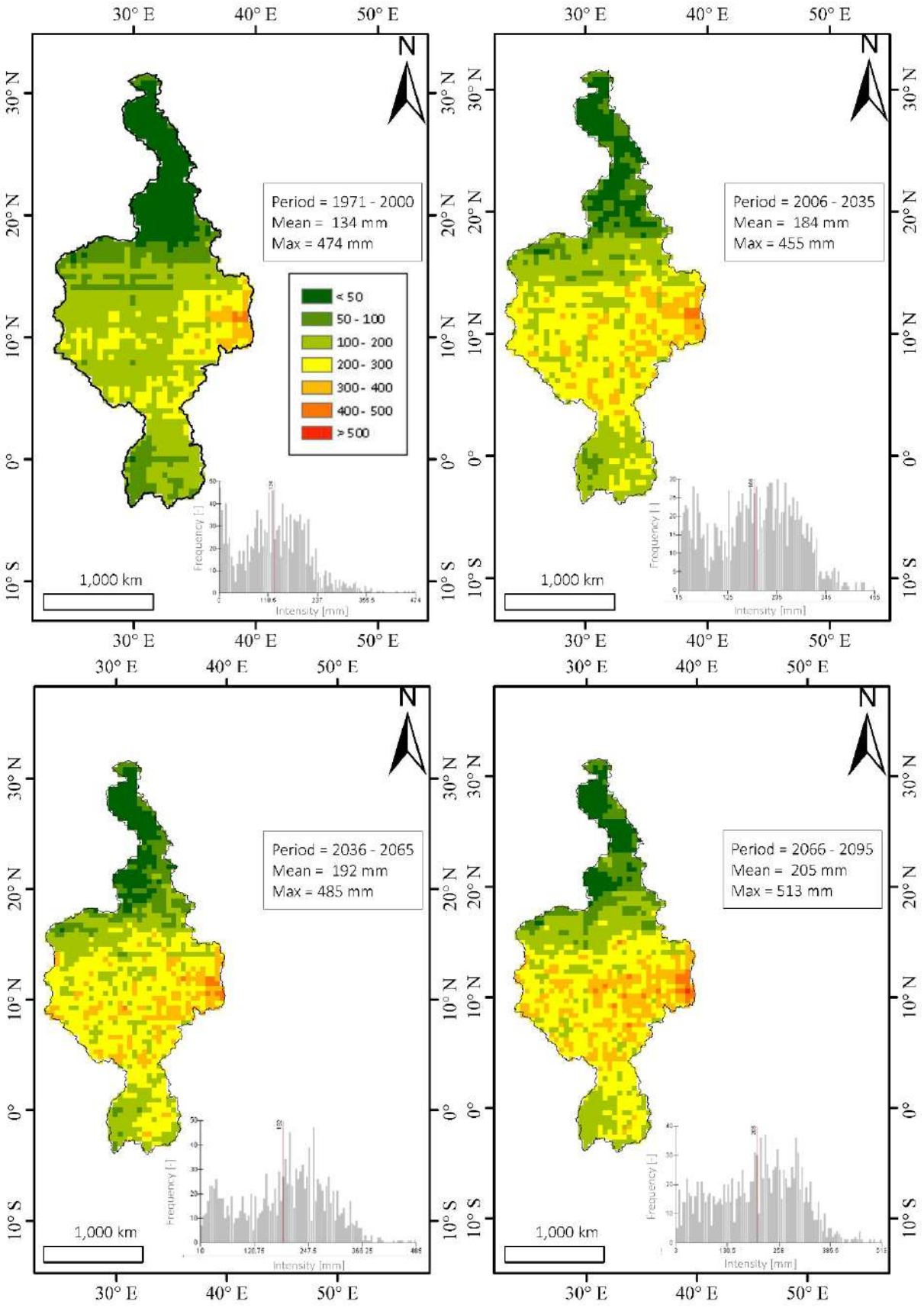

Figure 10: IDF grid map sample (RCP scenario = 4.5, Duration = 1 day, Frequency = 100 a).

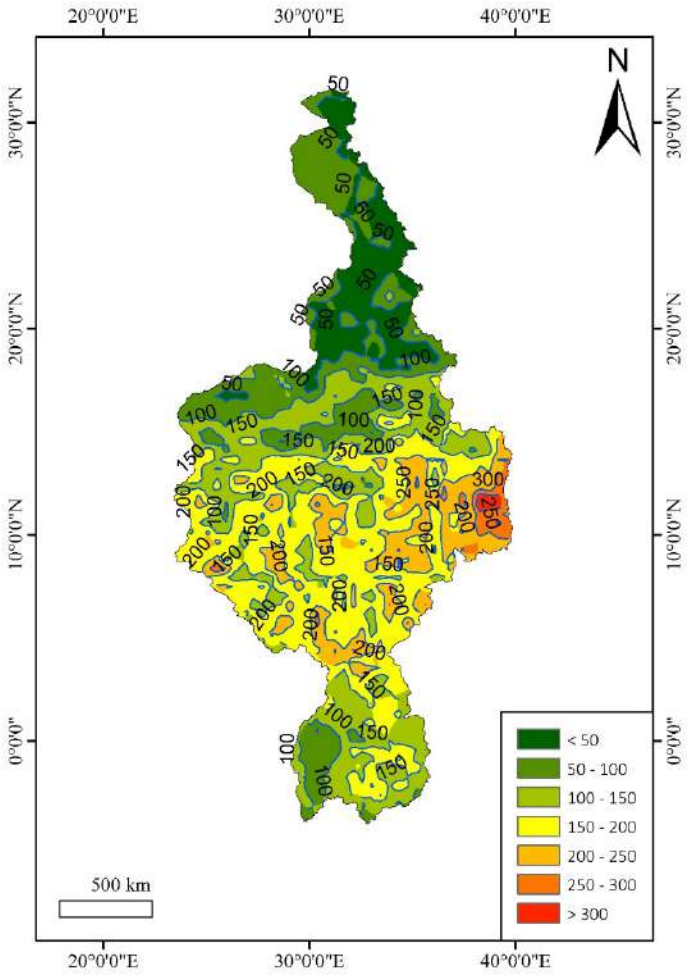

Figure 11: IDF contour map sample (RCP scenario = 4.5, period= 2006-2035, Duration = 1 day, Frequency = 100 a).

4.3.3.1 Cluster definition

The Nile basin has been divided into clusters. During the clustering process, the following factors have been considered:

- Climate zones (arid, semi-arid, humid)
- Geographical boundaries (plains , mountains, plateaus)
- Political boundaries (countries)

Figure 12 depicts the clustering process, where the basin has been divided into 11 clusters. The figure depicts the political boundaries, climate zones and geography to display that the clusters are significantly matching the aforementioned factors.

The clusters can be changed to have a higher resolution or consider other factors. This will occur in agreement with the Nile SEC.

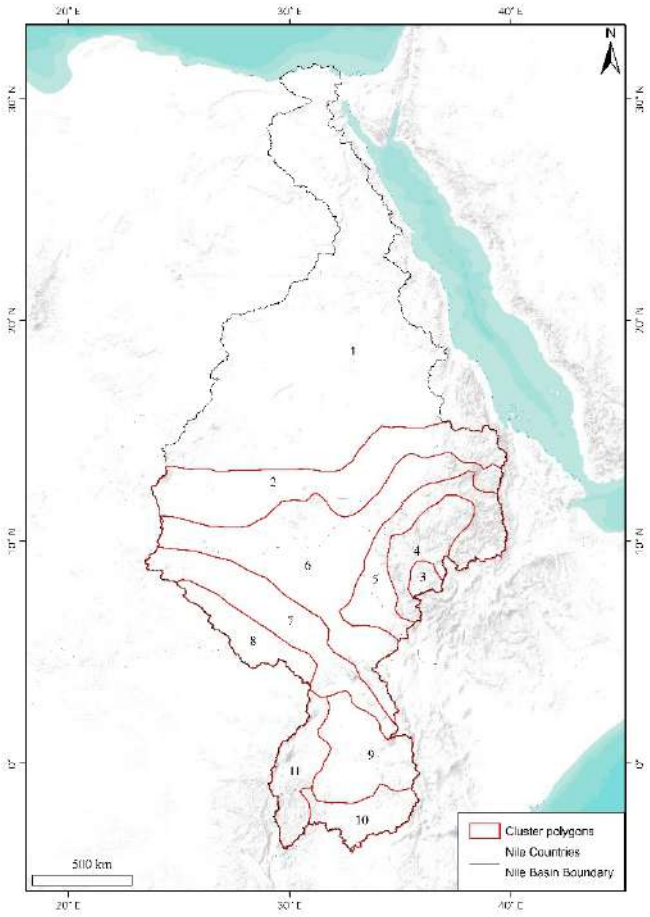

Figure 12: Cluster definition.

4.3.3.2 Radar change diagrams

After the clusters were defined, the relative change of the future projected IDF values to the historical IDF values in terms of the following four variables was calculated:

1- Change in rainfall intensity
2- Change in rainfall duration
3- Change in rainfall frequency
4- Spatial extent of extreme rainfall

Based on this approach, the mean value of the first three variables in both the historical period and future periods were calculated and the relative change between the historical period and future period was calculated for each cluster. The fourth variable requires an ArcGIS analysis to determine the changes in the spatial distribution of the rainfall by counting the number of grids that exceed the mean value of rainfall of the cluster for the historical and future projected periods. To represent the relative change values, a radar diagram was applied for each cluster. Figure 13 shows a sample of the generated map showing the Radar diagram. The corners of the radar diagram are marked with I = Intensity, D = Duration, F = Frequency, E = Extent and the relative change is calculated in percentage.

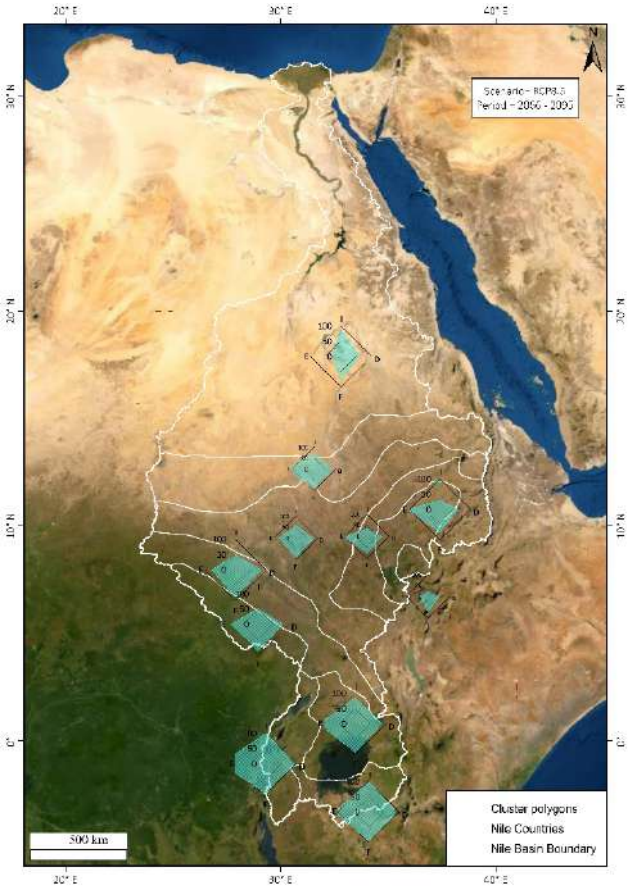

Figure 13: Sample of radar diagrams for each cluster (RCP scenario=4.5, period= 2006-2035).

5 PROBABLE MAXIMUM PRECIPITATION (PMP)

5.1 Definition and WMO approach

According to the (WMO, 1986), the Probable Maximum Precipitation (PMP) can be defined as "the greatest depth of precipitation for a given duration meteorologically possible for a given size storm area at a particular location at a particular time of year, with no allowance made for long-term climatic trends".

Due to the greenhouse effect which resulted in a change in the meteorological conditions in the 21st century, the PMP definition has been changed by (WMO, 2009). The updated definition of the Probable Maximum Precipitation (PMP) is the theoretical maximum precipitation for a given duration under modern meteorological conditions. The precipitation value calculated via PMP method may occur over a certain watershed at a certain design storm at certain time of the year.

PMP can aid hydrologists to determine the Probable Maximum Flood (PMF) prior to designing water infrastructures such as dams. The PMF is defined by (WMO, 1986) as the theoretical maximum flood that poses extremely serious threats to the flood control of a given project in a design watershed. Such a flood could plausibly occur in a locality at a particular time of year under current meteorological conditions.

The WMO recommends different approaches to estimate the PMP. Some methods are based on the physical estimation using meteorological data such as dew-point, moisture content, and wind speed. Whereas the latter methods are based on the statistical estimation by analysing the rainfall time series for a certain period. The following approaches are recommended by the WMO:

1- Local method (physical method)
2- Transposition method (physical method)
3- Combination method (physical method)
4- Inferential method (physical method)
5- Generalized method (physical method)
6- Statistical method (statistical method)

Due to lack of data availability related to dew-point moisture and wind speed, it is unpassable to apply the statistical methods to estimate the PMP for the Nile Basin. Thus, the statistical method was chosen to estimate the PMP values. The statistical procedure for estimating PMP is recommended by WMO wherever sufficient precipitation data is available and when dew point and wind records are lacking. The CORDEX scenarios will provide sufficient data when extremes are collected from all scenarios. The idea of the statistical approach is to envelope the value k that determines the PMP as a function of the annual maximum precipitation and the standard deviation of different rainfall durations. It could also be interpreted as a maximisation of skewness of a distribution function.

To estimate the PMP using the statistical approach, an equation has been formulated by (Hershfield, 1961) as follows:

$$X_m = \bar{X} + K_m.S$$

With

X_m	:	Point PMP for a specific station
$\bar{X}$	:	Average annual maximum precipitation
K_m	:	Statistical maximisation parameter
S	:	Standard deviation

The steps for estimating PMP are as follows as recommended by WMO manual:

1- Calculating the series of annual maximum precipitation for the CORDEX scenarios.
2- Determining the K_m parameter values according to the WMO approach.
3- Carrying out a spatial analysis to identify homogenous areas for the K_m values.
4- Determining an area-reduction factor based on the results.
5- Calculating PMP for the previously identified homogeneous areas.
6- Drawing PMP maps.

5.2 Assumptions for calculation

The WMO statistical approach was proposed to calculate the PMP for a defined watershed. However in our case, the input rainfall time series are different for each grid cell. Therefore, the following assumptions have been adopted:

1- K_m has been determined for each grid cell based on the statistical analysis of the maximum annual precipitation, and is hence also spatially variable.
2- The $\bar{X}$ and S statistical parameters have been adjusted using the adjustment factor mentioned in WMO manual, where the adjustment factor $\bar{X}$ and S are 1.02 and 1.04 respectively for the duration equal or greater than 24 hours.
3- The area reduction factor can be specified depending on the sub-basin size.
4- The PMP for the durations less than 24 h was estimated based on a graph developed by (Huff, 1967), which is also recommended by the WMO.

5.3 PMP Estimation Approach

5.3.1 Calculating the series of annual maximum precipitation for the CORDEX scenarios

The series of annual maximum precipitation is necessary to calculate certain statistical parameters required for estimating the PMP (average annual maximum precipitation and standard deviation of the average annual maximum precipitation), and was generated using python scripts. Figure 14 demonstrates a sample of the series of annual maximum precipitation for a chosen grid cell for the historical period (1971-2000). Afterwards, the average annual maximum precipitation $\bar{X}$ and the standard deviation S have been determined for each grid cell. Figure *15* demonstrate the spatial distribution of the mean and standard deviation.

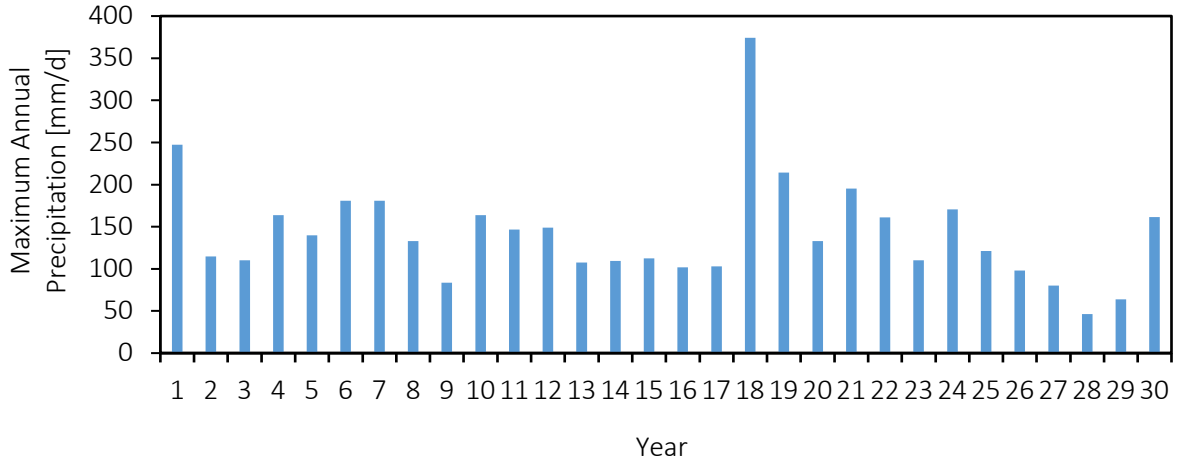

Figure 14: Annual maximum precipitation time series for a chosen grid.

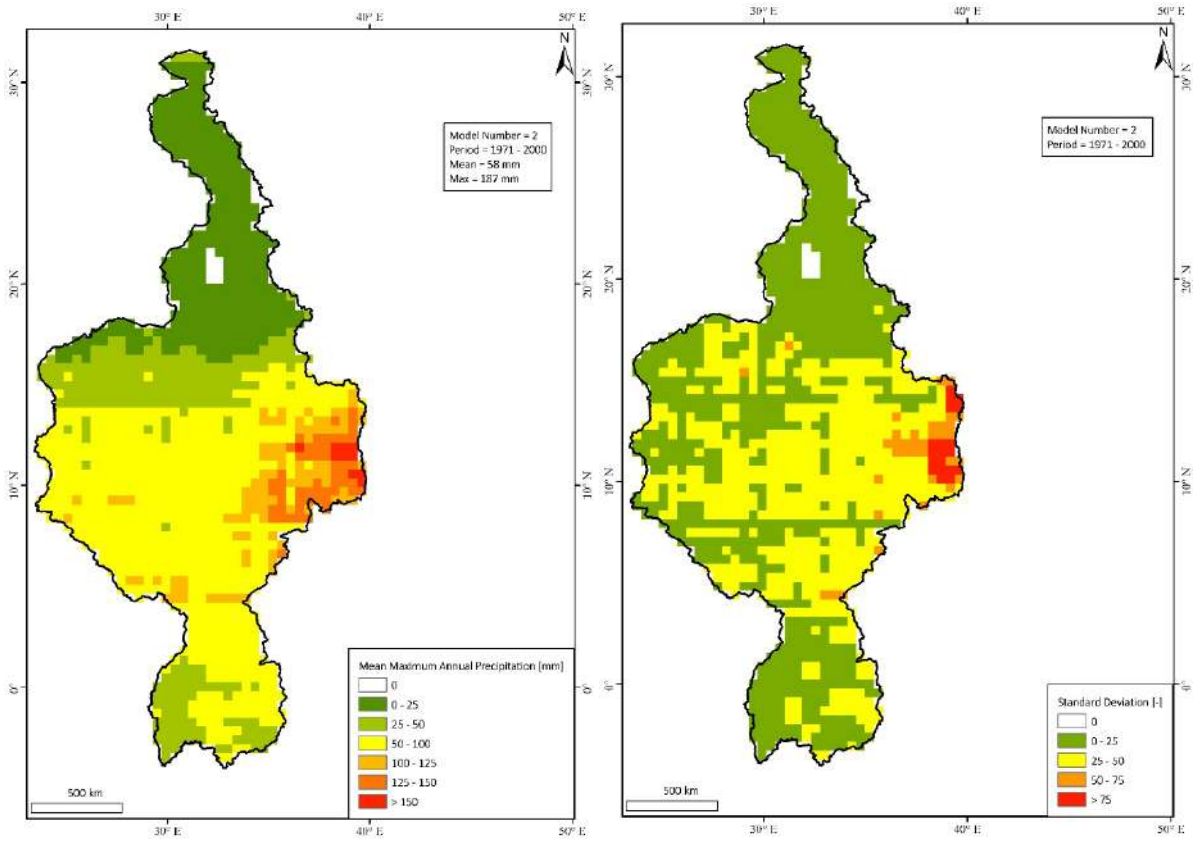

Figure 15: Spatial distribution of the mean maximum annual precipitation and standard deviation for the historical period.

5.3.2 Determining the K_m values according to the WMO approach

The Statistical maximization parameter K_m has been estimated based on the average annual maximum precipitation. (Hershfield, 1965) developed a relationship between the average annual maximum precipitation and K_m as shown in Figure 16 (a) . To determine the K_m values corresponding to the average annual maximum precipitation $\bar{X}$ of each grid cell, a linear interpolation based on the curve in Figure *16* (a) has been applied using a python script.

5.3.3 Conducting the spatial analysis over all locations to identify homogenous areas for the K_m values

The K_m Parameter was calculated for each grid. Figure *16* (b) represents the spatial distribution of K_m for the historical period. The figure shows that K_m ranges from around 14 to approximately 20. It was observed that low K_m values are located at the grids characterized by a high average annual mean precipitation.

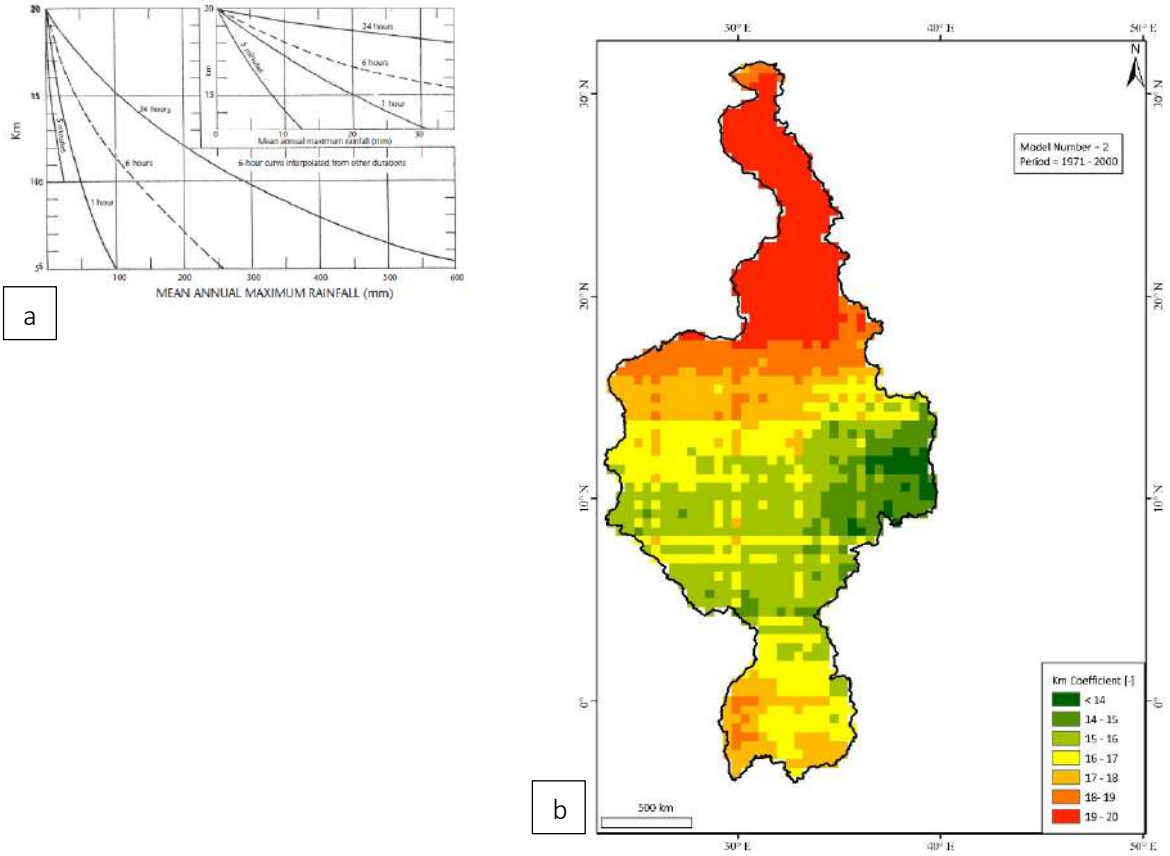

Figure 16: (a) K_m as a function of rainfall duration and mean of annual series (after: (Hershfield, 1965)). (b) Spatial distribution of the K_m parameter for the historical period.

5.3.4 Determining an area-reduction factor based on the results

The area reduction factor was determined by utilizing the graph developed by (United States Weather Bureau, 1960) as shown in Figure *17*, which is recommended by WMO. As shown in Figure 17, the area reduction factor depends on the sub-basin area.

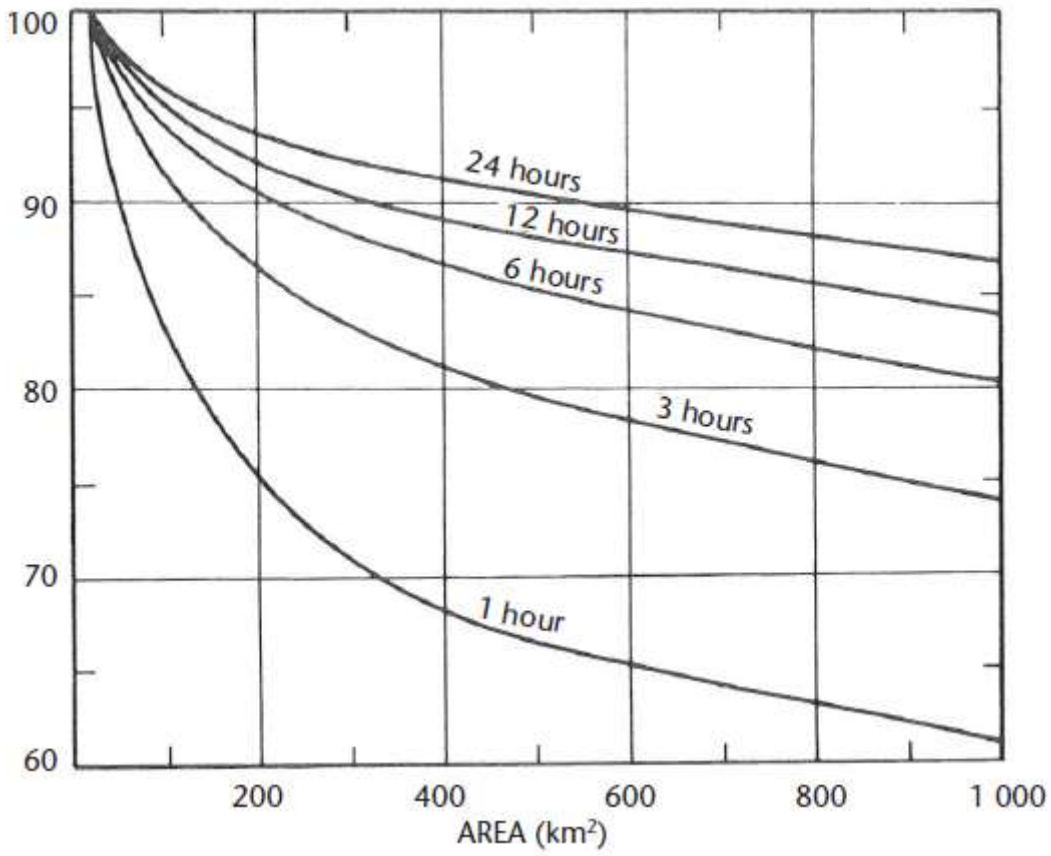

Figure 17: Depth-area, or area-reduction curves for western United States (after: (United States Weather Bureau, 1960)).

5.3.5 Calculating the PMP for the previously identified homogeneous areas

After acquiring the different parameters including the average annual maximum precipitation ($\bar{X}$), the statistical maximisation parameter (K_m), and the standard deviation (S), the PMP for a 24 h duration was estimated using the aforementioned equation. To determine the PMP at lower duration (less than 24 h), a relationship was developed by (Huff, 1967) between the PMP at durations less than 24 h and PMP at a 24 h duration. This relationship is represented in a graph as shown in Figure *18*. The graph was applied in our case to acquire the PMP at 1h, 3h, 6h, and 12h durations. Figure *19* represents the PMP result.

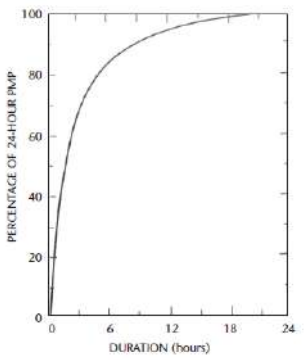

Figure 18: Maximum depth duration curve (after: (Huff, 1967))

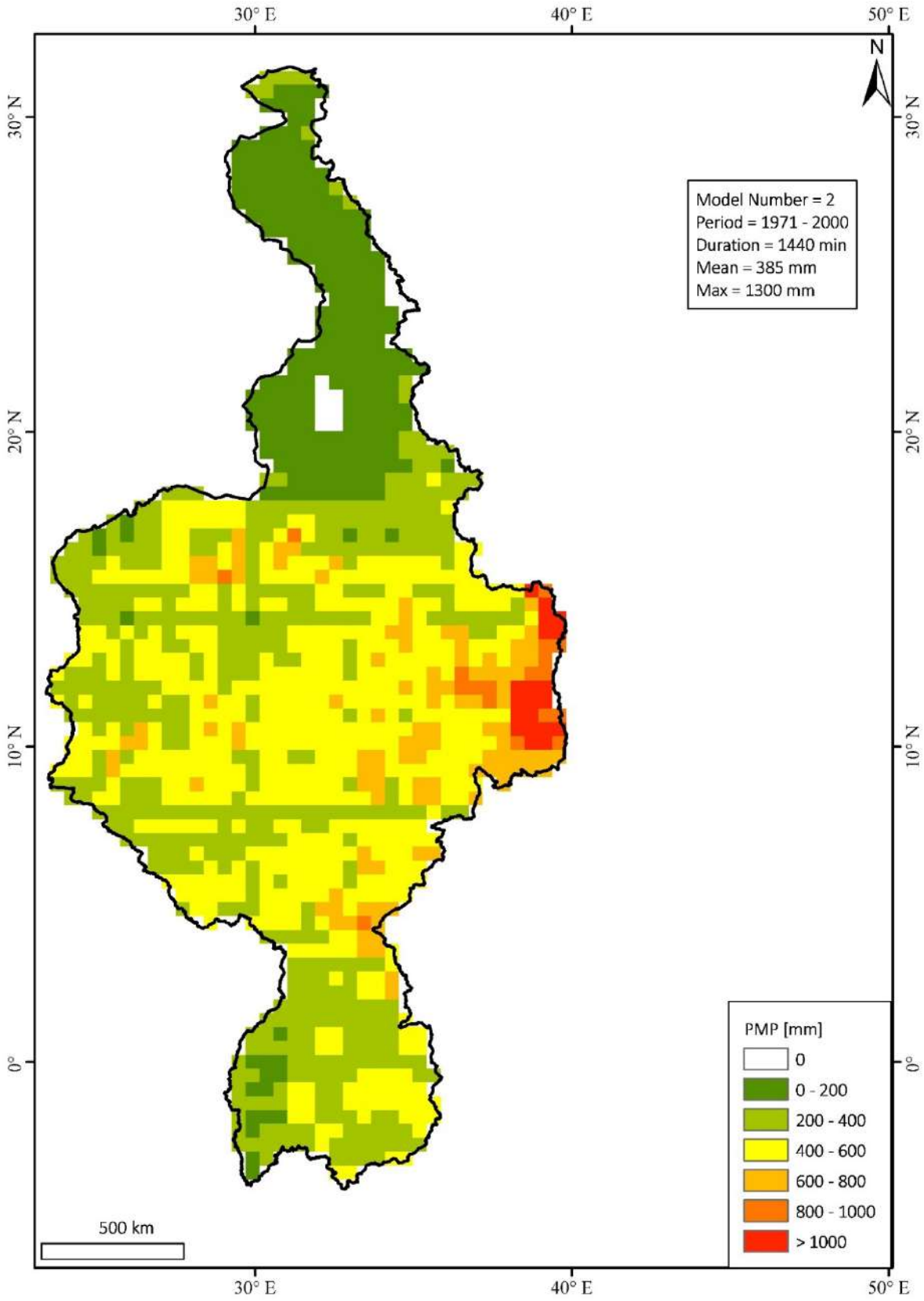

Figure 19: PMP (duration = 24 h, Period = 1971- 2000)

5.4 Maps

5.4.1 Grid maps

Grid maps were created to represent the PMP estimation results considering the spatial variation. Figure 20 shows a sample of the 24h PMP for the historical period. The map also indicates the mean and maximum values of the PMP and shows a histogram of the distribution of the grid cell values. Additionally, PMP maps have also been generated for the durations of 1h, 3h, 6h, and 24h.

5.4.2 Contour maps

Since the grid maps are not sufficient enough to be utilized by hydrologists to design the water infrastructure, contour maps could be generated to facilitate the map user to extract the values. To map contour lines from the grid maps, the grid maps were processed in ArcGIS Figure *11*: IDF contour map sample (RCP scenario = 4.5, period= 2006-2035, Duration = 1 day, Frequency = 100 a). Figure 21 depicts an example of a generated contour map for the historical period.

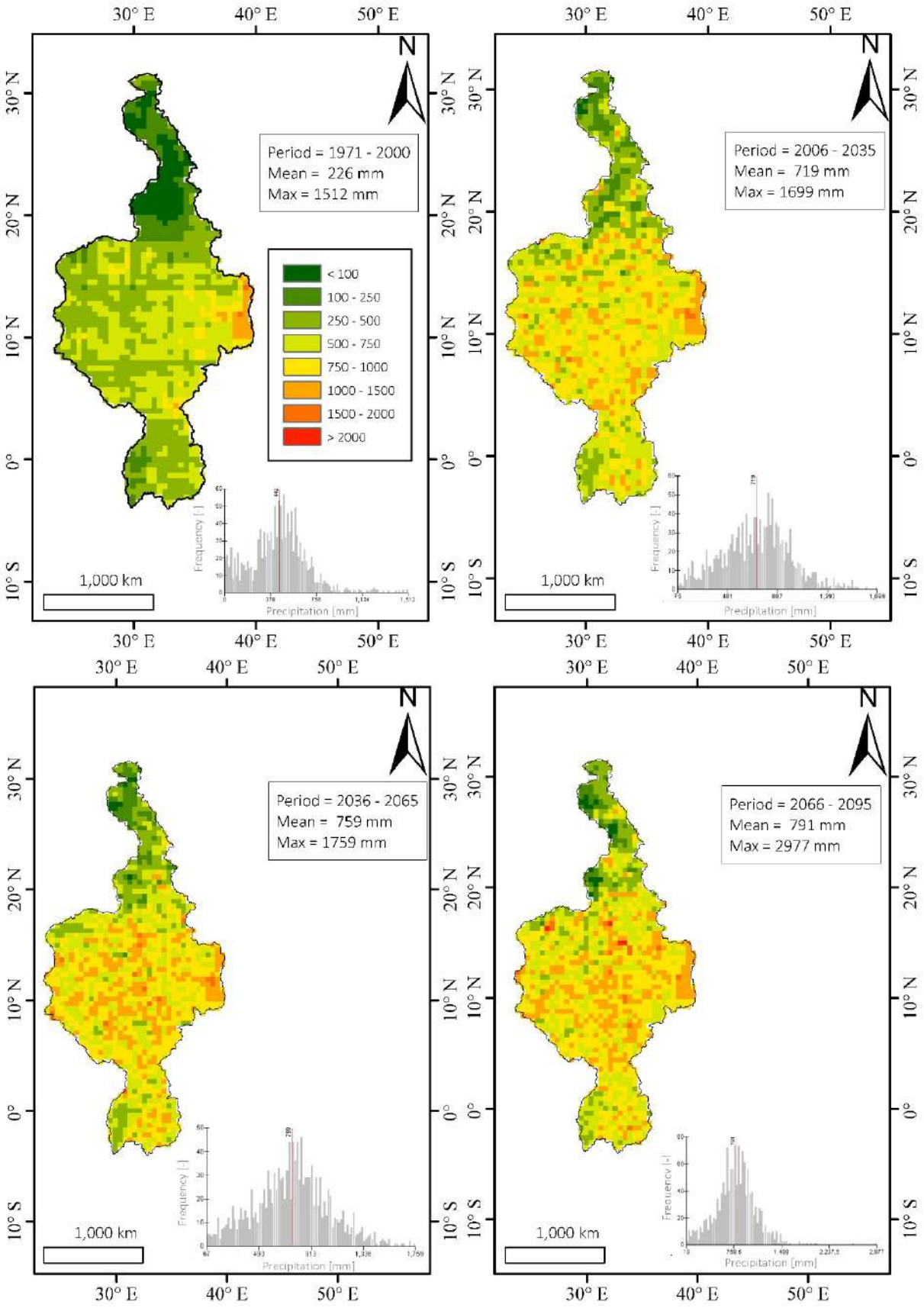

Figure 20: PMP grid map sample (RCP scenario = 4.5, Duration = 1440 min).

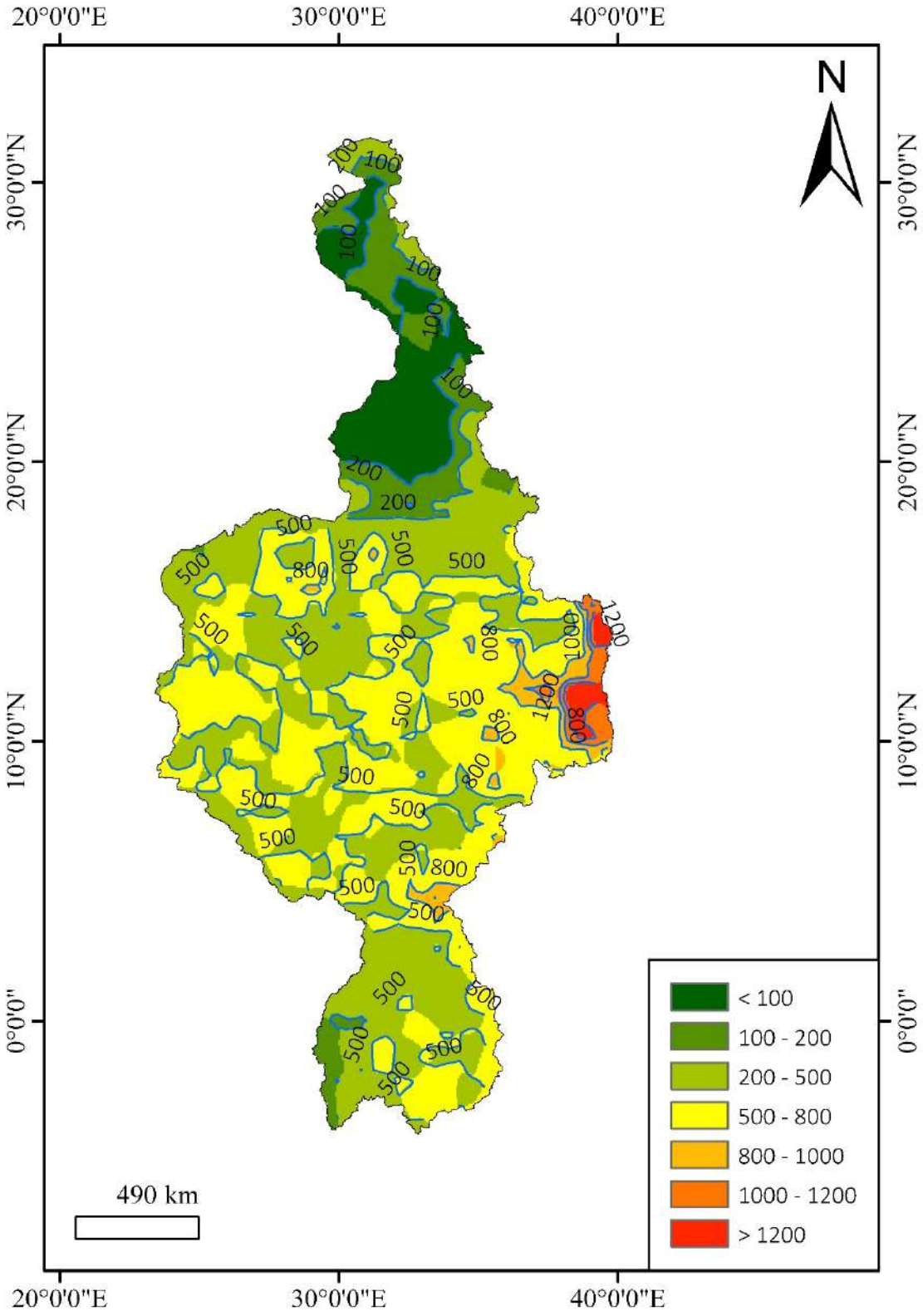

Figure 21: PMP contour map sample (RCP scenario = historical, Duration = 1440 min).

6 PROBABLE MAXIMUM FLOOD (PMF)

Probable Maximium Flood (PMF) is one of several conceptual flood events used in the design of hydrological structures to ensure the reliability and stability of these structures particularily the dams. PMF is estimated for the catchment area of a dam in order to design the spillway to minimize the risk of overtopping. In order to obtain the PMF at a given catchment, the PMP has to be transformed into streamflow using the catchment characteristics. The steps for calculating the PMF are as follows:

1- Deriving several design storm profiles for the PMP
2- Testing the derived desing storm profiles to obtain the maximum conditions at the water infrastructure

6.1 Derving several design storm profiles for the PMP

Design strom profiles are spatially variable because they mainly depend on the climate zone of the catchment. Different profiles were developed at different climate conditions. One of the widely used profiles among the hydrologists is the SCS strom profiles. SCS storm profiles were developed based on several storm observations conducted in the USA. The SCS storm profiles were generated in the form of percentage mass curves based on 24-hr rainfall of the desired frequency. SCS strom profiles comprise 4 types representing different storm conditions in USA (Figure 22): Type I, Type II, Type III, Type IV. The design storm profile for a certain catchment can be obtained by multiplying the fraction hour rainfall by the precipitation depth (PMP). Different durations and different storm profiles could be generated from PMP value. Driving the storm profiles depends on the study area location and the catchment characteristics and should be done for each case study separately.

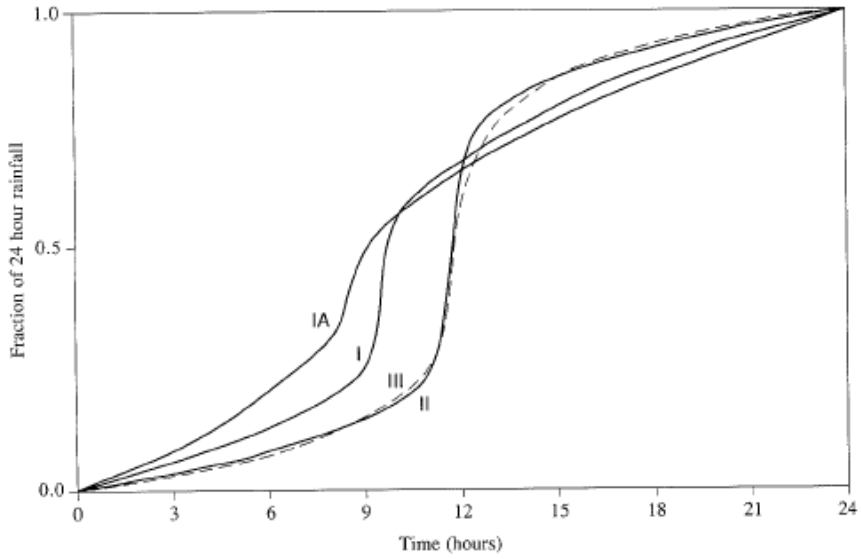

Figure 22: SCS storm profiles (after : (USACE Hydraulic Engineering Center, 2022)).

6.2 Testing the derived strom profile to obtain the maximum conditions at the water infrastructure

After generating different storm profiles, the profiles can be imported to a rainfall runoff model, where they can be used to run the model for the chosen catchment. The PMF can be generated by filtering out the maximum flood conditions that occurred by running the storm profiles. The PMF, unlike the

PMP, cannot be calculated for each grid of the Nile Basin as the calculation requires a delineated watershed.

7 DATABASE PORTAL

The climate products that were derived in the course of this assignment can be accessed through a data service portal website which entails downscaled CORDEX Data from 4 scenarios which represent the minimum and maximum signal changes of climate in terms of temperature (minimum and maximum) and precipitation. Those four selected datasets were used to derive Intensity-Duration-Frequency (IDF) matrices, and the Probable Maximum Precipitation (PMP). Figure 23 shows the website home page. Different file format types are available on the website including the CSV file Format, ASCII file format, and maps for visualising the results.

Figure 23: Database website portal homepage.

To enable users to use the website, a manual has been prepared to describe to them how to get access to the relevant climate products prior to utilizing the data in different applications. Additionally, an example of how to process the data before implementation has been added to the manual.

8 REFERENCES

Costa, J. E. (1985). *Floods from dam failures* . US Geological Survey

Donnell, C. R. (2015). ICOLD 2015 General Report Q97

Evans, J. E. (2000). Lessons from a dam failure. *The Ohio Journal of Science*, S. 121.

Hershfield, D. M. (1961). Estimating the probable maximum precipitation. *Journal of the Hydraulics Division*, *87*(5), 99–116.

Hershfield, D. M. (1965). Method for estimating probable maximum rainfall. *Journal-American Water Works Association*, *57*(8), 965–972.

Huff, F. A. (1967). Time distribution of rainfall in heavy storms. *Water Resources Research*, *3*(4), 1007–1009.

IPCC. (2007). The physical science basis. Summary for policy makers. In S. Solomon, D. Qin, M. Manning, Z. Chen, M. Marquis, K. Averyt, … H. Miller (Eds.), *Contribution of working group I to the fourth assessment report* (Intergover). Cambridge: Cambridge University Press.

United States Weather Bureau. (1960). *Internal Report*.

USACE Hydraulic Engineering Center. (2022). *HEC-HMS Technical Reference Manual.* Von https://www.hec.usace.army.mil/confluence/hmsdocs/hmstrm/precipitation/scs-storm abgerufen

Willmott, C. J., & Matsuura, K. (2005). Advantages of the mean absolute error (MAE) over the root mean square error (RMSE) in assessing average model performance. *Climate Research*, *30*(1), 79–82. https://doi.org/10.3354/cr030079

WMO (World Meteorological Organization). (1986). *Manual for estimation of probable maximum precipitation. Operational hydrology.* (Vol. Report1). Geneva, Switzerland: WMO (World Meteorological Organization).

WMO (World Meteorological Organization). (2009). *Manual for estimation of probable maximum precipitation* (WMO No. 10). Geneva, Switzerland: WMO (World Meteorological Organization).

Zhang, L. Y. (2009). Analysis of earth dam failures. A database approach. In *Georisk* (S. 184-189).

9 ANNEX – CORDEX DATA

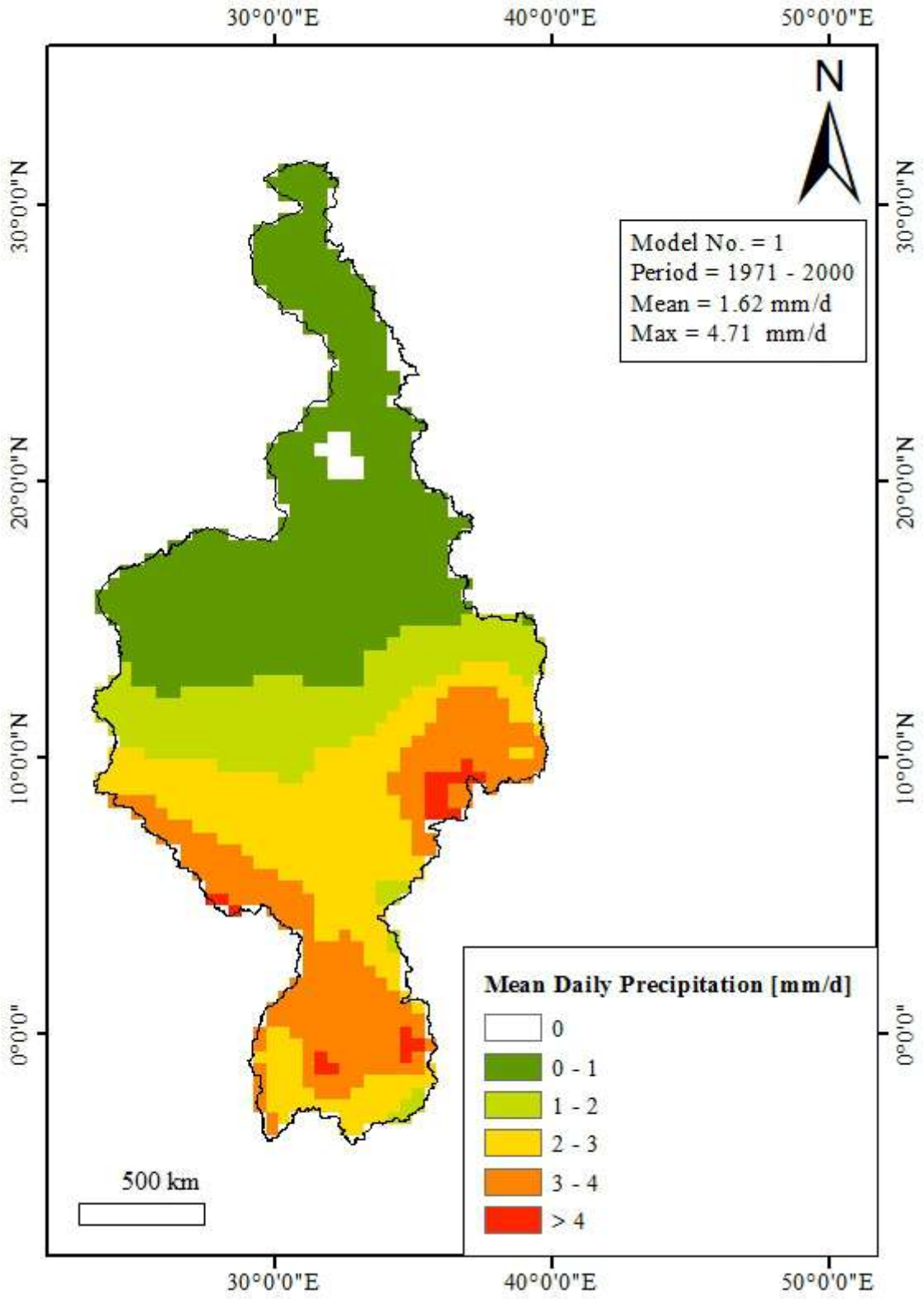

Figure 24: Mean historical daily precipitation (Model = BCCR_WRF331NCC_NorESM1_M , Period = 1971-2000).

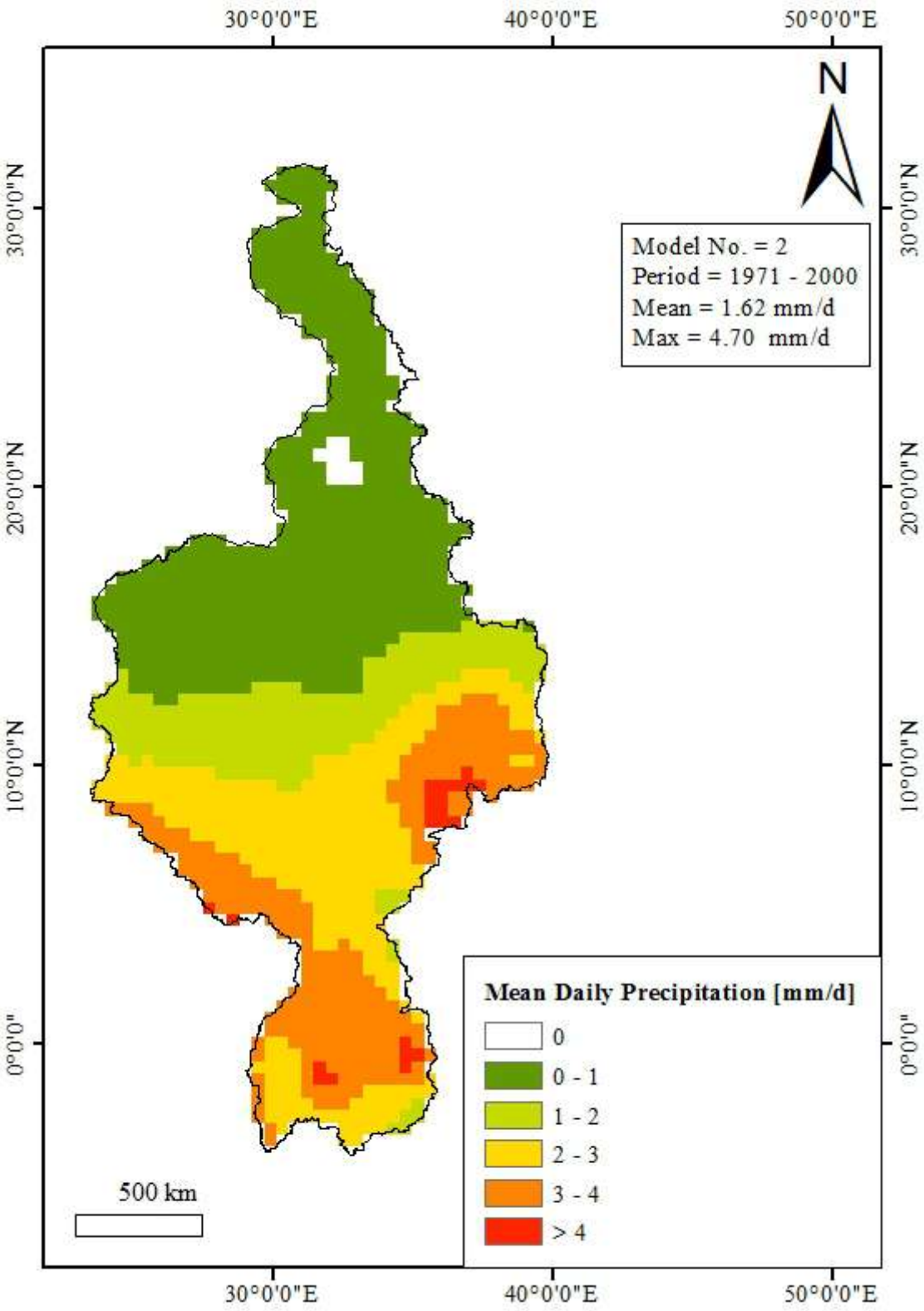

Figure 25: Mean historical daily precipitation (Model = CLMcom_CCLM4817CNRM_CERFACS_CNRM_CM5 , Period = 1971-2000).

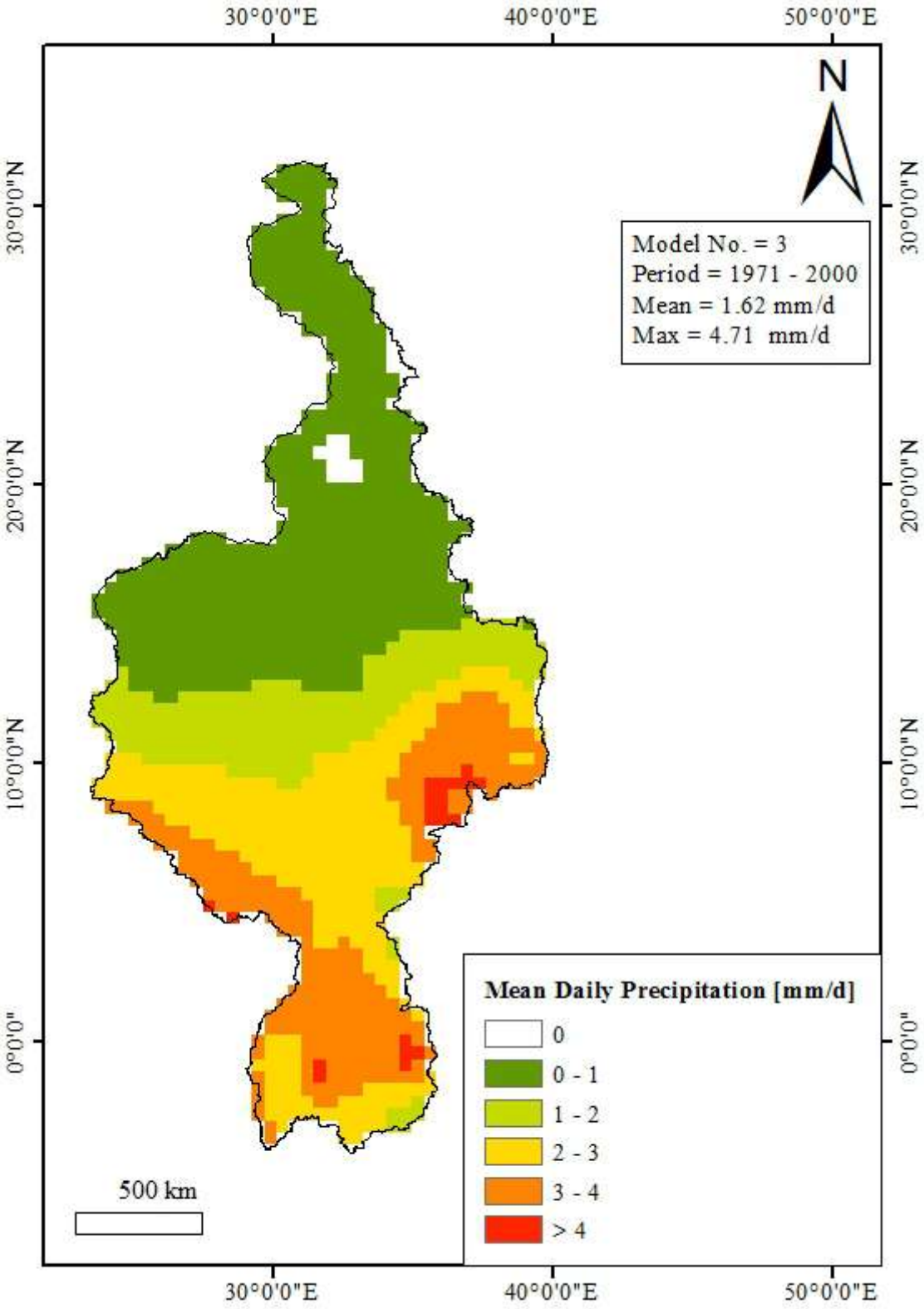

Figure 26: Mean historical daily precipitation (Model = CLMcom_CCLM4817ICHEC_EC_EARTH , Period = 1971-2000).

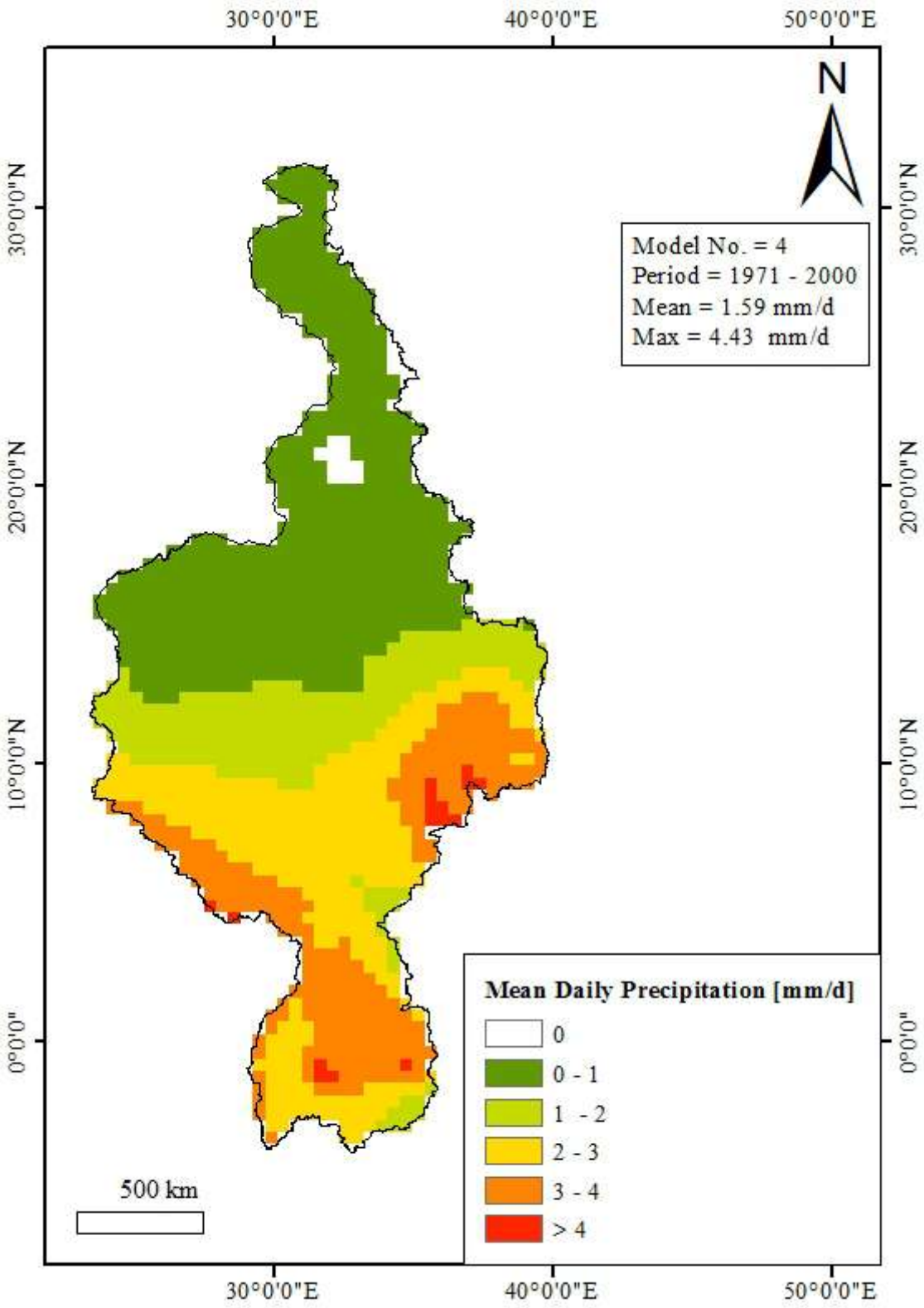

Figure 27: Mean historical daily precipitation (Model = CLMcom_CCLM4817MOHC_HadGEM2_ES , Period = 1971-2000).

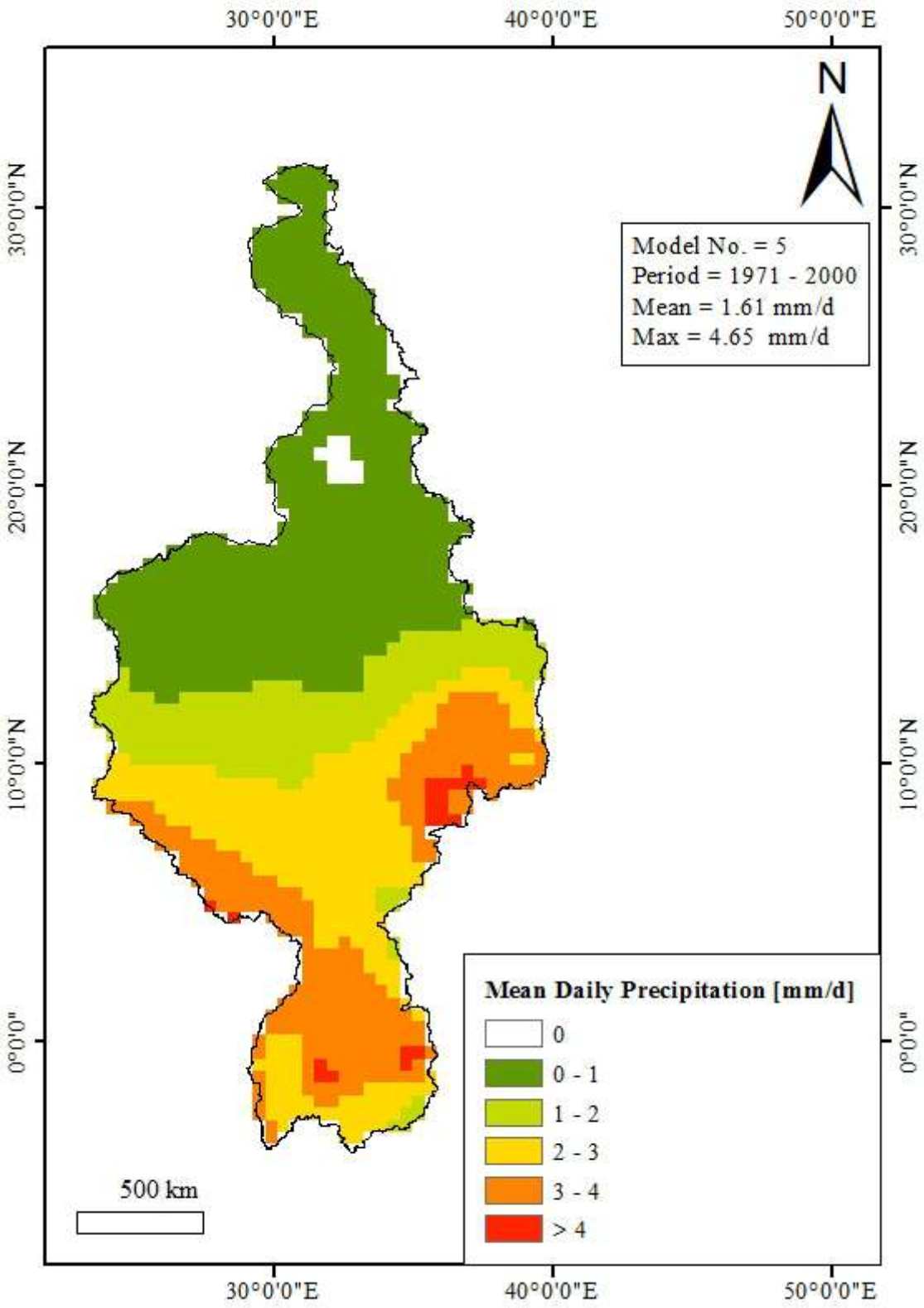

Figure 28: Mean historical daily precipitation (Model = CLMcom_CCLM4817MPI_M_MPI_ESM_LR , Period = 1971-2000).

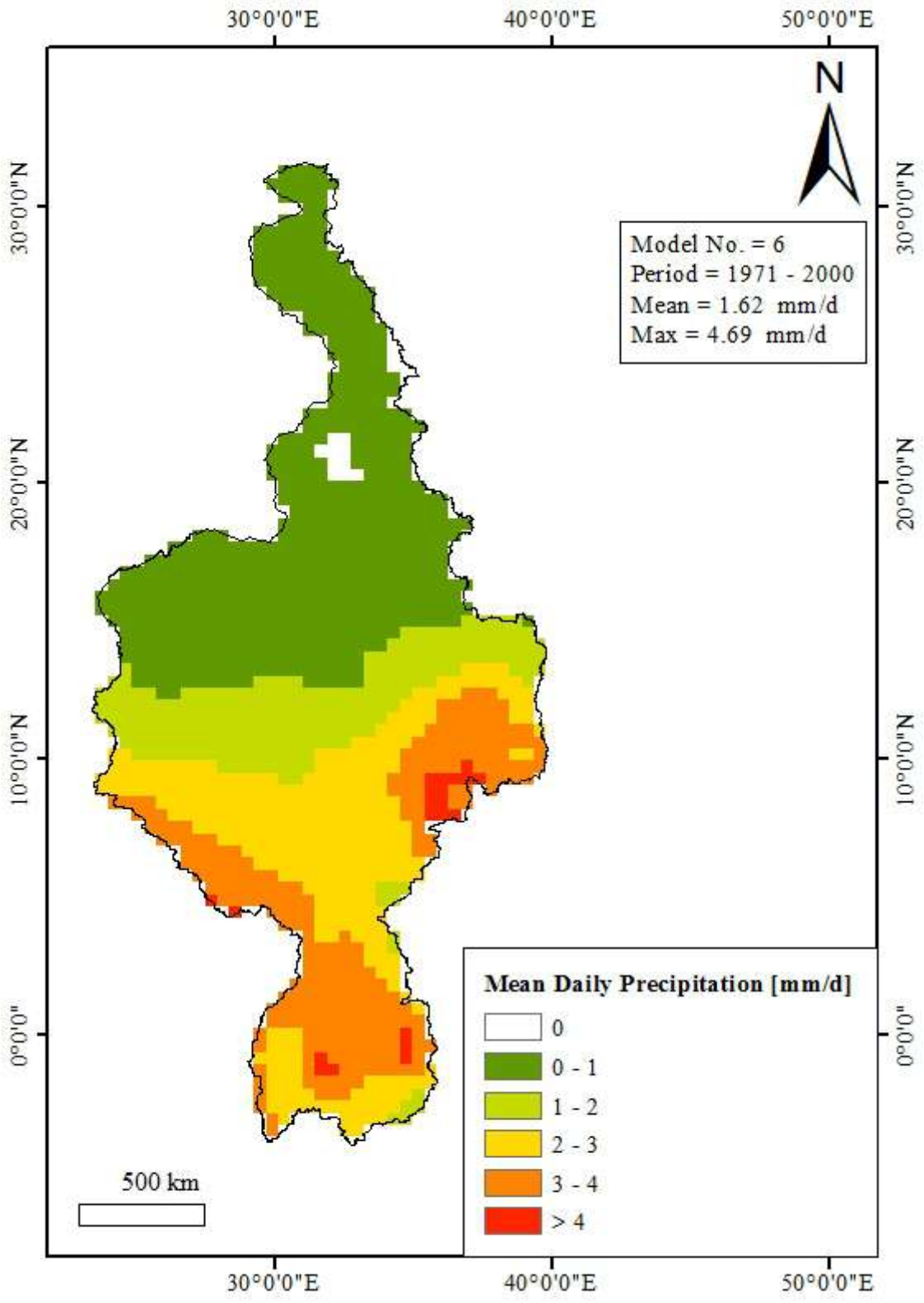

Figure 29: Mean historical daily precipitation (Model = DMI_HIRHAM5ICHEC_EC_EARTH , Period=1971-2000).

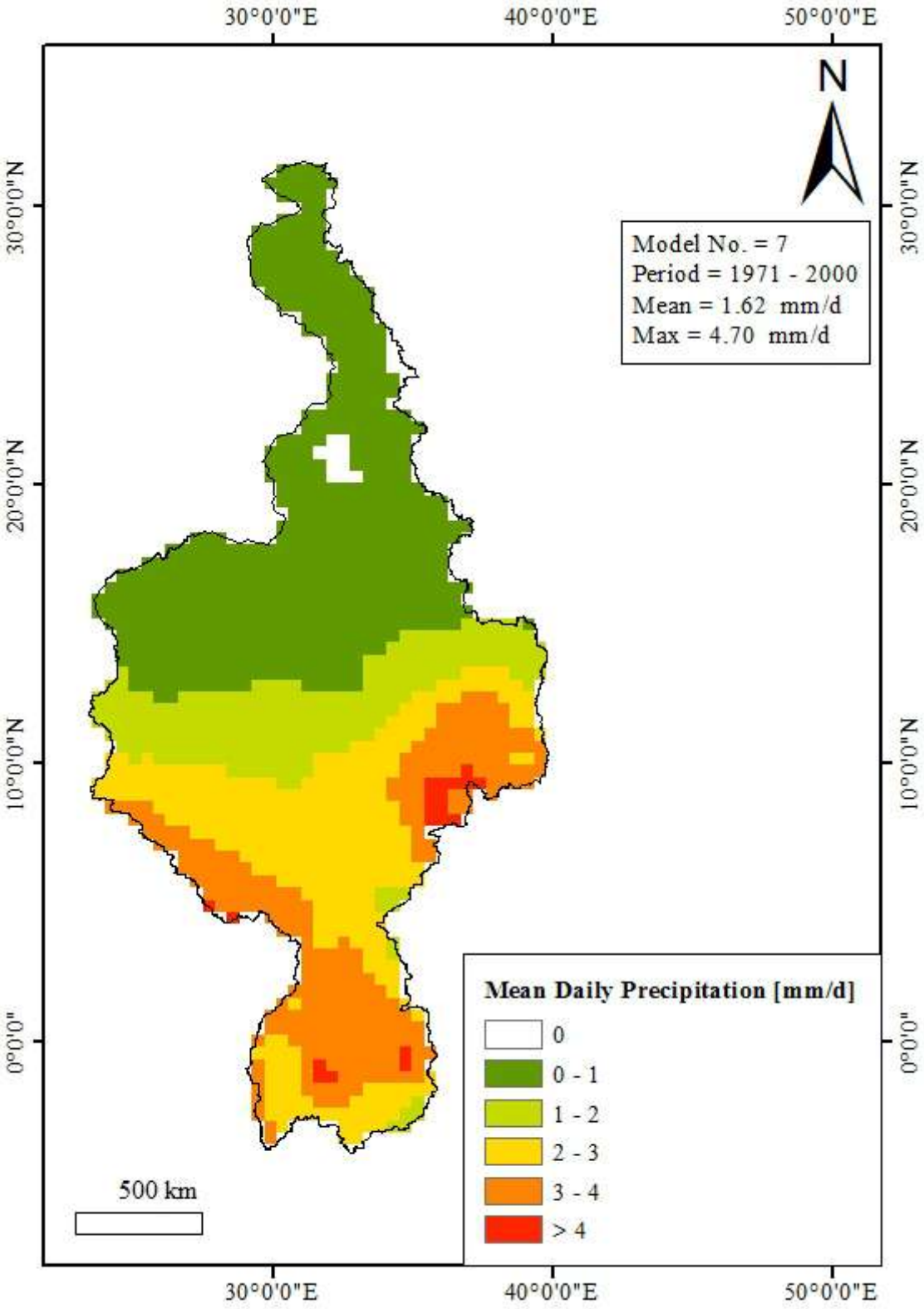

Figure 30: Mean historical daily precipitation (Model = KNMI_RACMO22TICHEC_EC_EARTH , Period = 1971-2000).

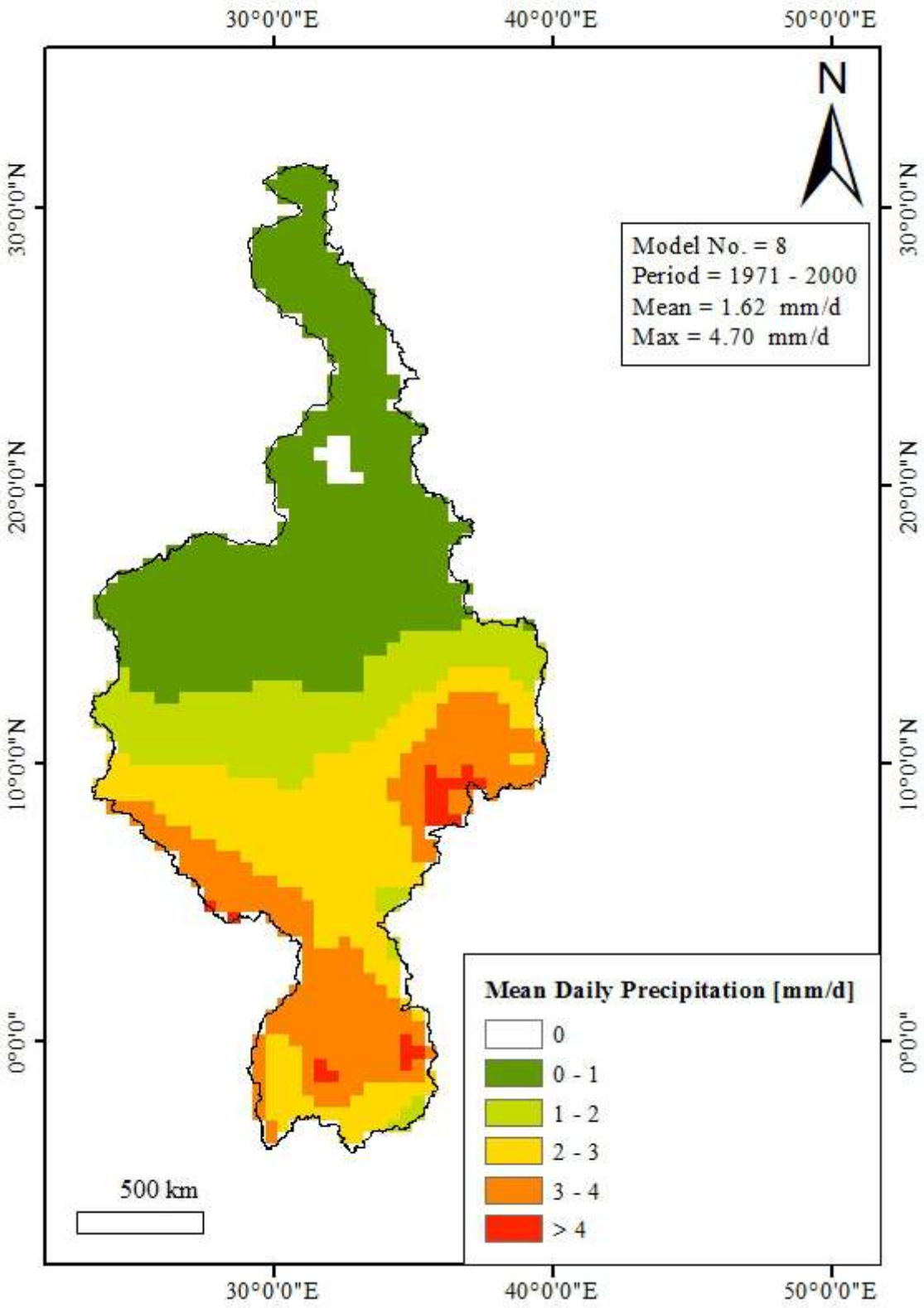

Figure 31: Mean historical daily precipitation (Model = MPI_CSC_REMO2009MPI_M_MPI_ESM_LR , Period = 1971-2000).

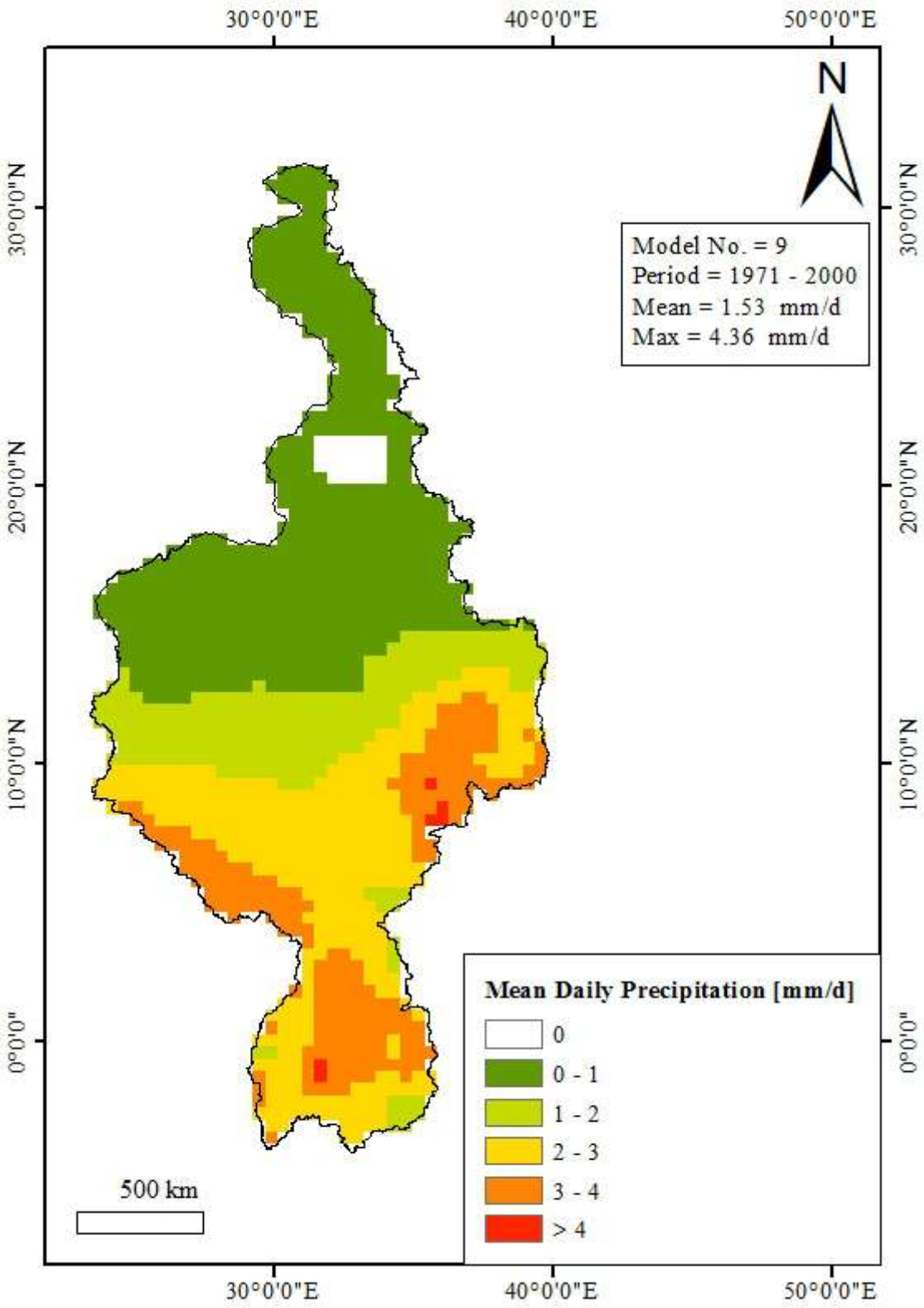

Figure 32: Mean historical daily precipitation (Model = SMHI_RCA4CCCma_CanESM2 , Period = 1971-2000).

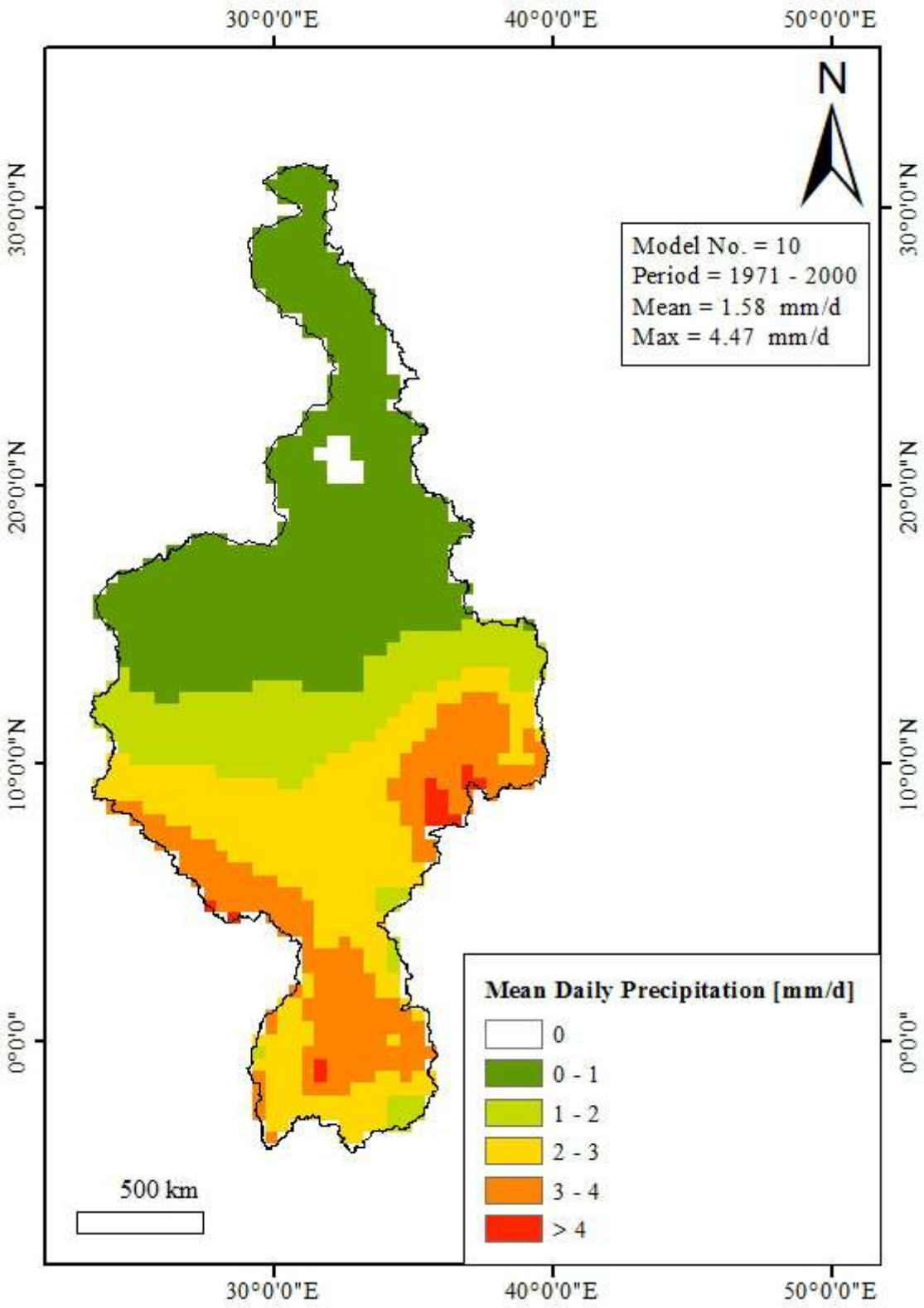

Figure 33: Mean historical daily precipitation (Model = SMHI_RCA4CCCma_CanESM2 , Period = 1971-2000).

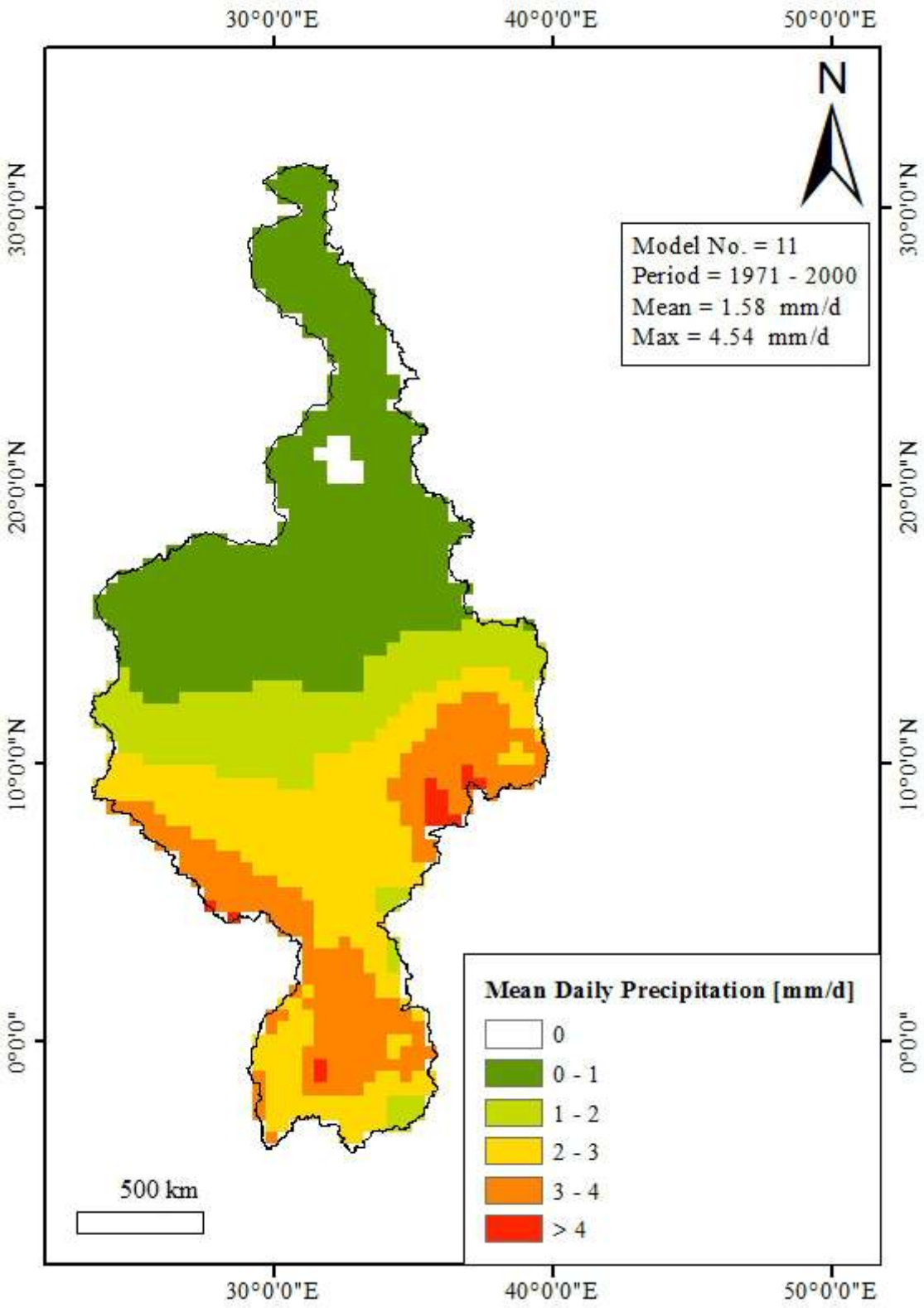

Figure 34: Mean historical daily precipitation (Model = SMHI_RCA4CNRM_CERFACS_CNRM_CM5 , Period = 1971-2000).

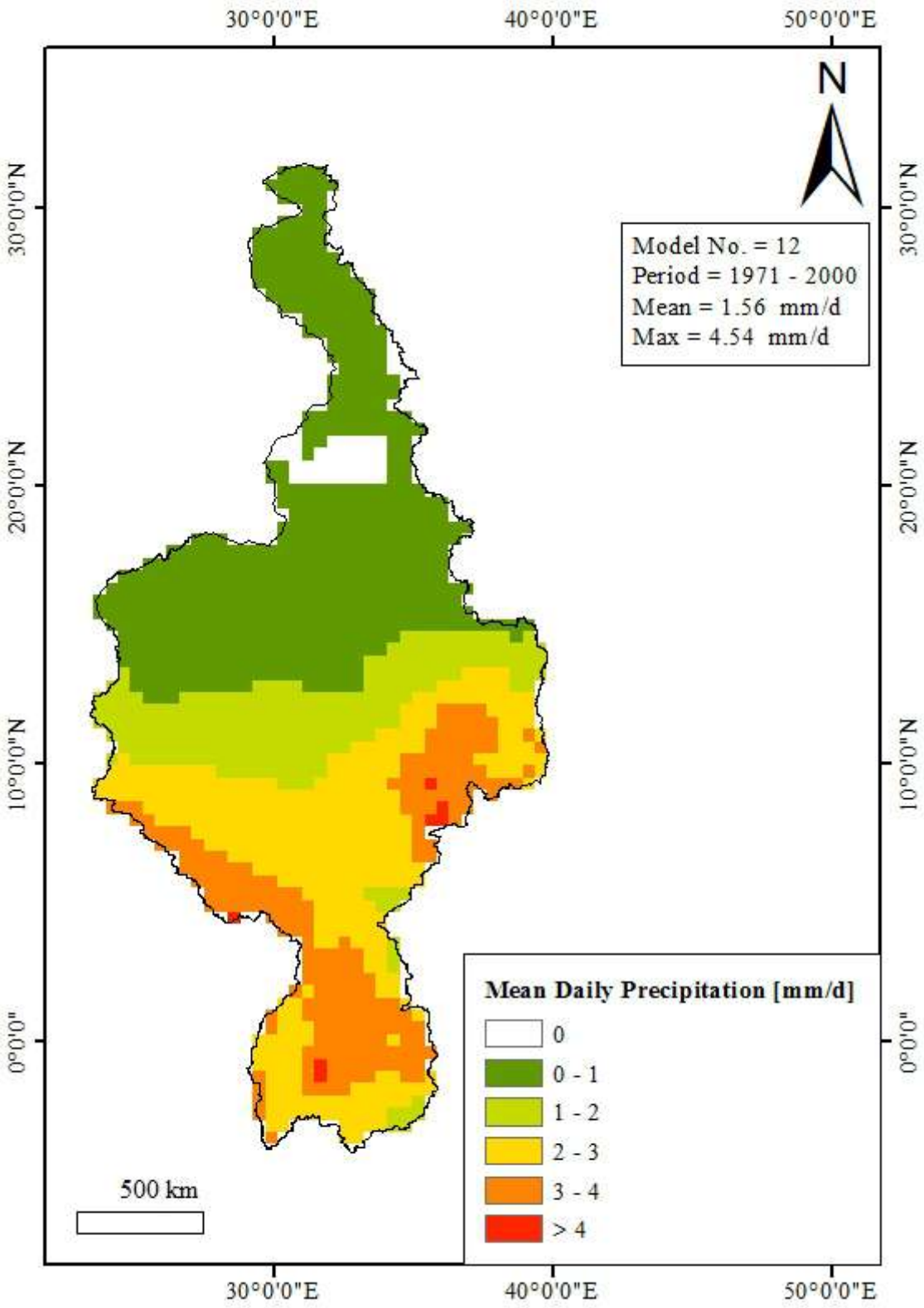

Figure 35: Mean historical daily precipitation (Model = SMHI_RCA4ICHEC_EC_EARTH_pr , Period = 1971-2000).

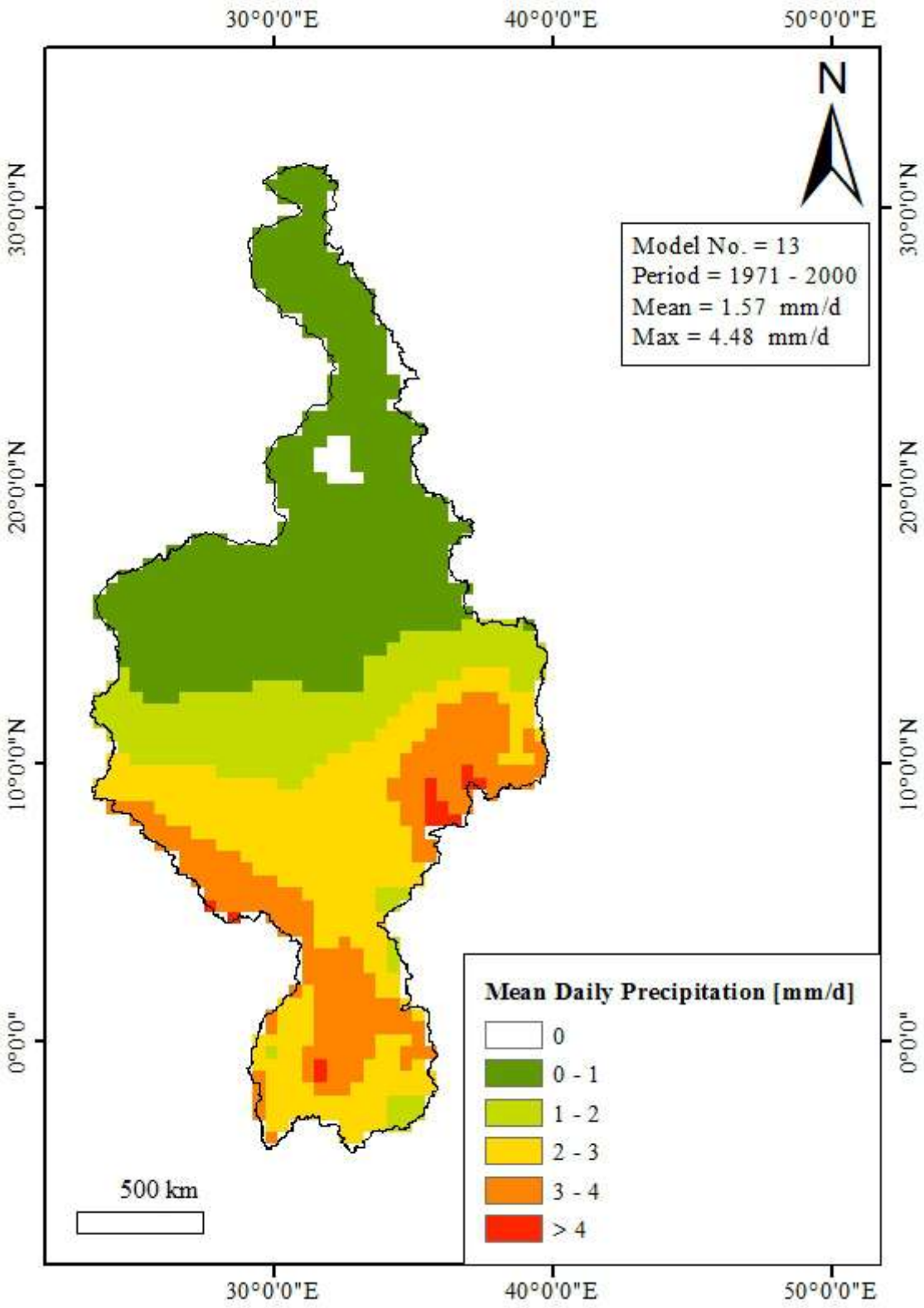

Figure 36: Mean historical daily precipitation (Model = SMHI_RCA4IPSL_IPSL_CM5A_MR , Period = 1971-2000).

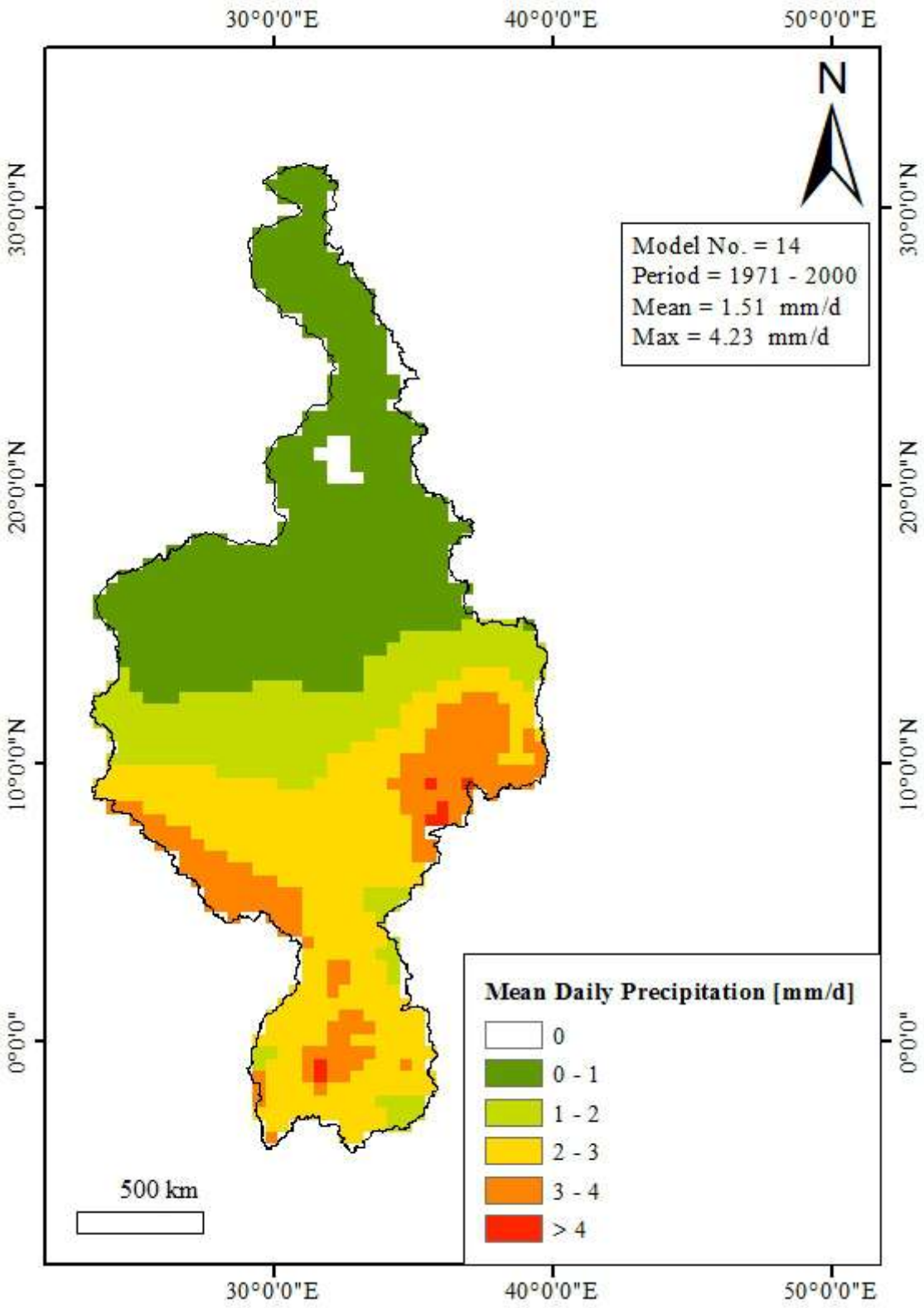

Figure 37: Mean historical daily precipitation (Model = SMHI_RCA4MIROC_MIROC5 , Period = 1971-2000).

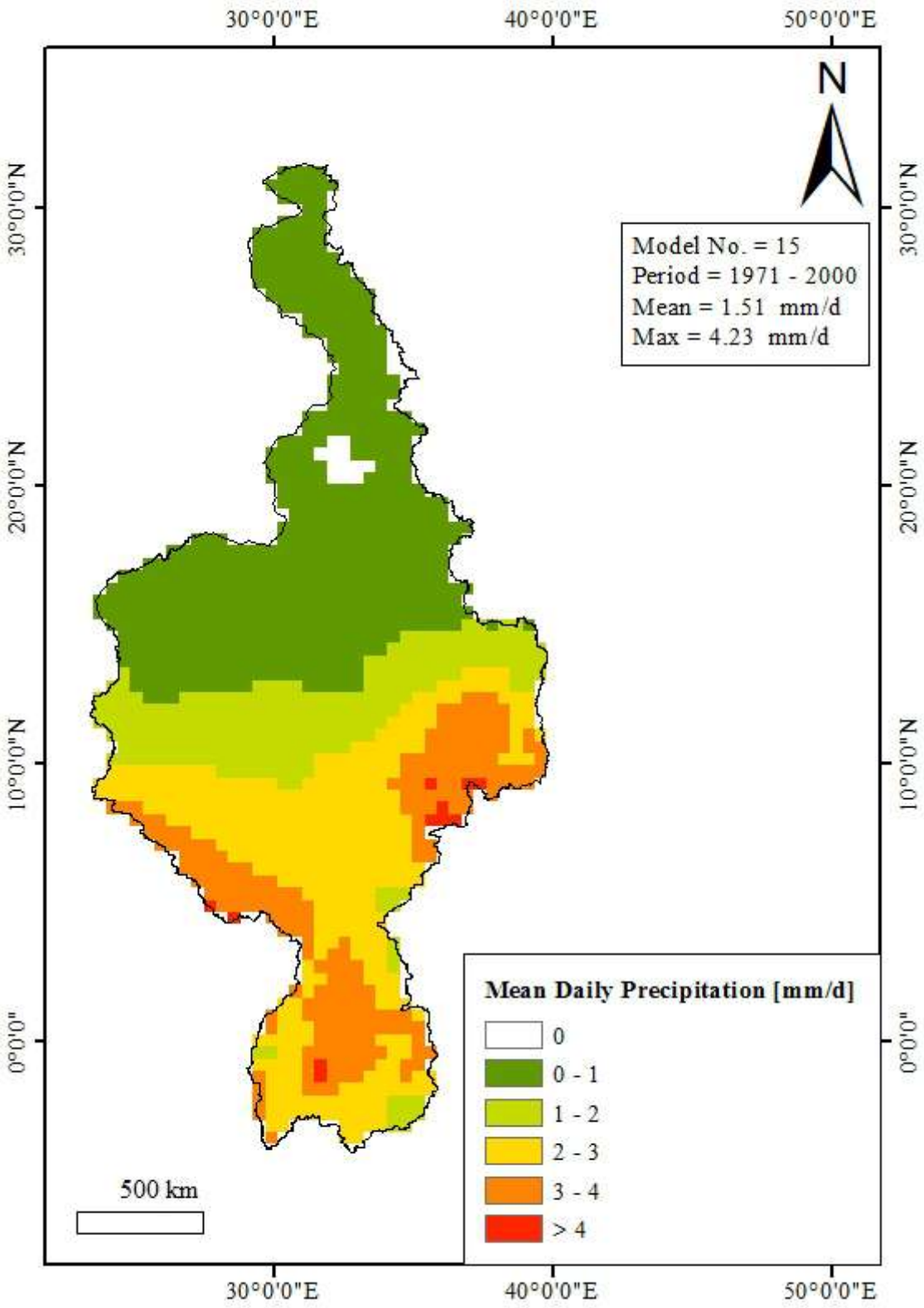

Figure 38: Mean historical daily precipitation (Model = SMHI_RCA4MOHC_HadGEM2 , Period = 1971-2000).

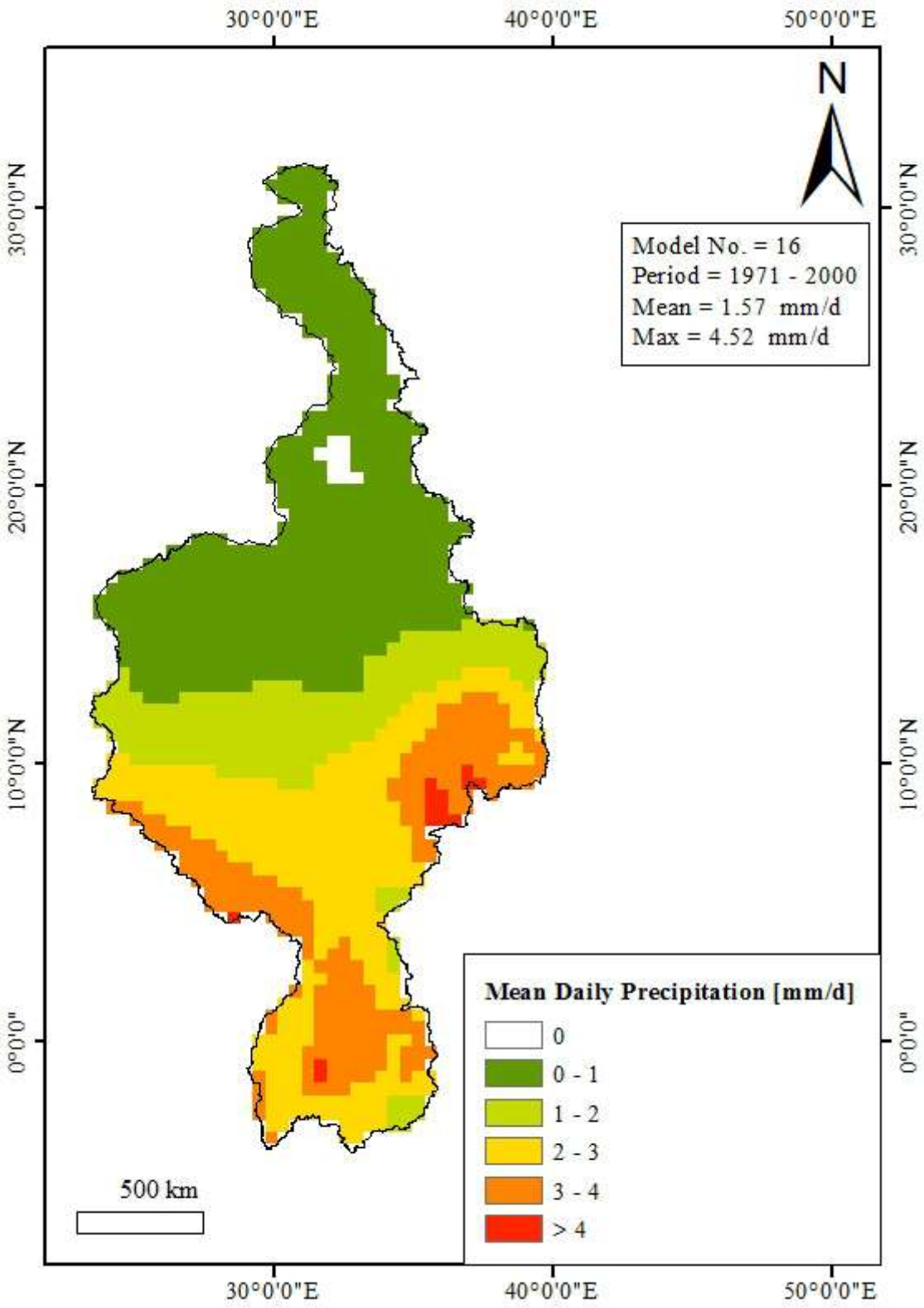

Figure 39: Mean historical daily precipitation (Model = SMHI_RCA4NCC_NorESM1_M , Period = 1971-2000).

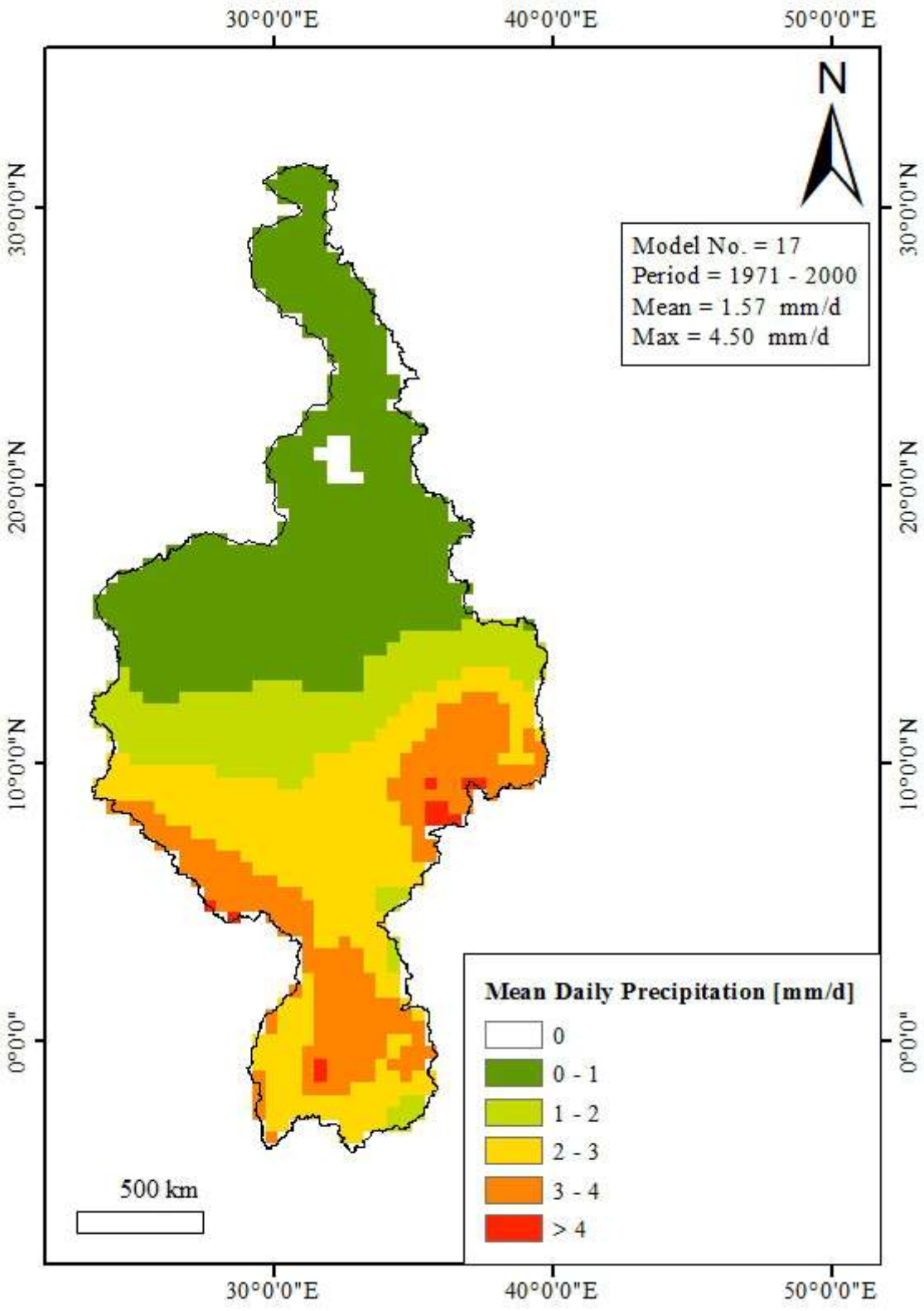

Figure 40: Mean historical daily precipitation (Model = SMHI_RCA4MPI_M_MPI_ESM_LR , Period = 1971-2000).

10 ANNEX – IDF GRID MAPS

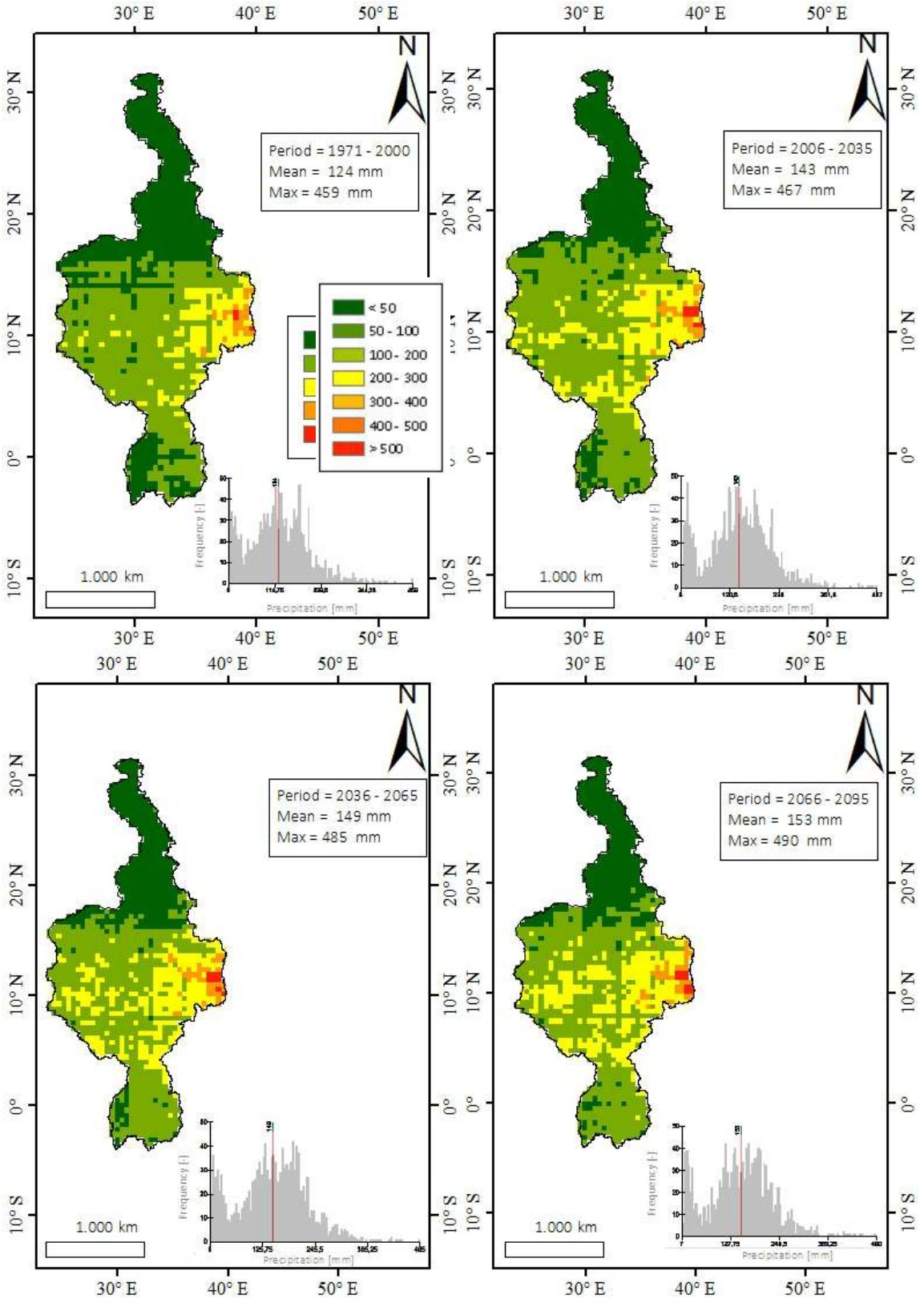

Figure 41: IDF grid map (Model No. = BCCR_WRF331NCC_NorESM1_M, RCP scenario = 4.5, Duration = 1 day, Frequency = 100 year).

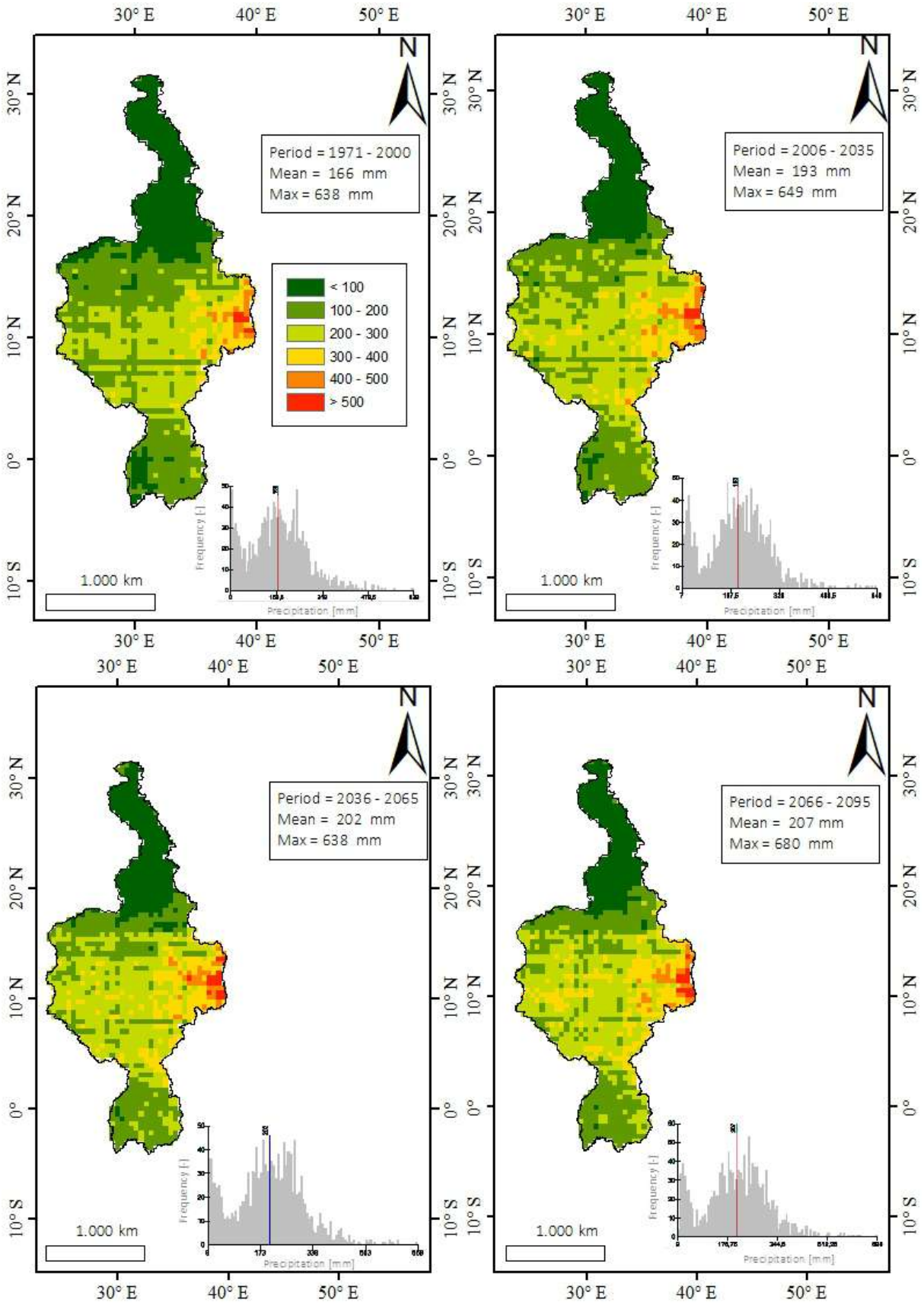

Figure 42: IDF grid map (Model = BCCR_WRF331NCC_NorESM1_M , RCP scenario = 4.5, Duration = 1 day, Frequency = 1000 year).

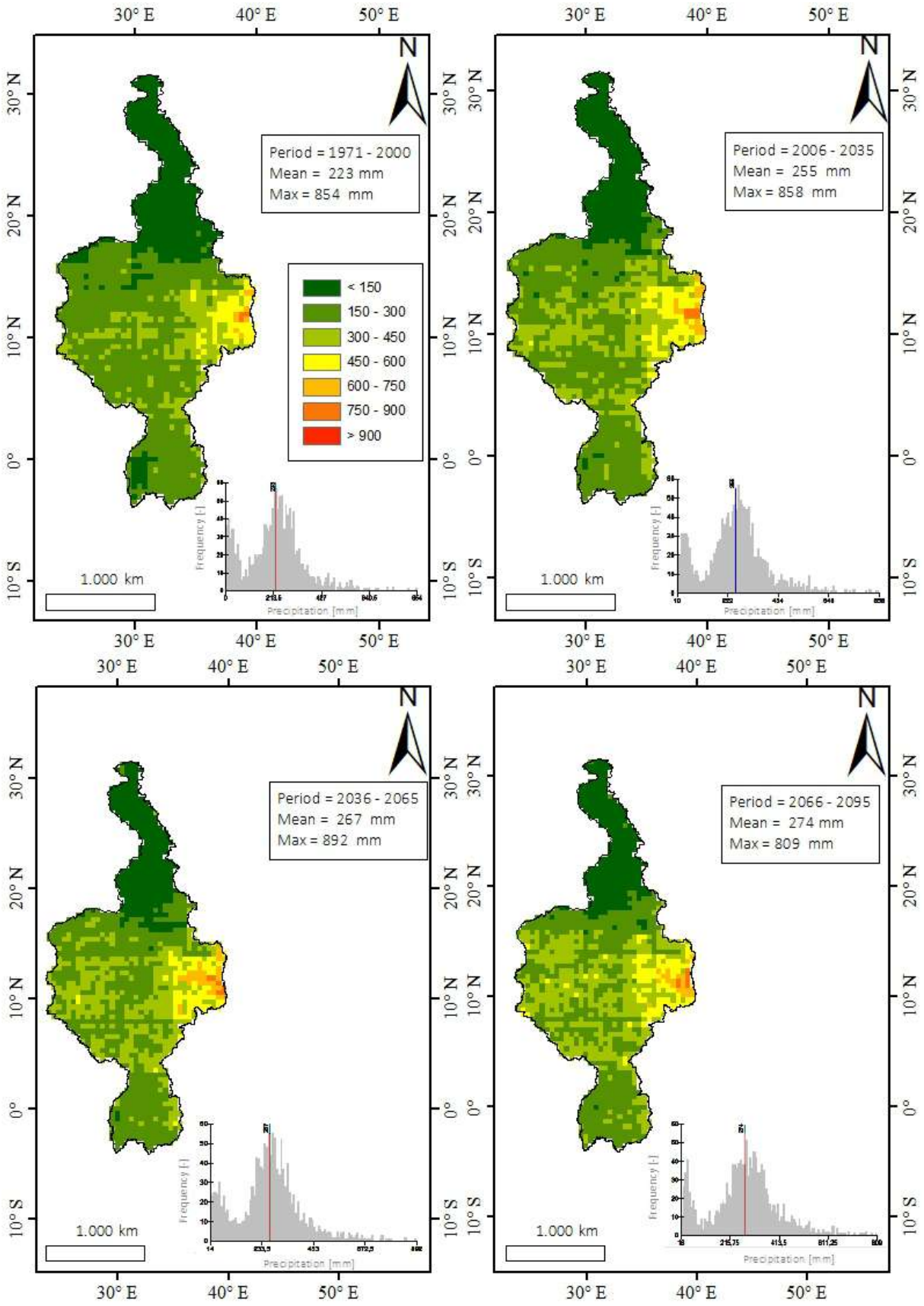

Figure 43: IDF grid map (Model No. = BCCR_WRF331NCC_NorESM1_M, RCP scenario = 4.5, Duration = 6 day, Frequency = 100 year).

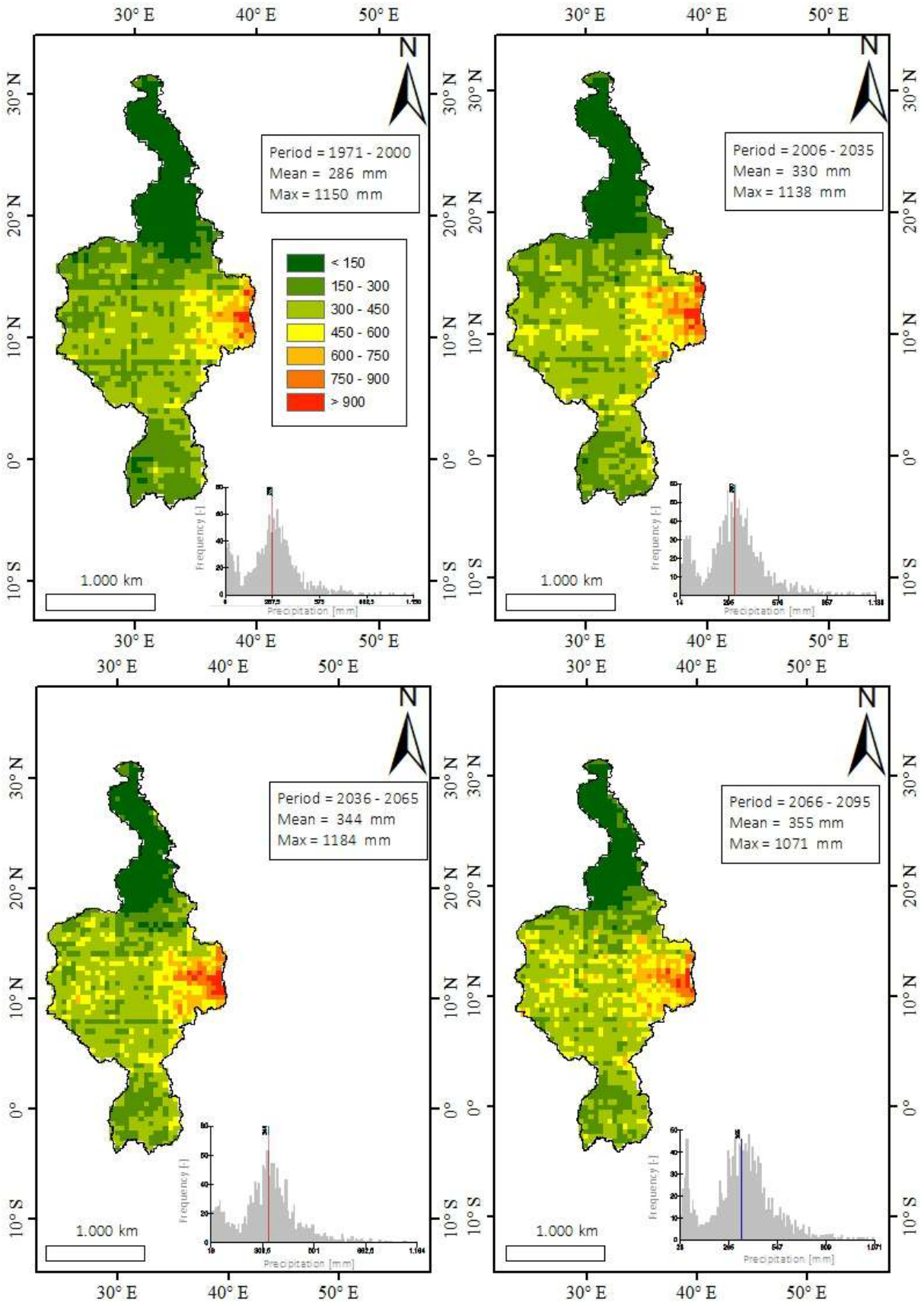

Figure 44: IDF grid map (Model No. = BCCR_WRF331NCC_NorESM1_M , RCP scenario = 4.5, Duration = 6 day, Frequency = 1000 year).

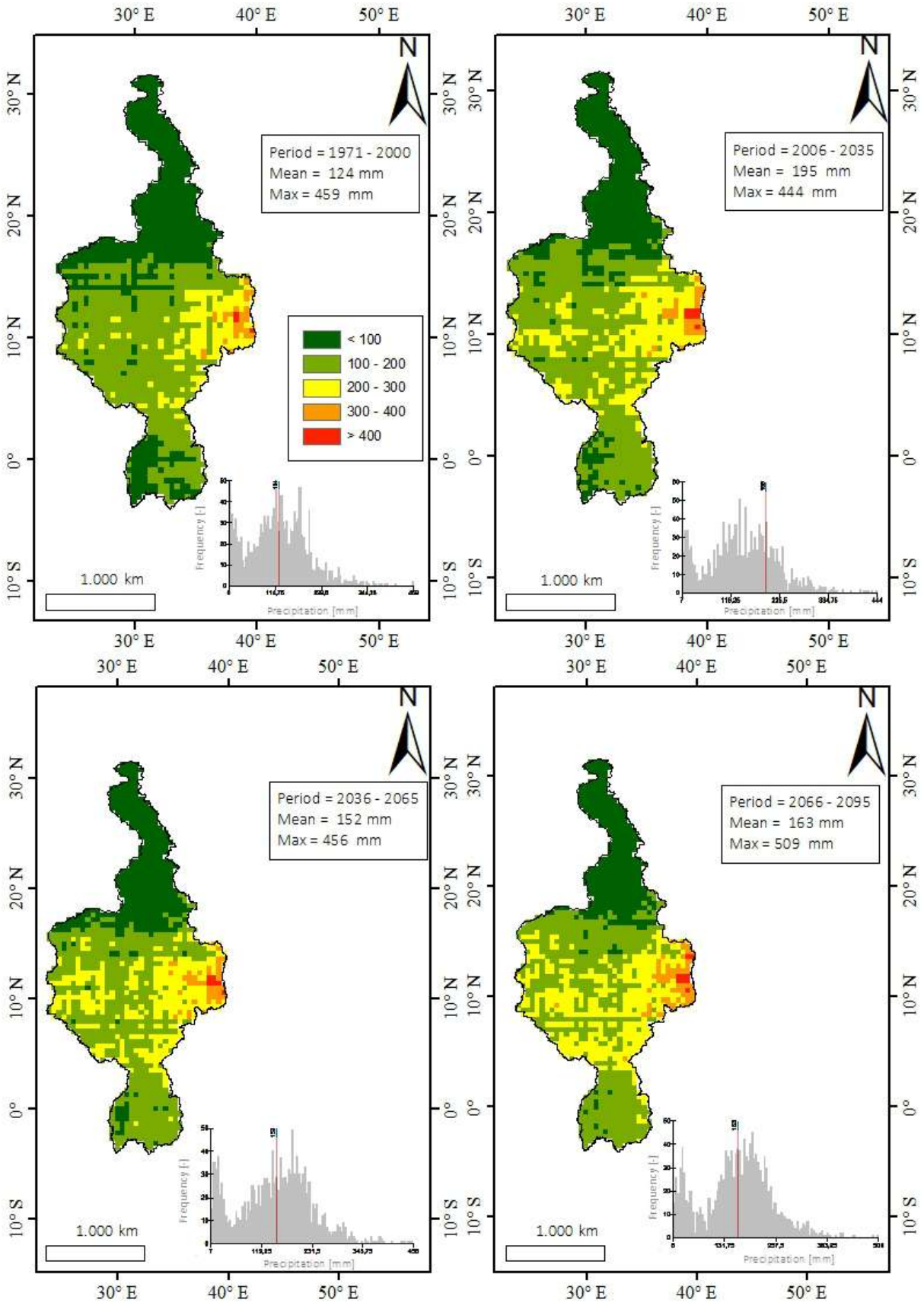

Figure 45: IDF grid map (Model No. = BCCR_WRF331NCC_NorESM1_M , RCP scenario = 8.5, Duration = 1 day, Frequency = 100 year).

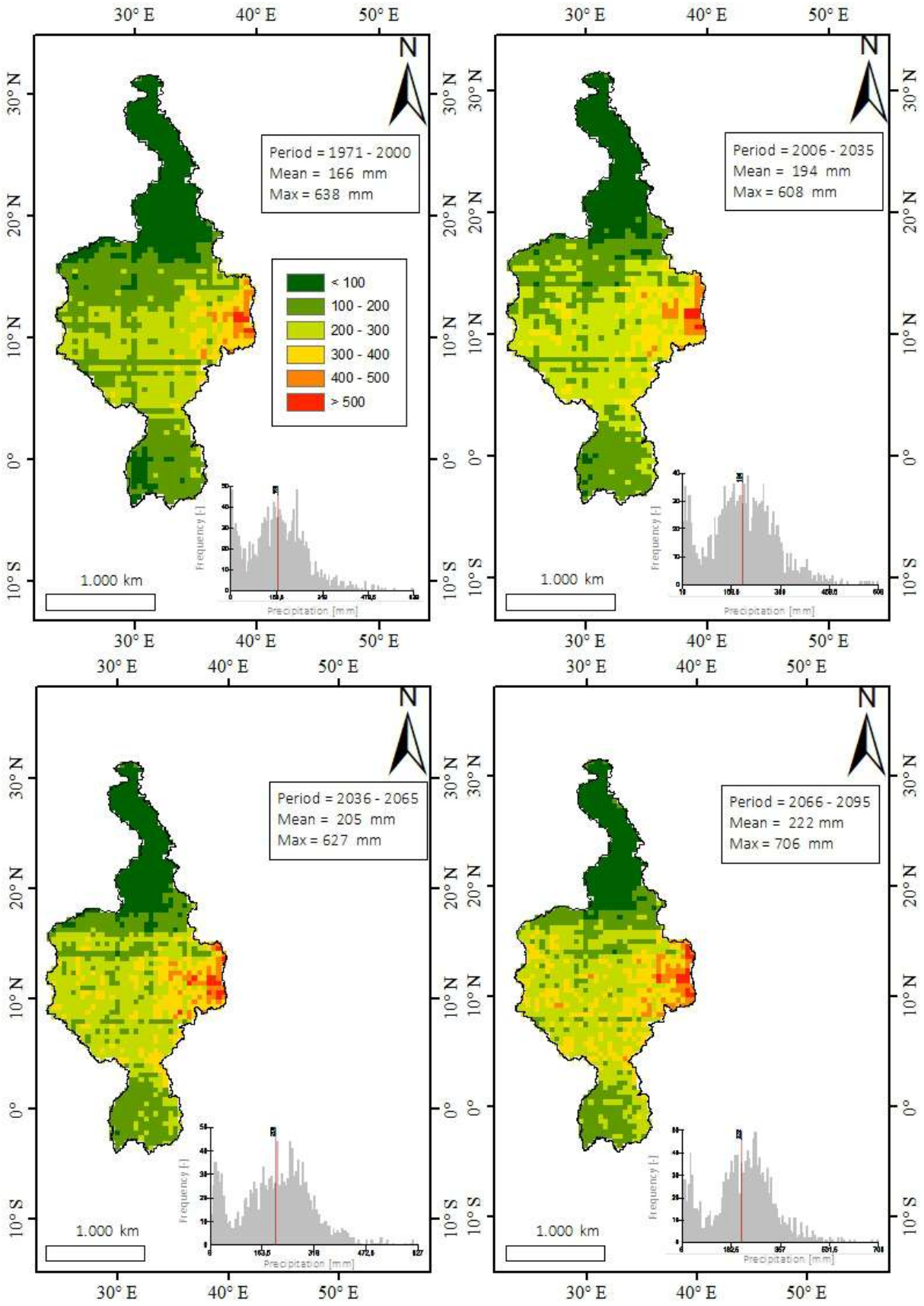

Figure 46: IDF grid map (Model No. = BCCR_WRF331NCC_NorESM1_M , RCP scenario = 8.5, Duration = 1 day, Frequency = 1000 year).

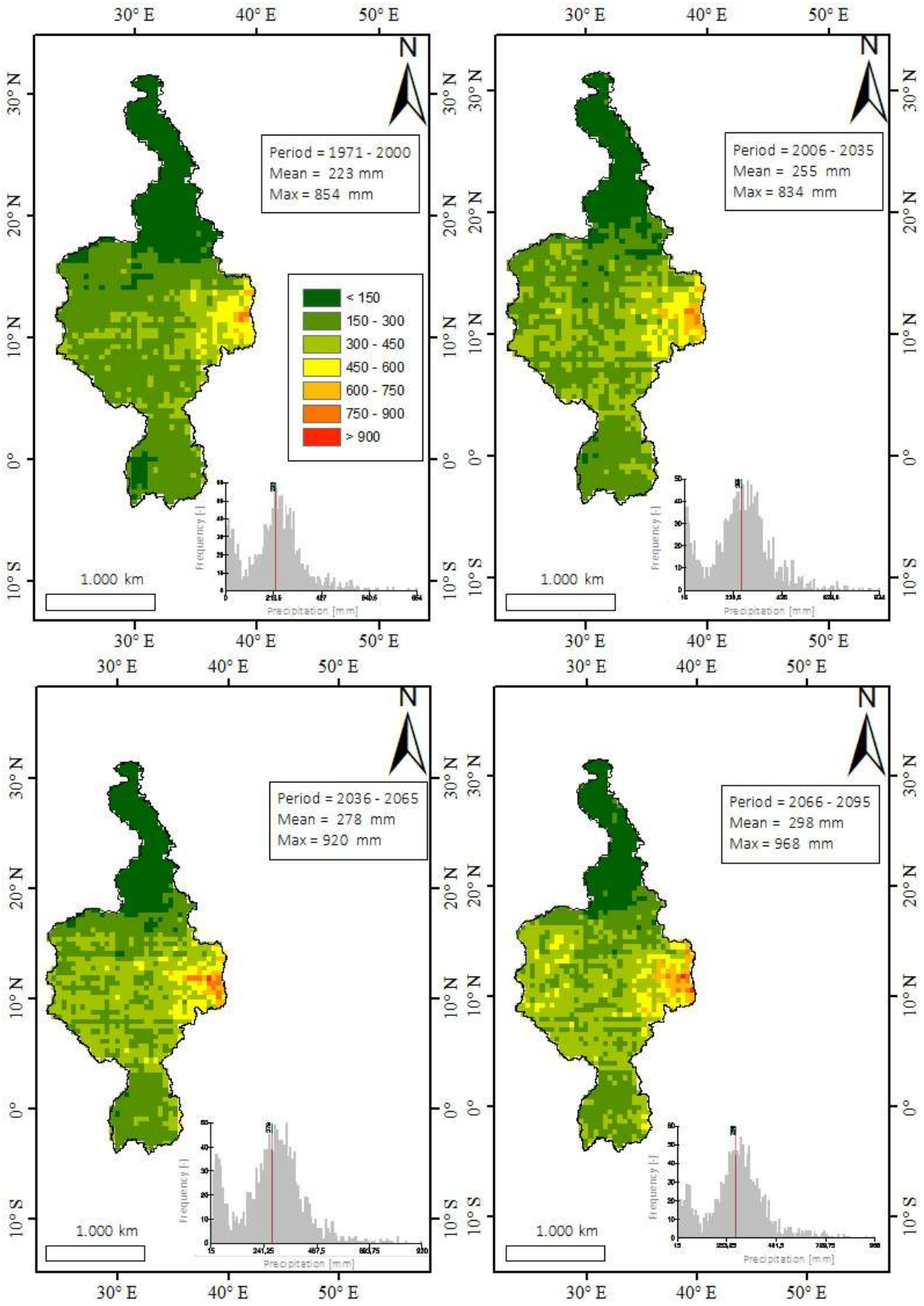

Figure 47: IDF grid map (Model No. = BCCR_WRF331NCC_NorESM1_M , RCP scenario = 8.5, Duration = 6 day, Frequency = 100 year).

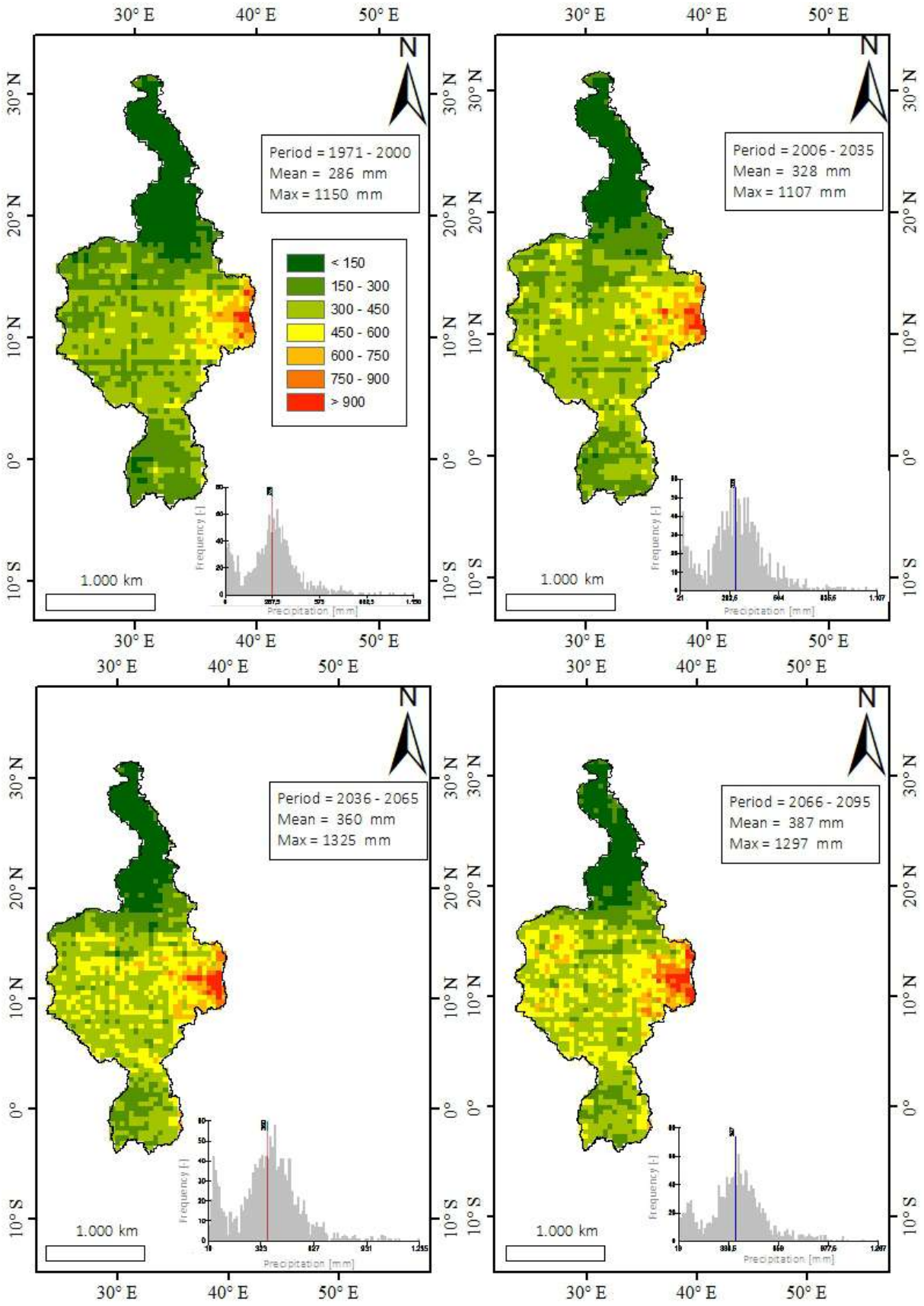

Figure 48: IDF grid map (Model No. = BCCR_WRF331NCC_NorESM1_M , RCP scenario = 8.5, Duration = 6 day, Frequency = 1000 year).

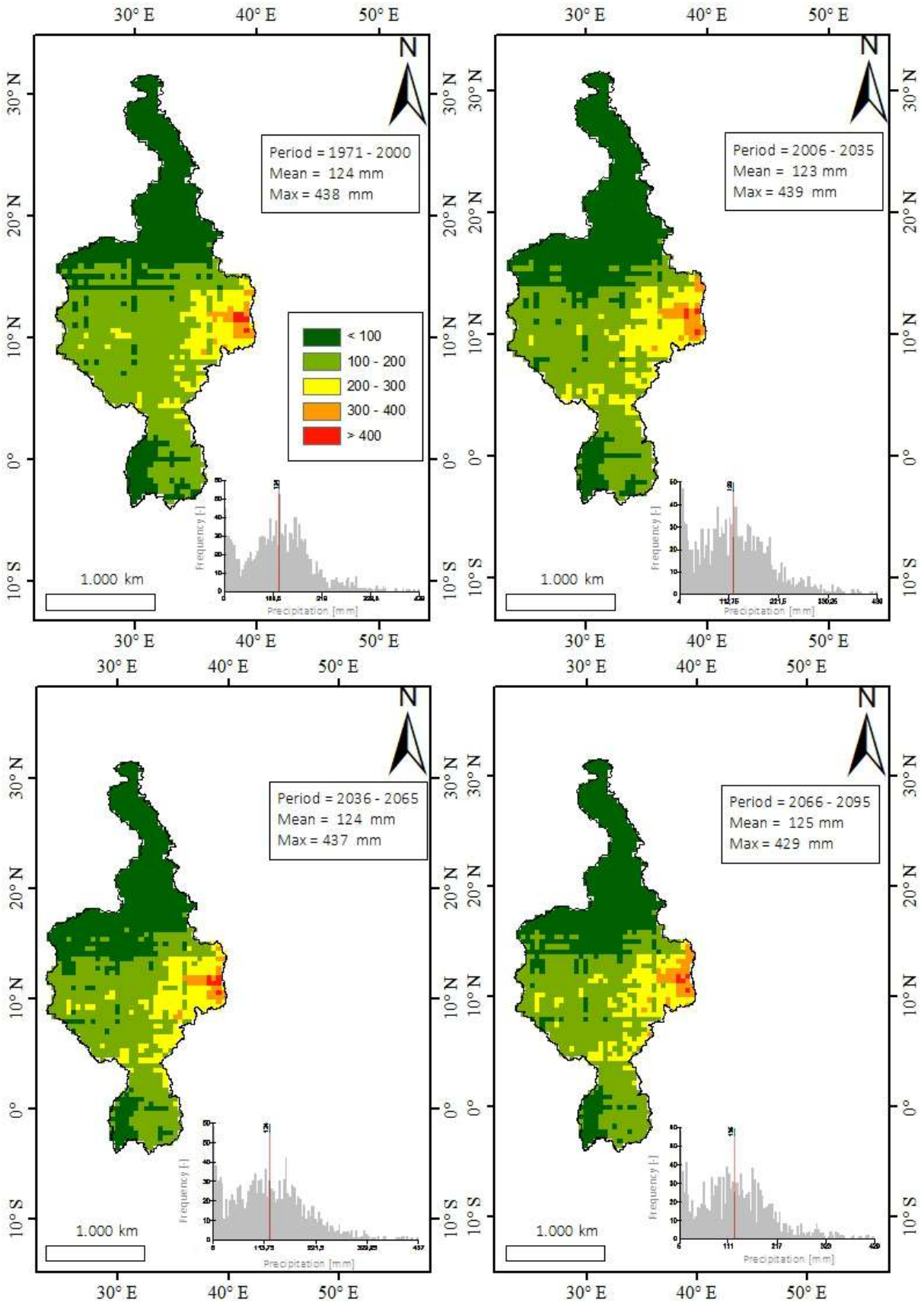

Figure 49: IDF grid map (Model No. = SMHI_RCA4MOHC_HadGEM2, RCP scenario = 4.5, Duration = 1 day, Frequency = 100 year).

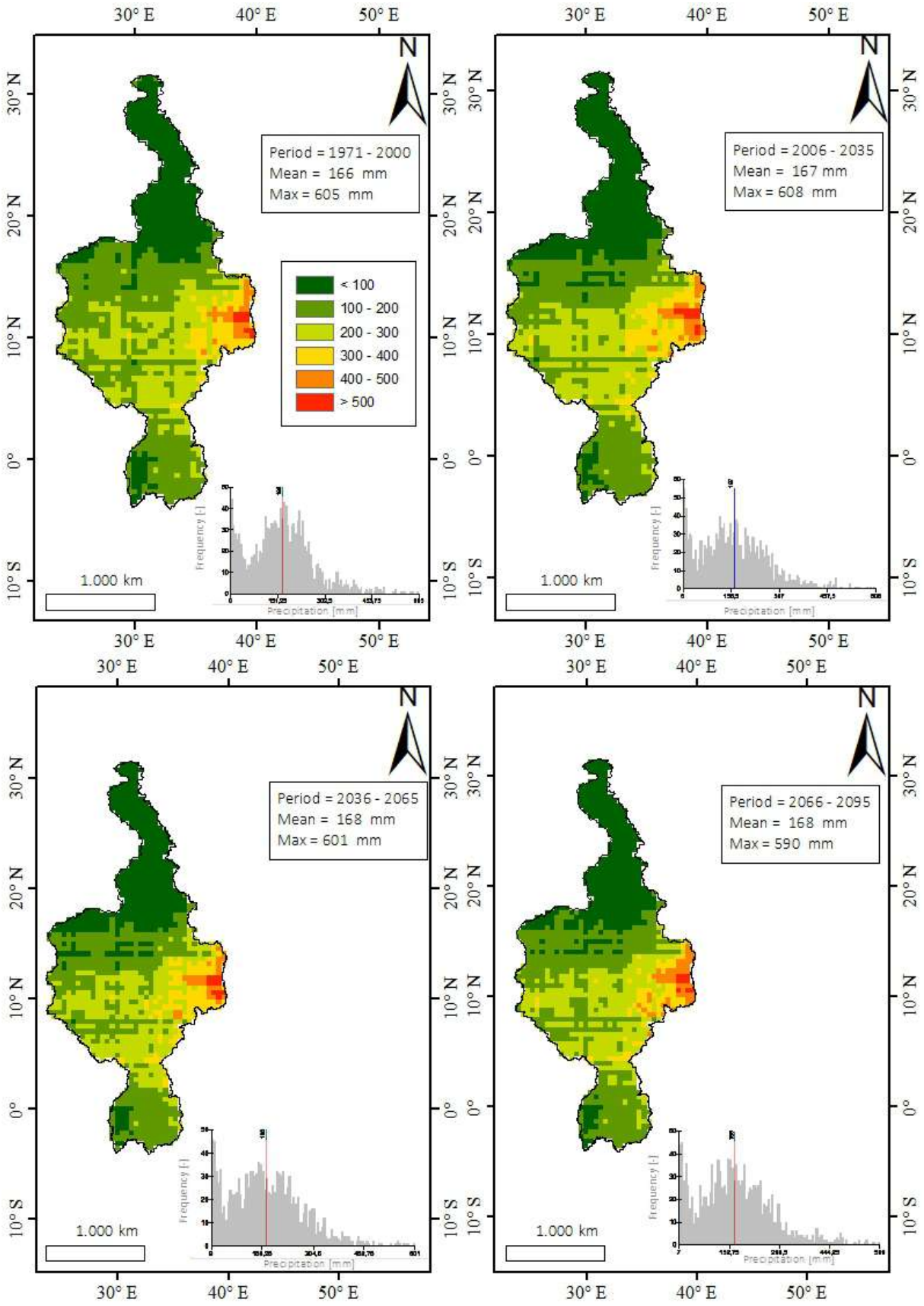

Figure 50: IDF grid map (Model No. = SMHI_RCA4MOHC_HadGEM2, RCP scenario = 4.5, Duration = 1 day, Frequency = 1000 year).

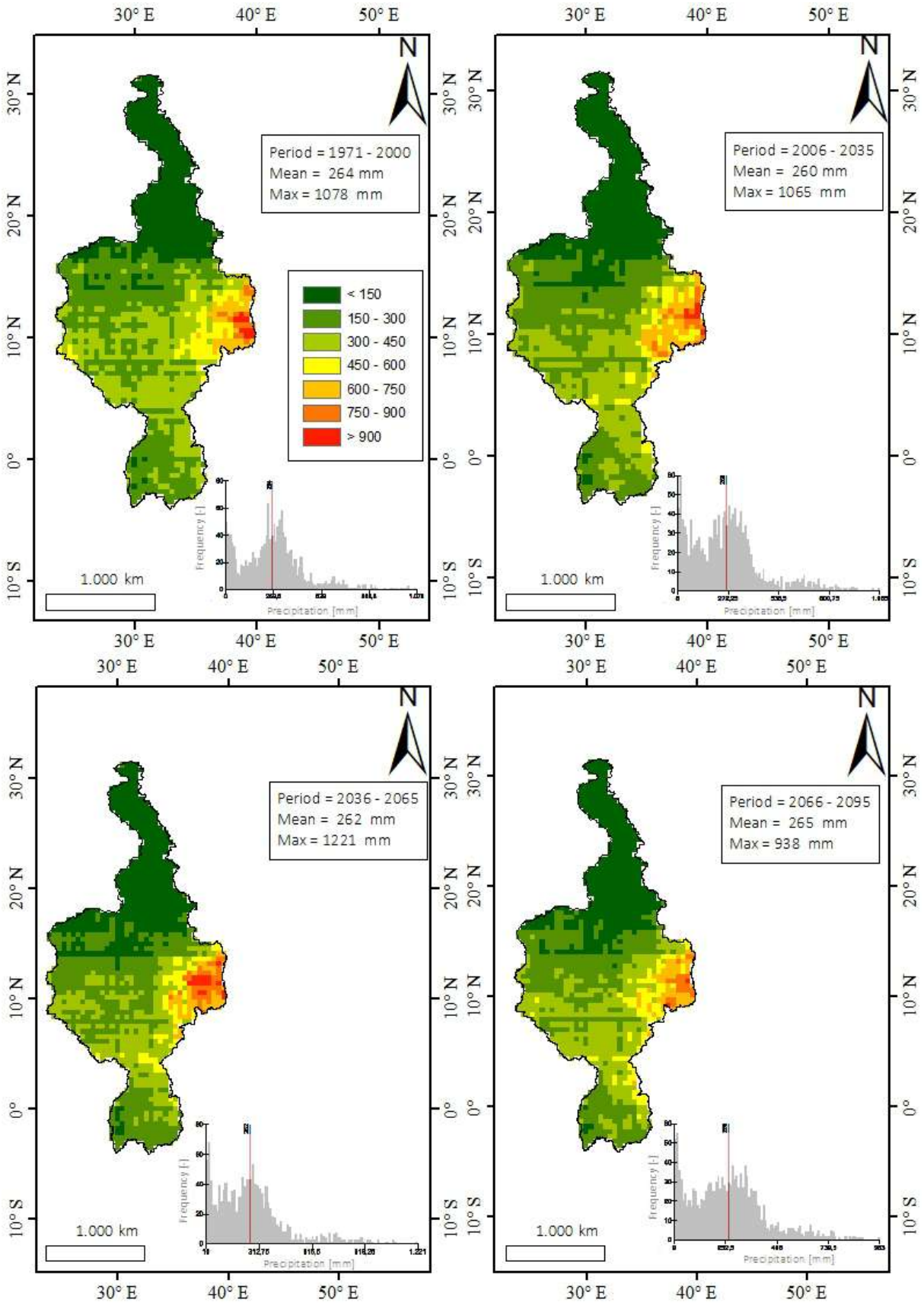

Figure 51: IDF grid map (Model No. = SMHI_RCA4MOHC_HadGEM2, RCP scenario = 4.5, Duration = 6 day, Frequency = 100 year).

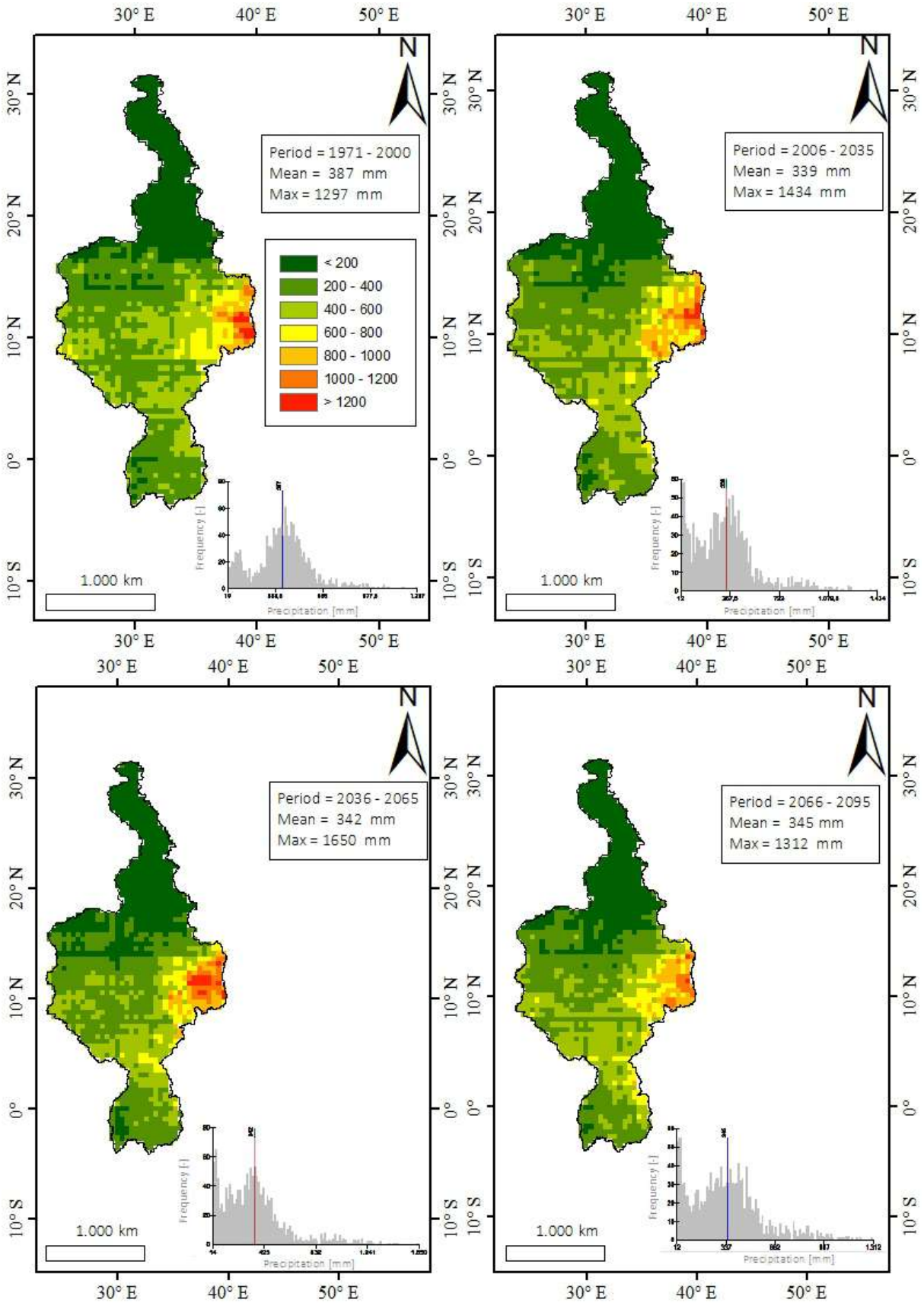

Figure 52: IDF grid map (Model No. = SMHI_RCA4MOHC_HadGEM2, RCP scenario = 4.5, Duration = 6 day, Frequency = 1000 year).

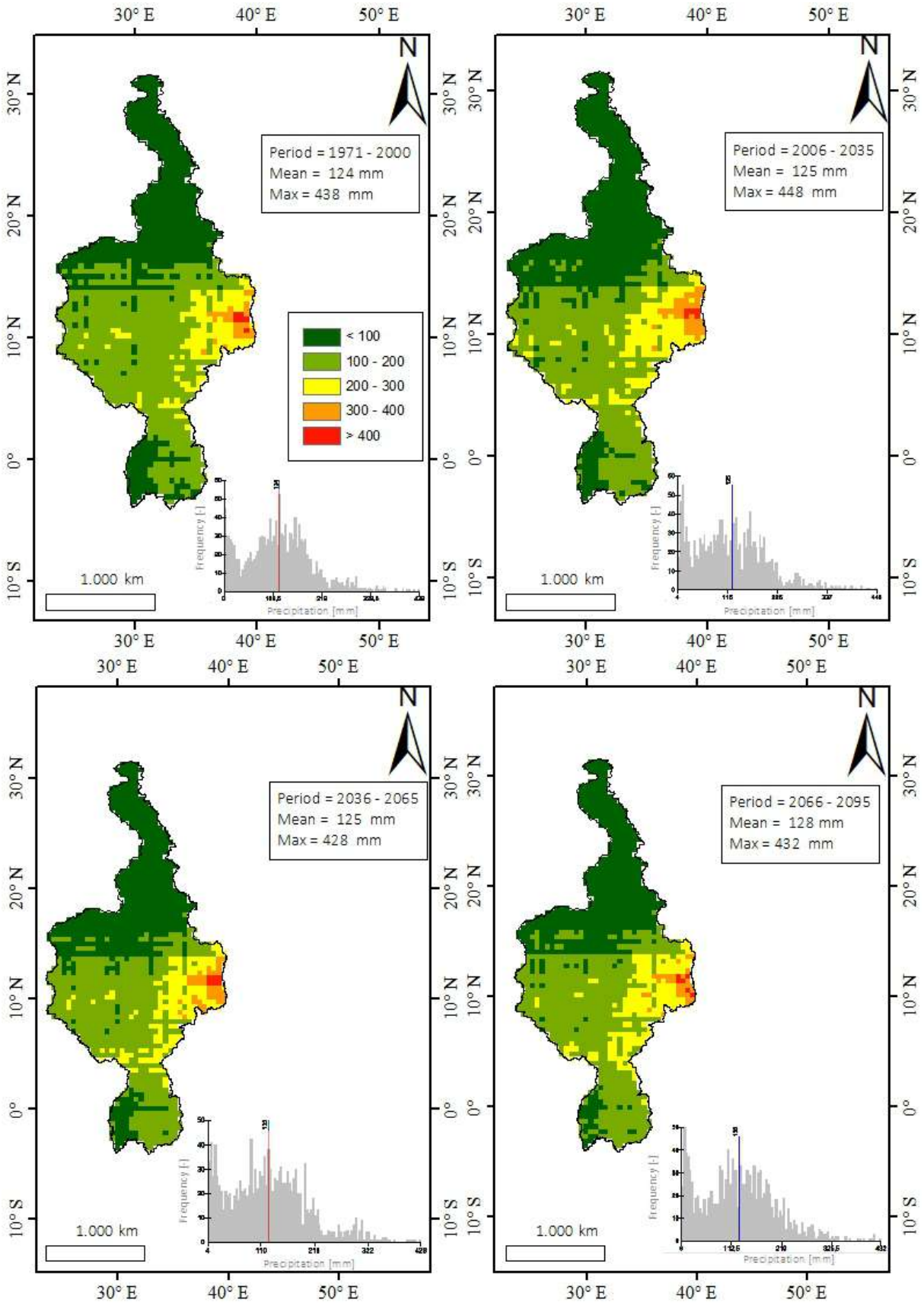

Figure 53: IDF grid map (Model No. = SMHI_RCA4MOHC_HadGEM2, RCP scenario = 8.5, Duration = 1 day, Frequency = 100 year).

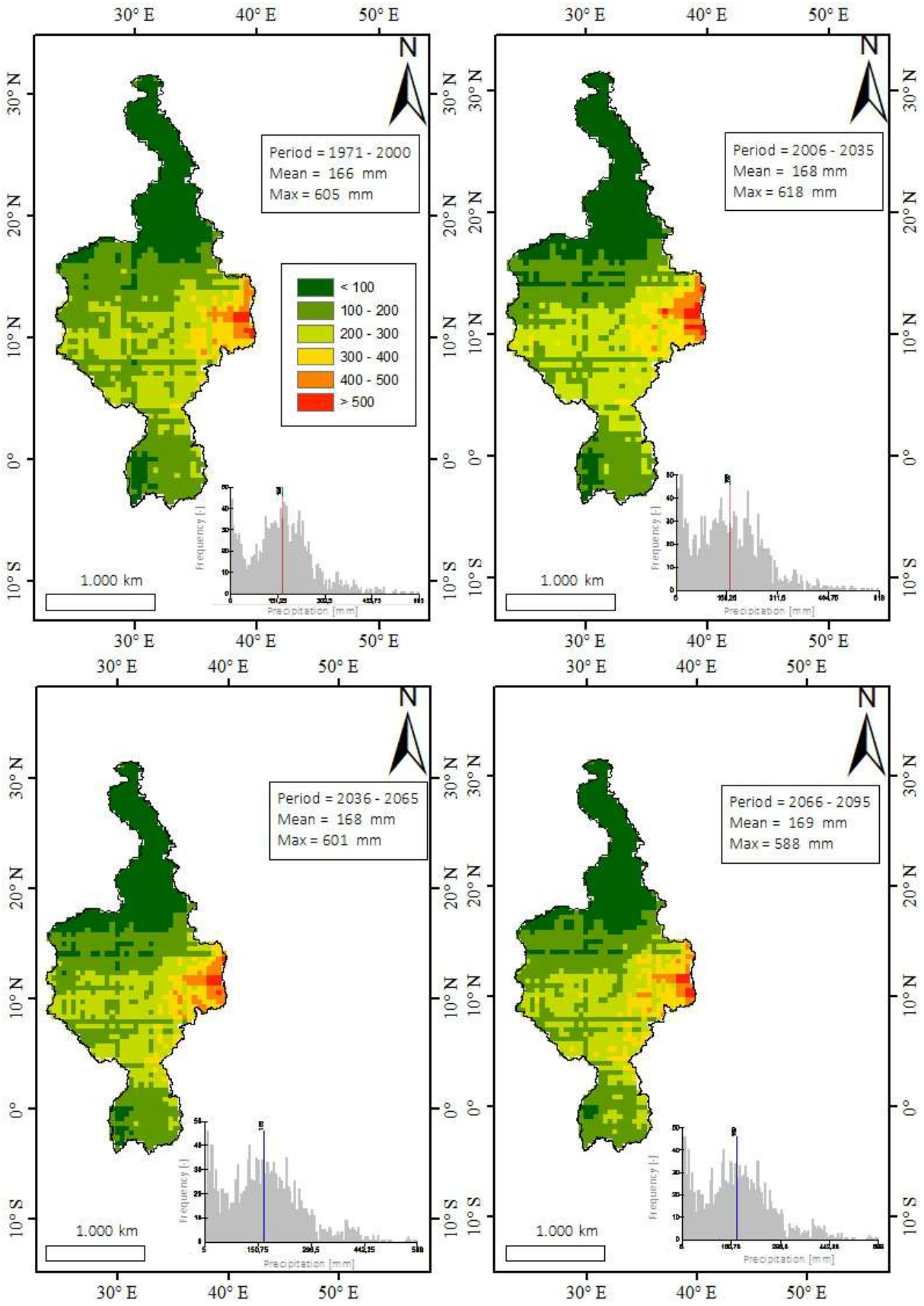

Figure 54: IDF grid map (Model No. = SMHI_RCA4MOHC_HadGEM2, RCP scenario = 8.5, Duration = 1 day, Frequency = 1000 year).

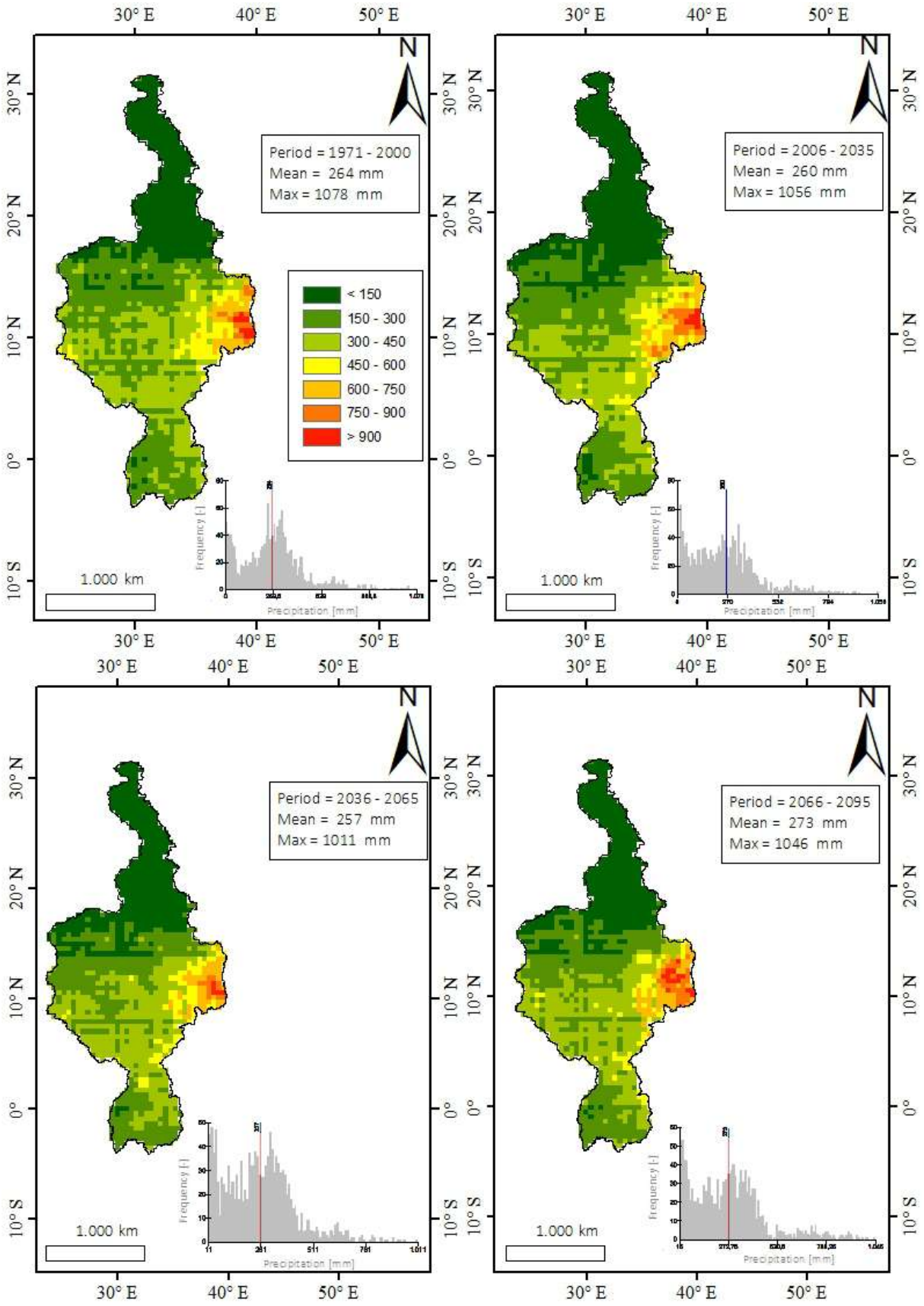

Figure 55: IDF grid map (Model No. = SMHI_RCA4MOHC_HadGEM2, RCP scenario = 8.5, Duration = 6 day, Frequency = 100 year).

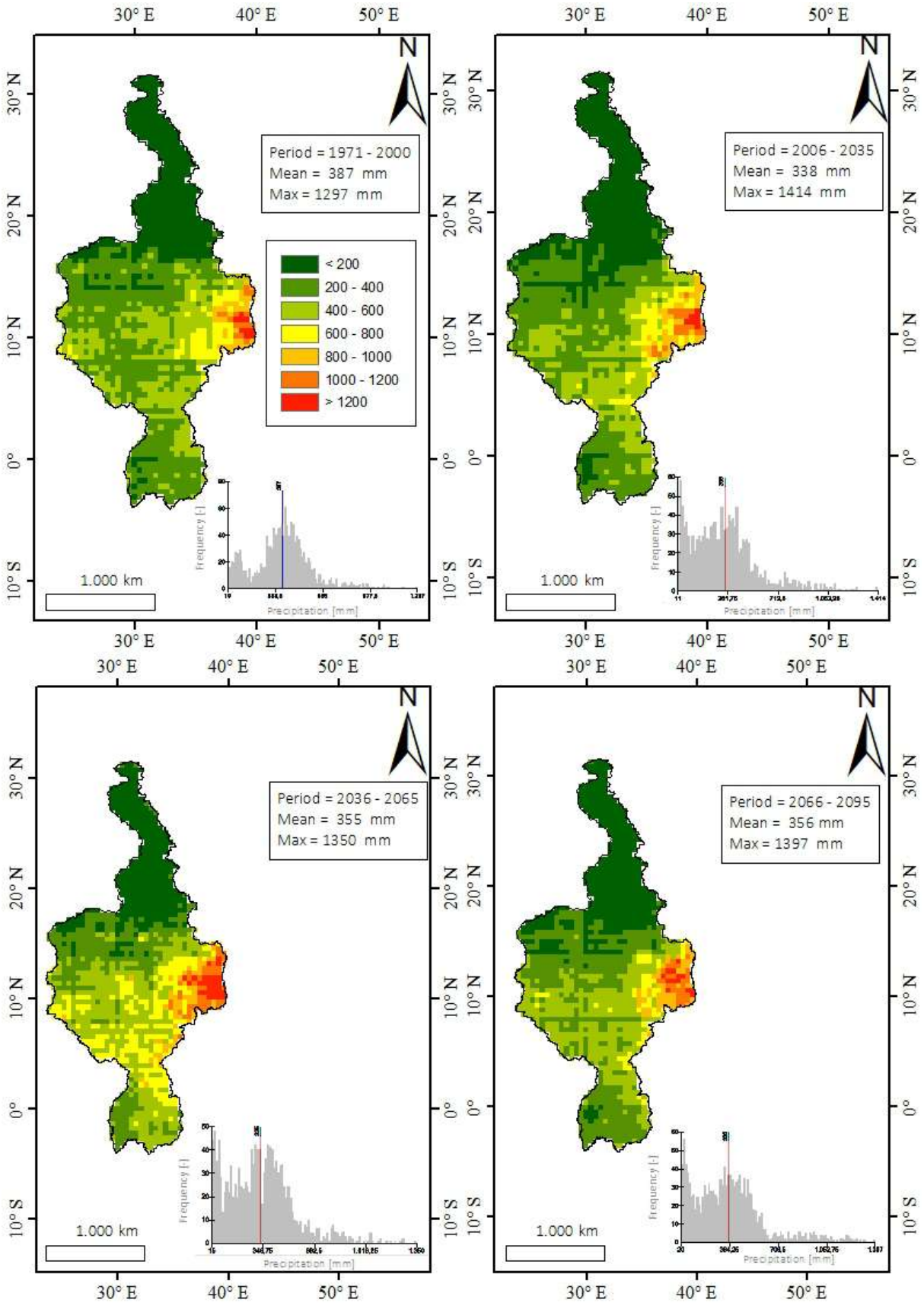

Figure 56: IDF grid map (Model No. = SMHI_RCA4MOHC_HadGEM2, RCP scenario = 8.5, Duration = 6 day, Frequency = 1000 year).

11 ANNEX – IDF CLUSTER MAPS

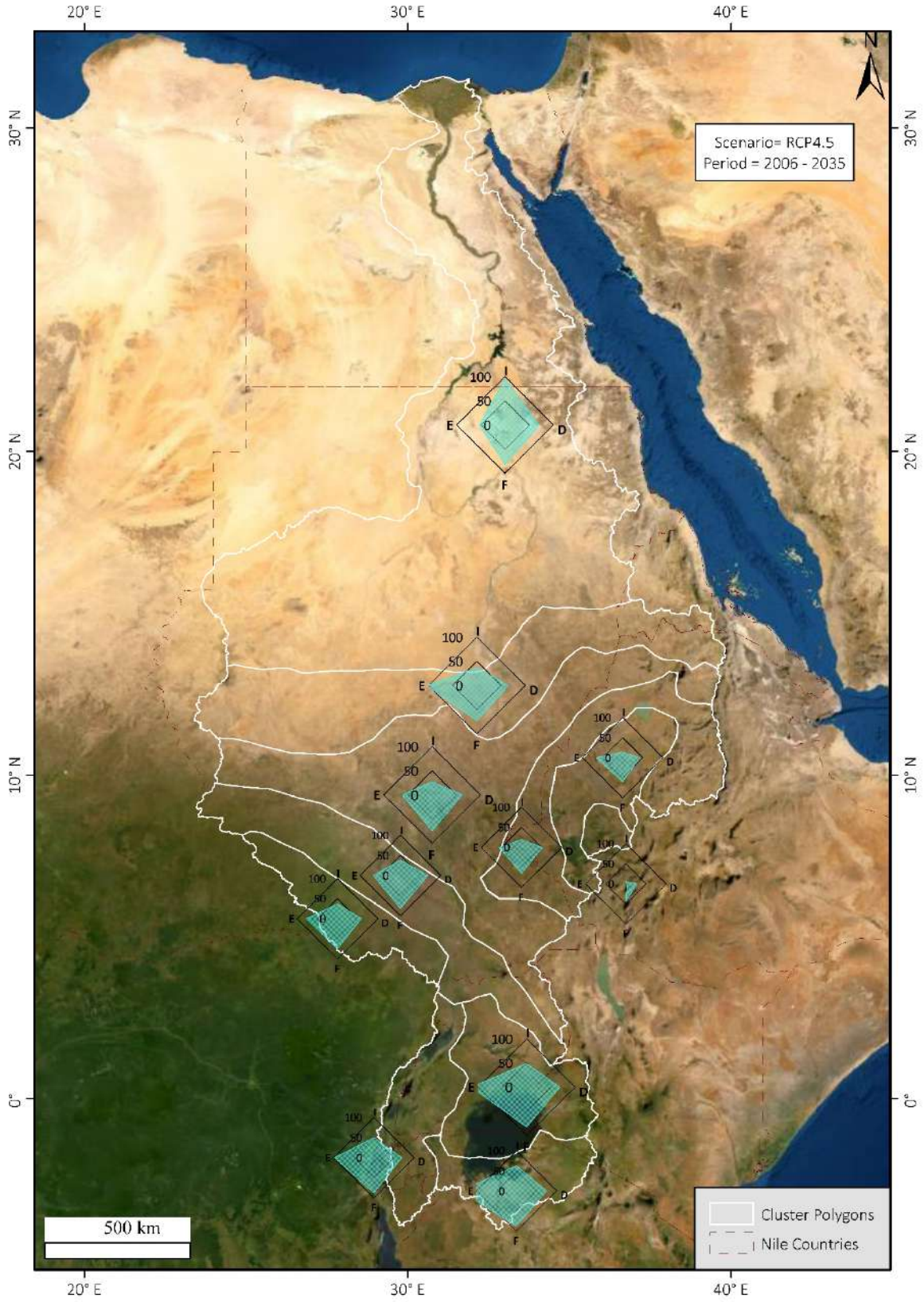

Figure 57: Cluster map (Model = BCCR_WRF331NCC_NorESM1_M, RCP scenario = 4.5, period = 2006-2035).

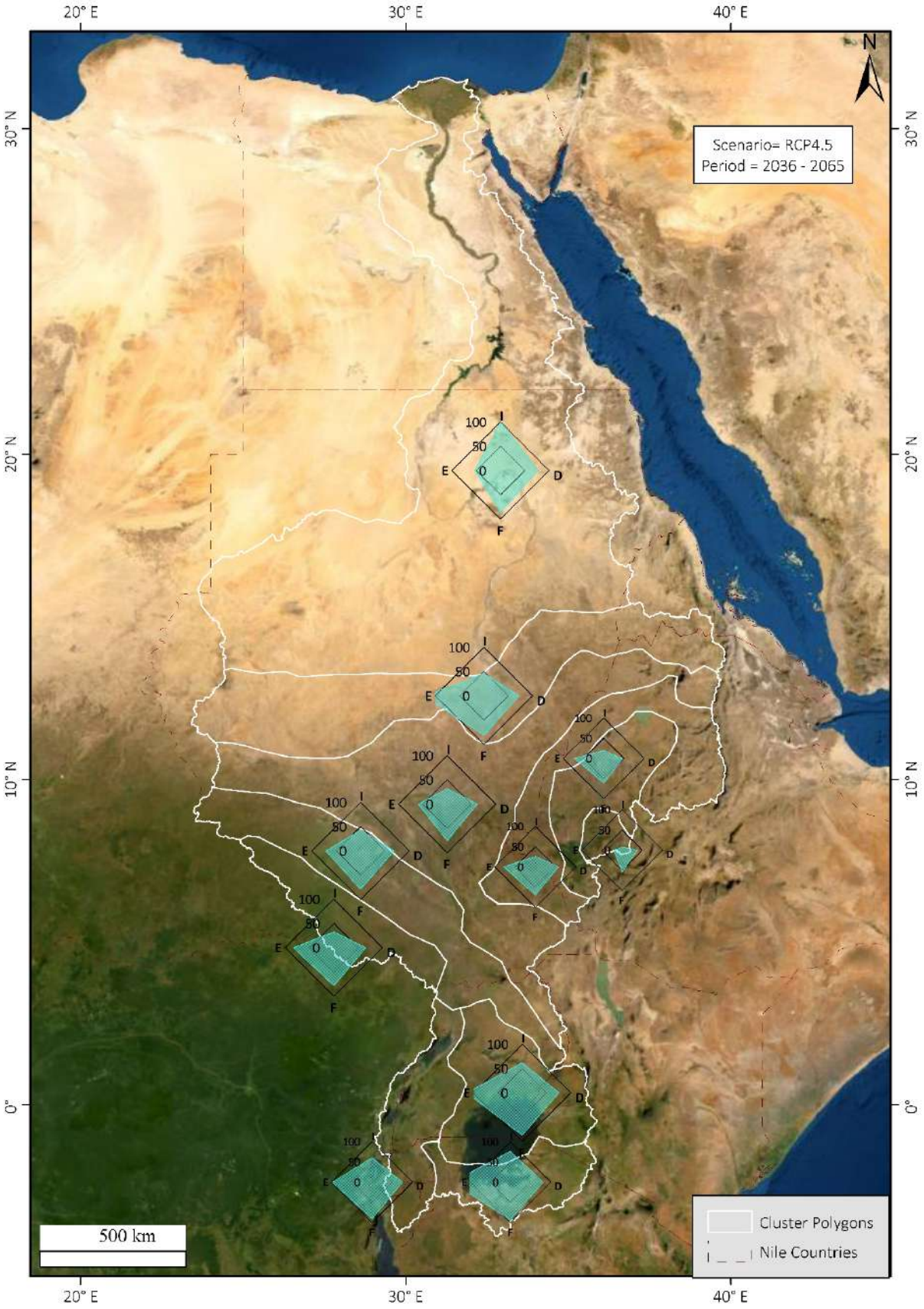

Figure 58: Cluster map (Model = BCCR_WRF331NCC_NorESM1_M, RCP scenario = 4.5, period = 2036-2065).

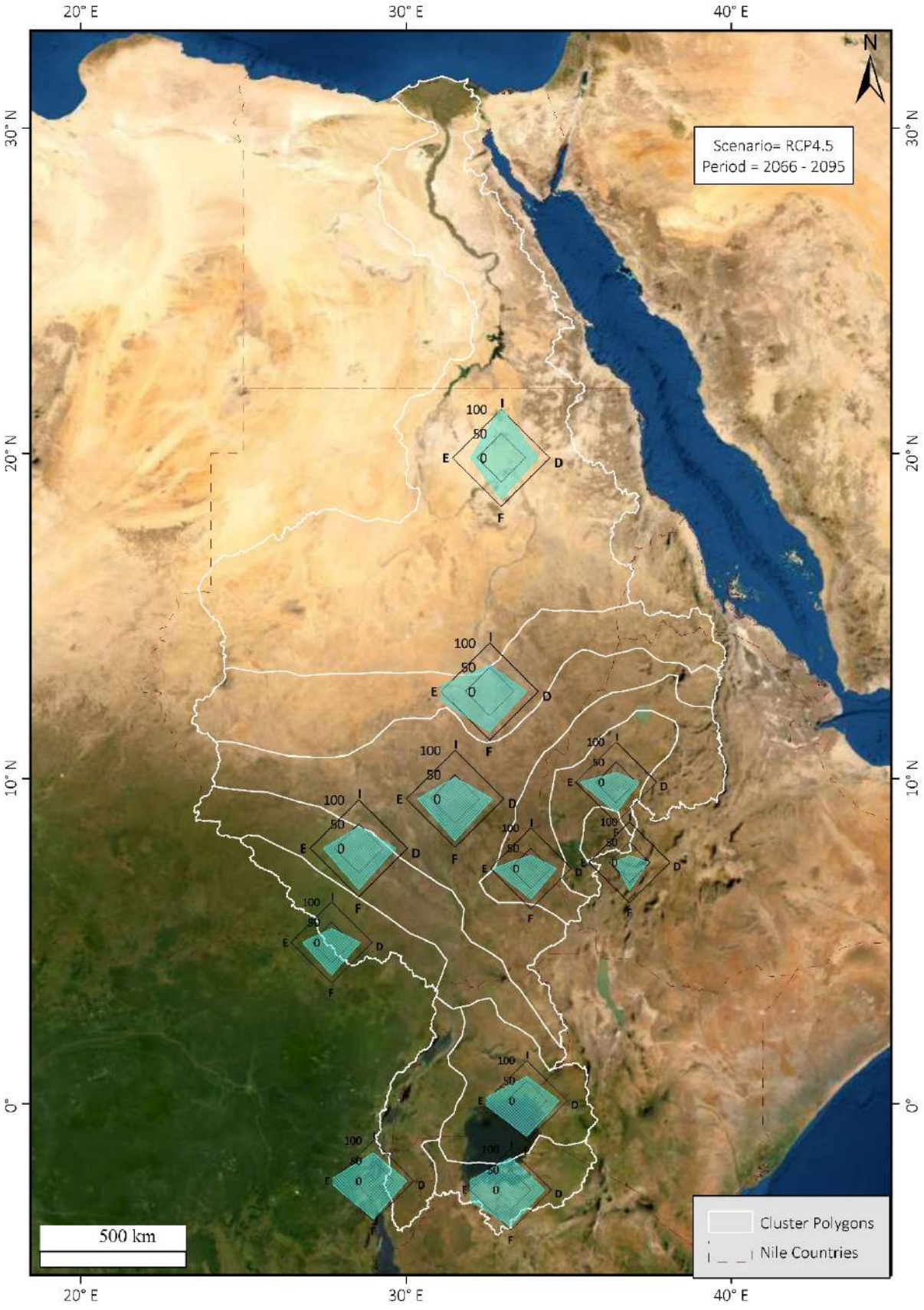

Figure 59: Cluster map (Model = BCCR_WRF331NCC_NorESM1_M , RCP scenario = 4.5, period = 2066-2095).

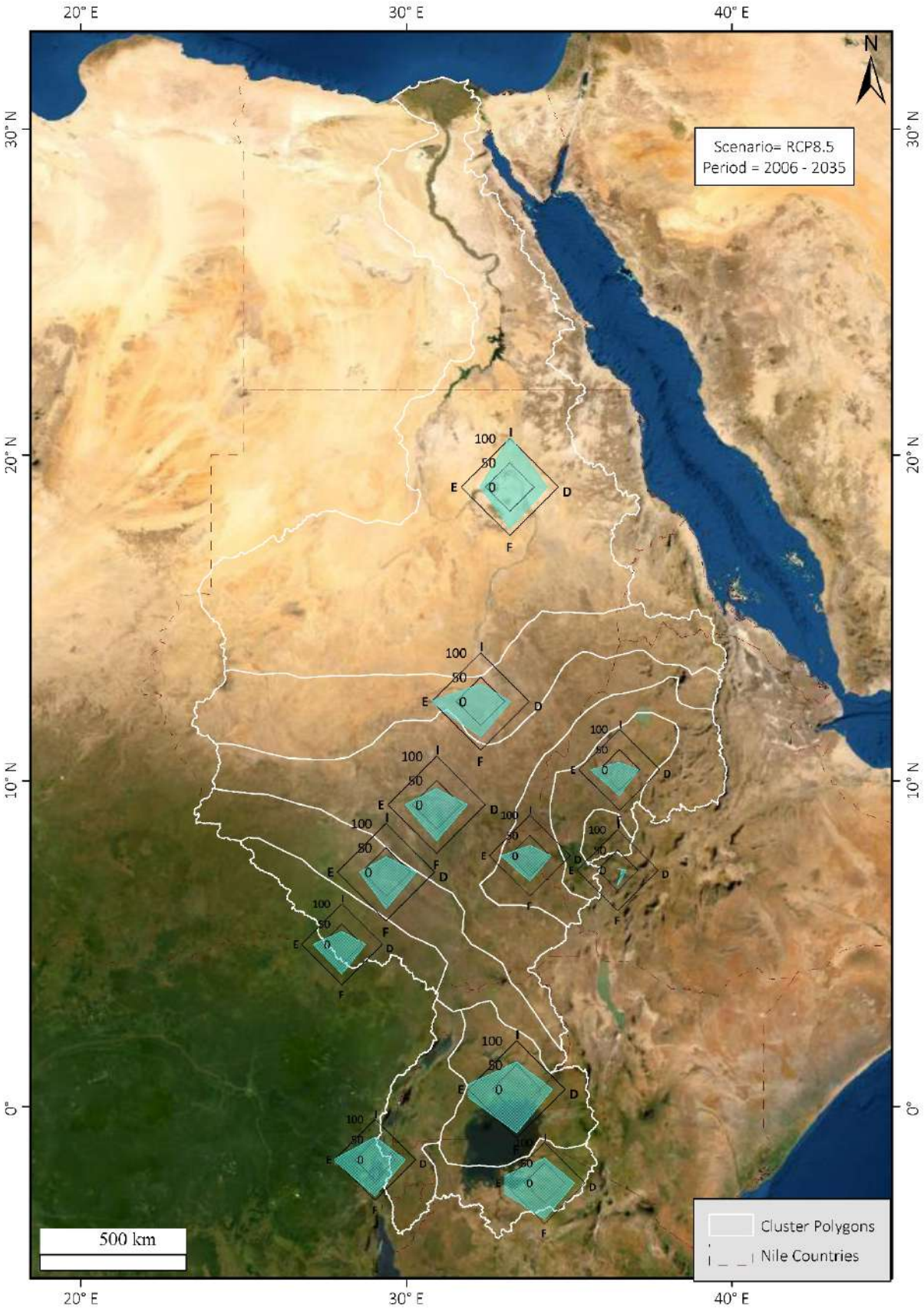

Figure 60: Cluster map (Model = BCCR_WRF331NCC_NorESM1_M , RCP scenario = 8.5, period = 2006-2035).

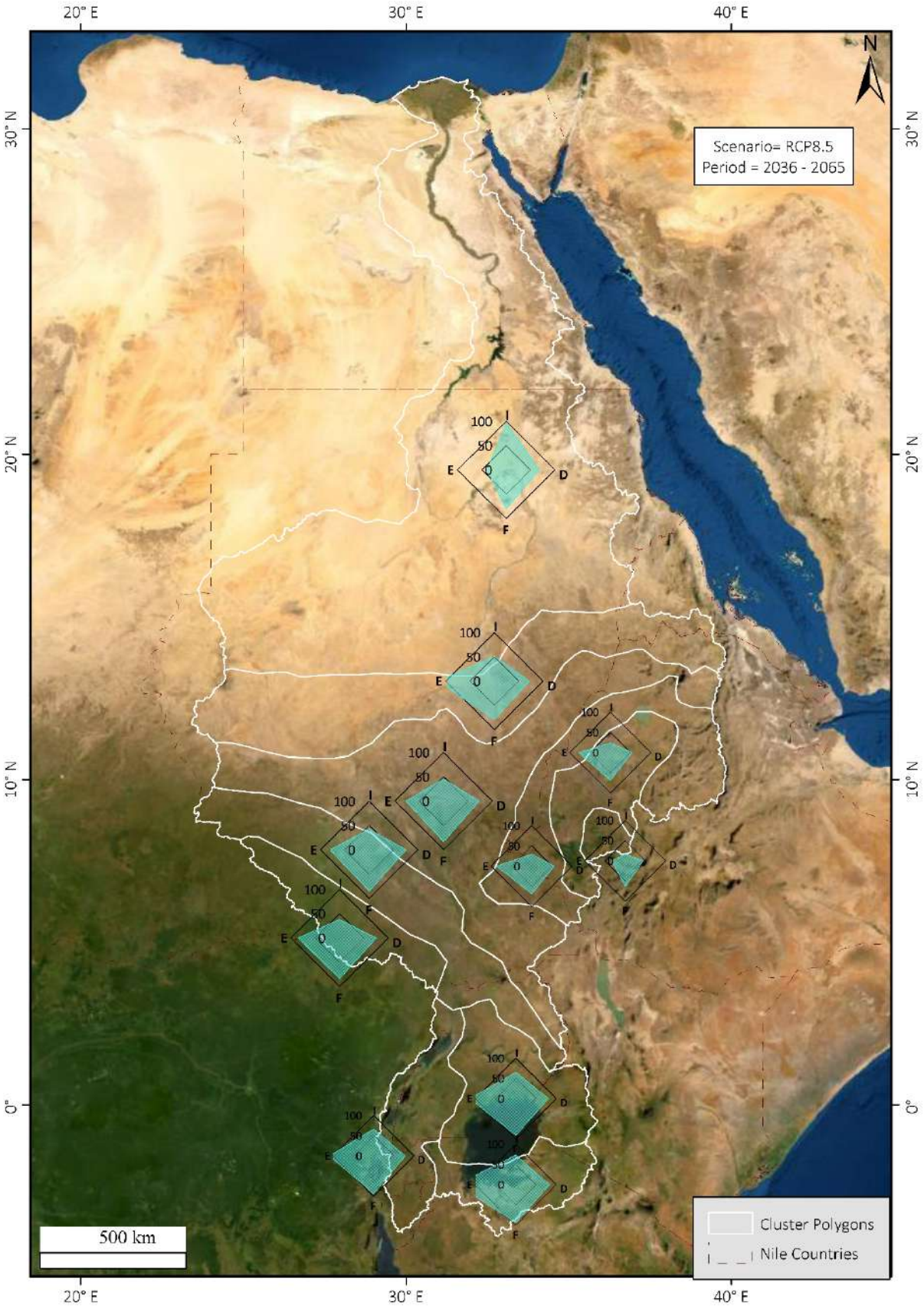

Figure 61: Cluster map (Model = BCCR_WRF331NCC_NorESM1_M , RCP scenario = 8.5, period = 2036-2065).

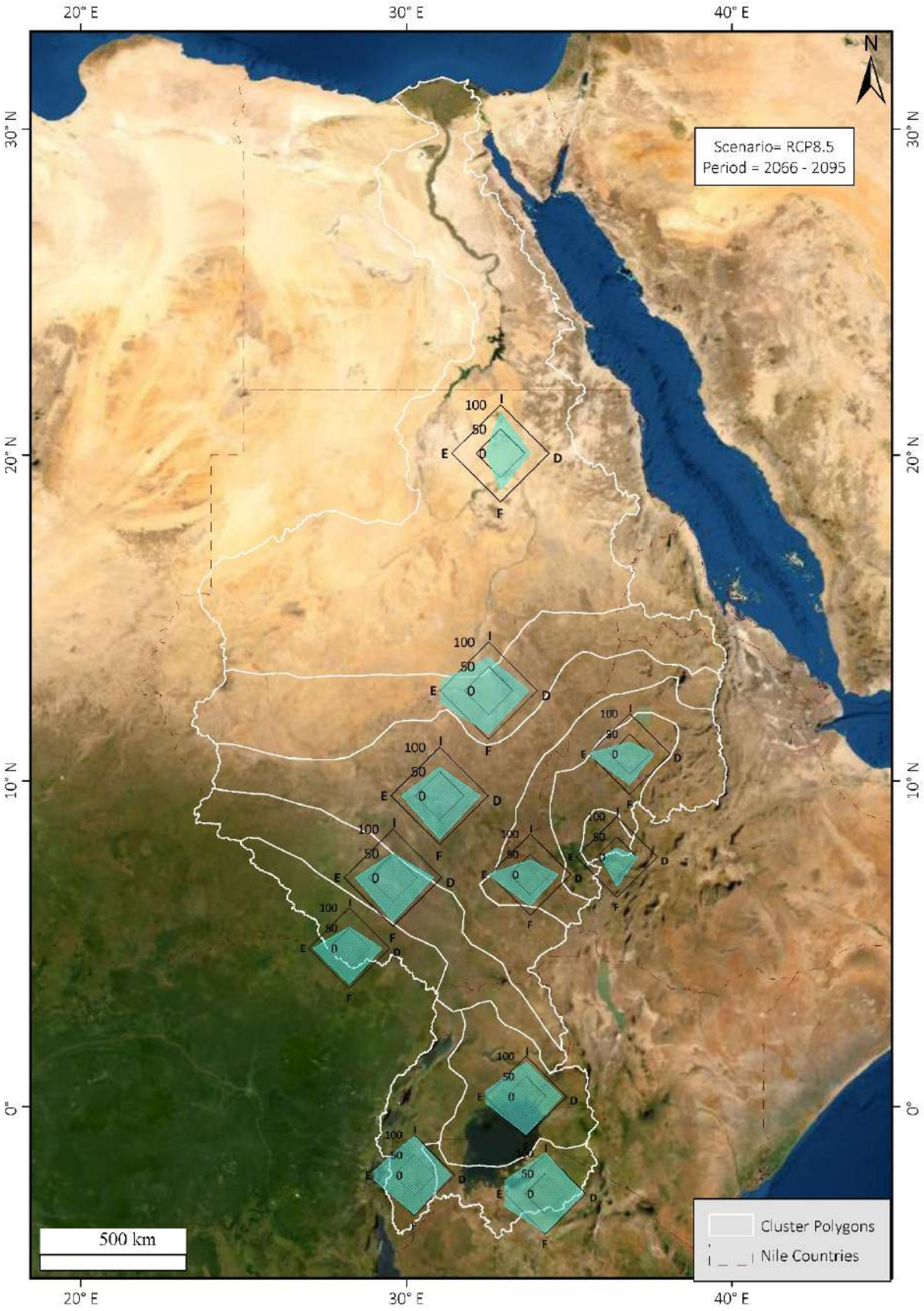

Figure 62: Cluster map (Model = BCCR_WRF331NCC_NorESM1_M , RCP scenario = 8.5, period = 2066-2095).

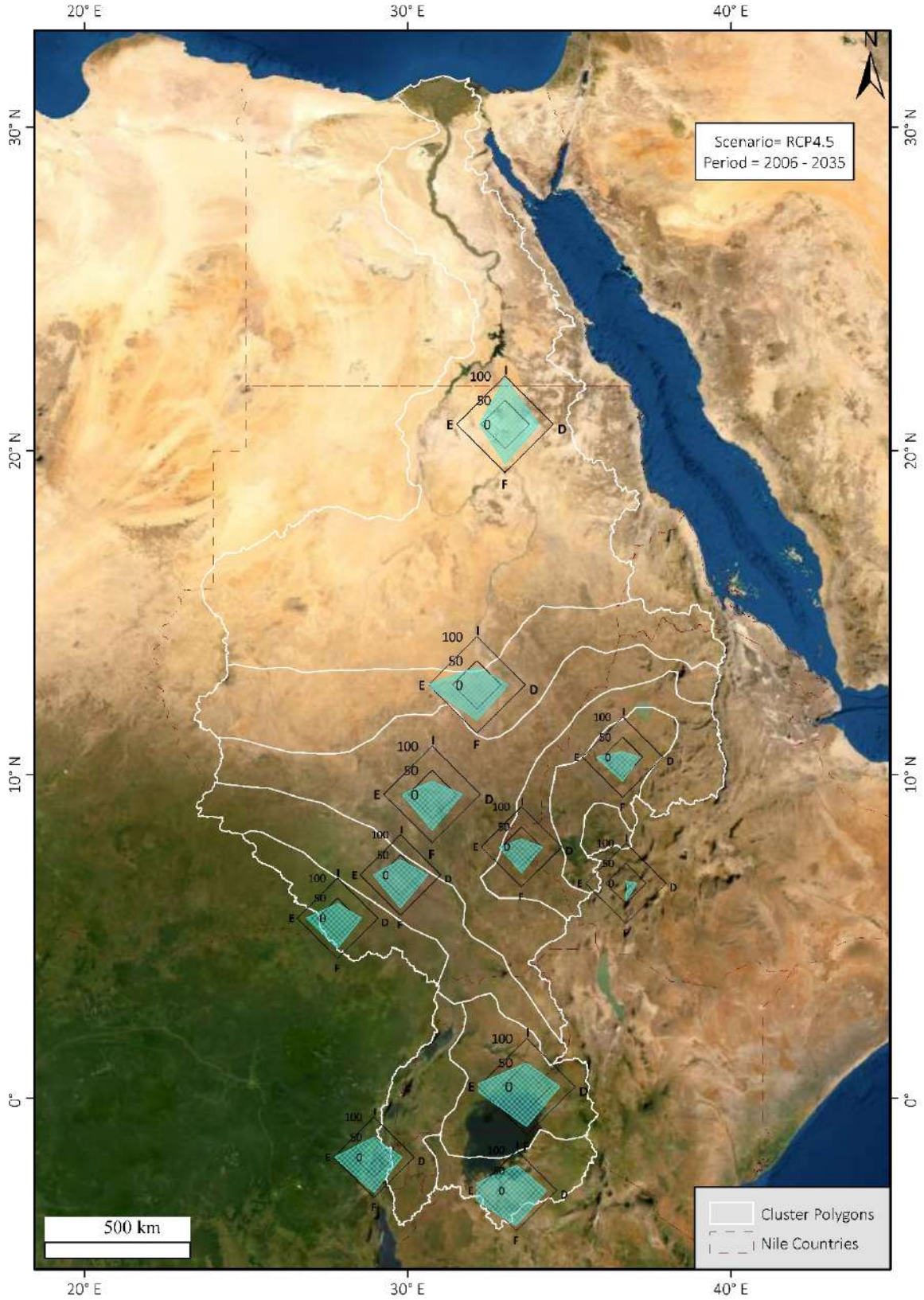

Figure 63: Cluster map (Model = SMHI_RCA4MOHC_HadGEM2, RCP scenario = 4.5, period = 2006-2035).

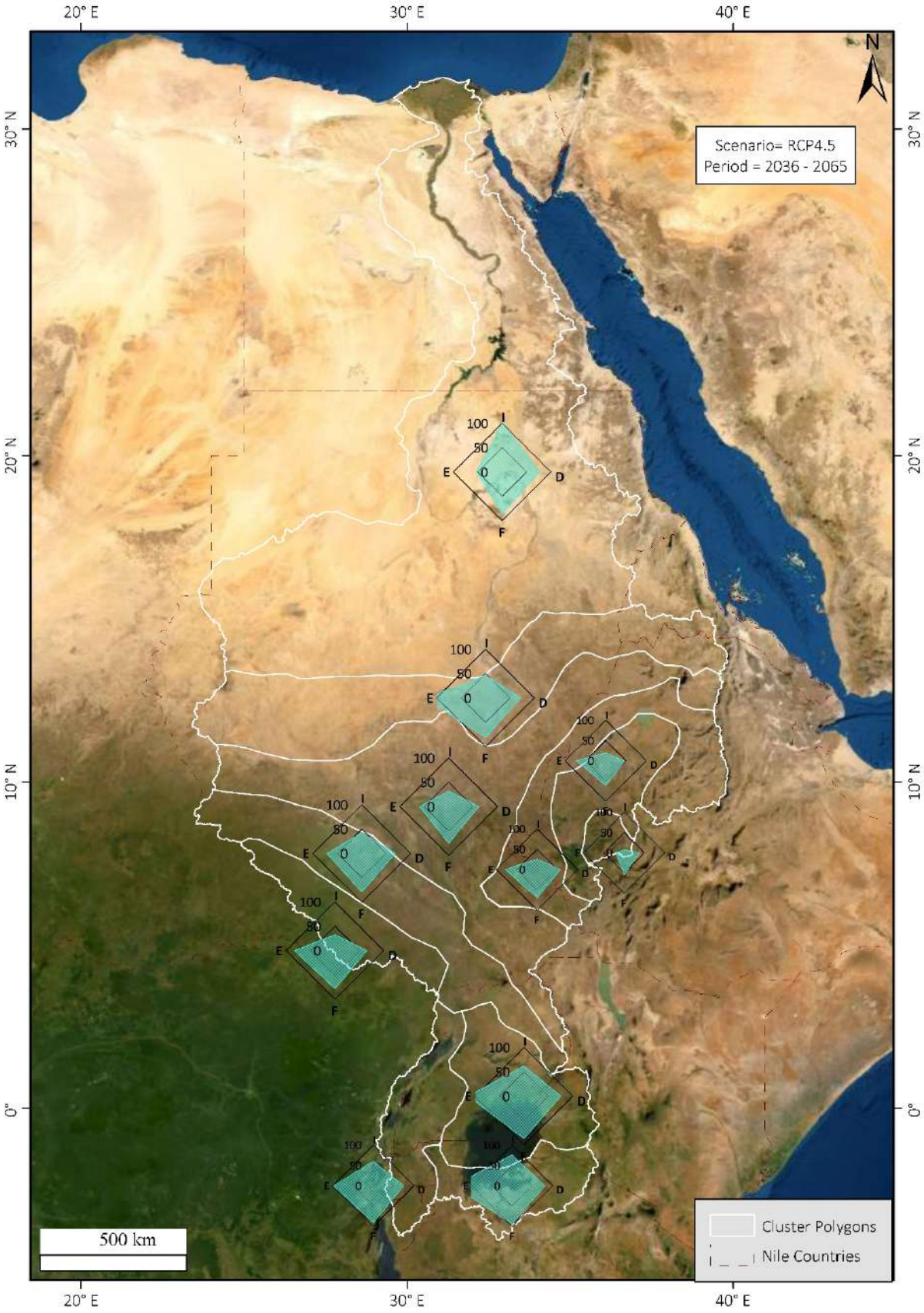

Figure 64: Cluster map (Model = SMHI_RCA4MOHC_HadGEM2, RCP scenario = 4.5, period = 2036-2065).

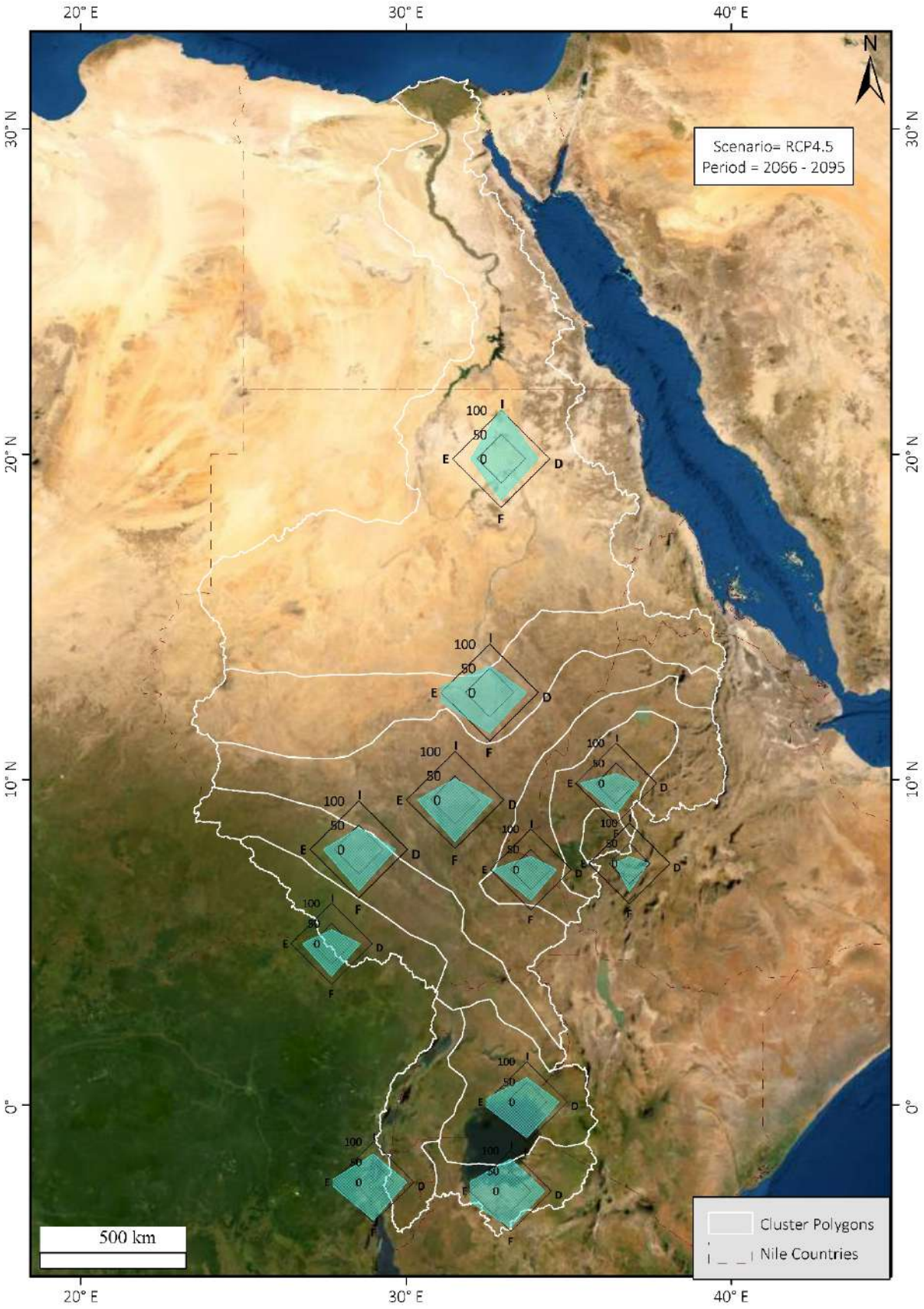

Figure 65: Cluster map (Model = SMHI_RCA4MOHC_HadGEM2, RCP scenario = 4.5, period = 2066-2095).

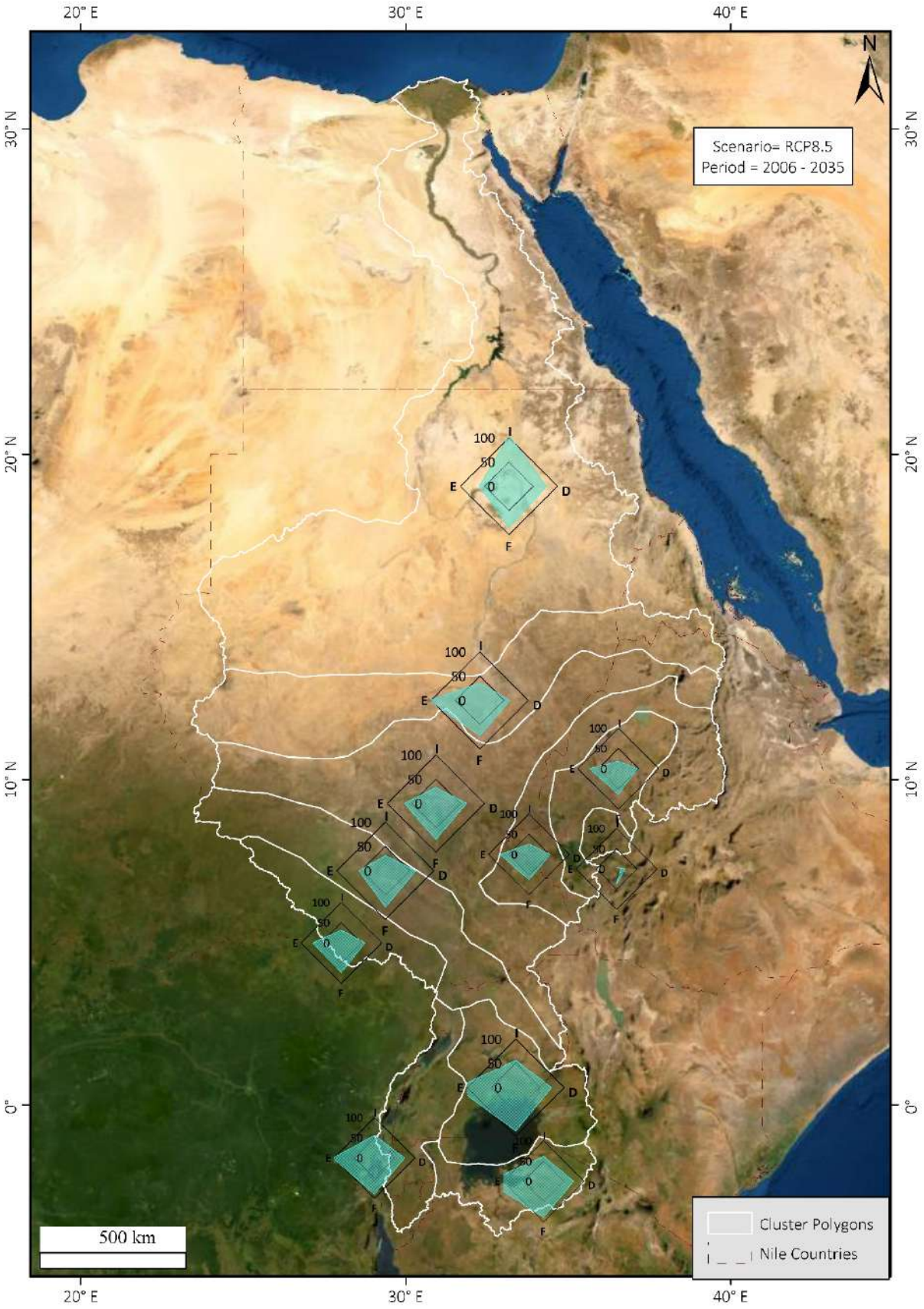

Figure 66: Cluster map (Model = SMHI_RCA4MOHC_HadGEM2, RCP scenario = 8.5, period = 2006-2035).

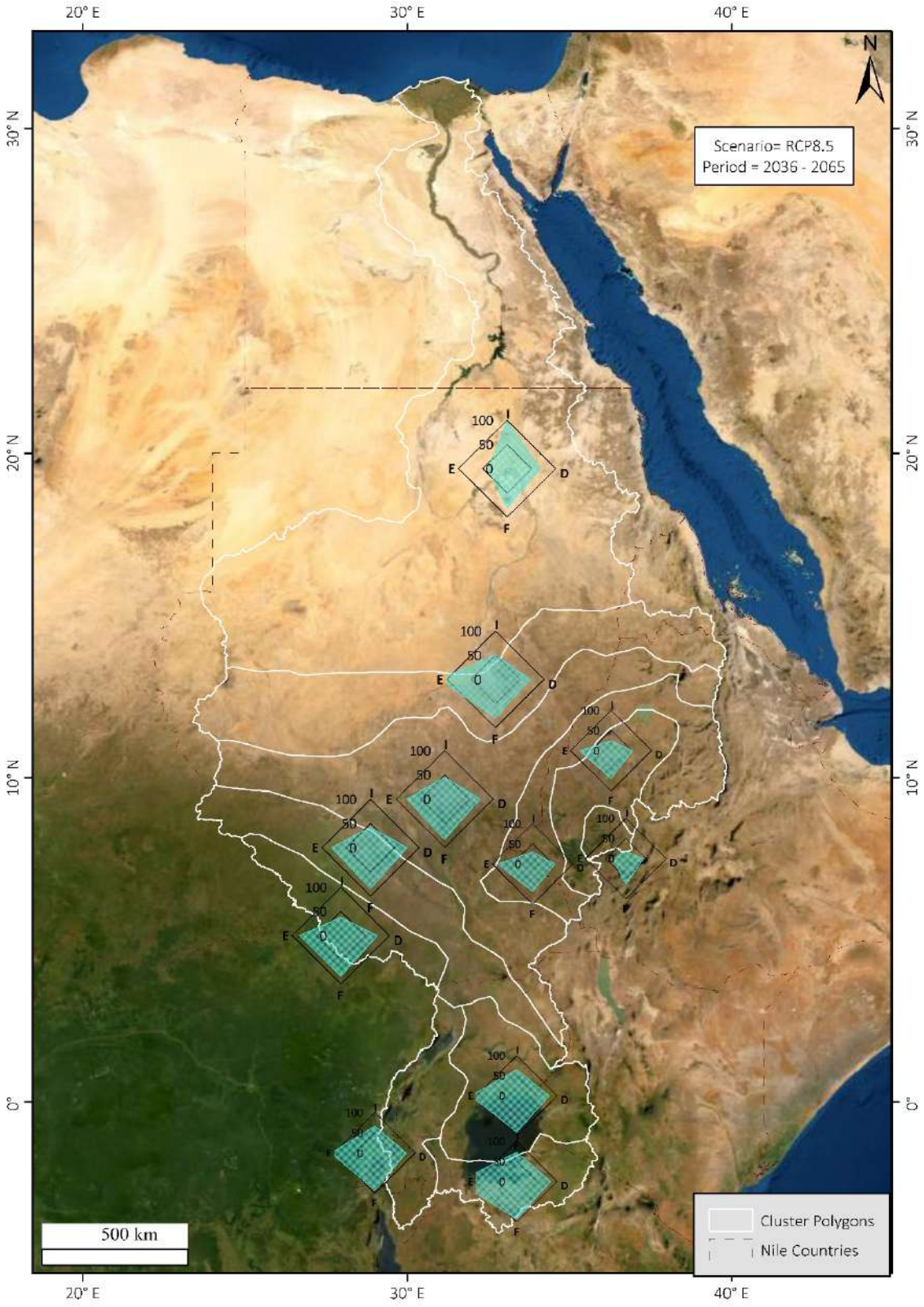

Figure 67: Cluster map (Model = SMHI_RCA4MOHC_HadGEM2, RCP scenario = 8.5, period = 2036-2065).

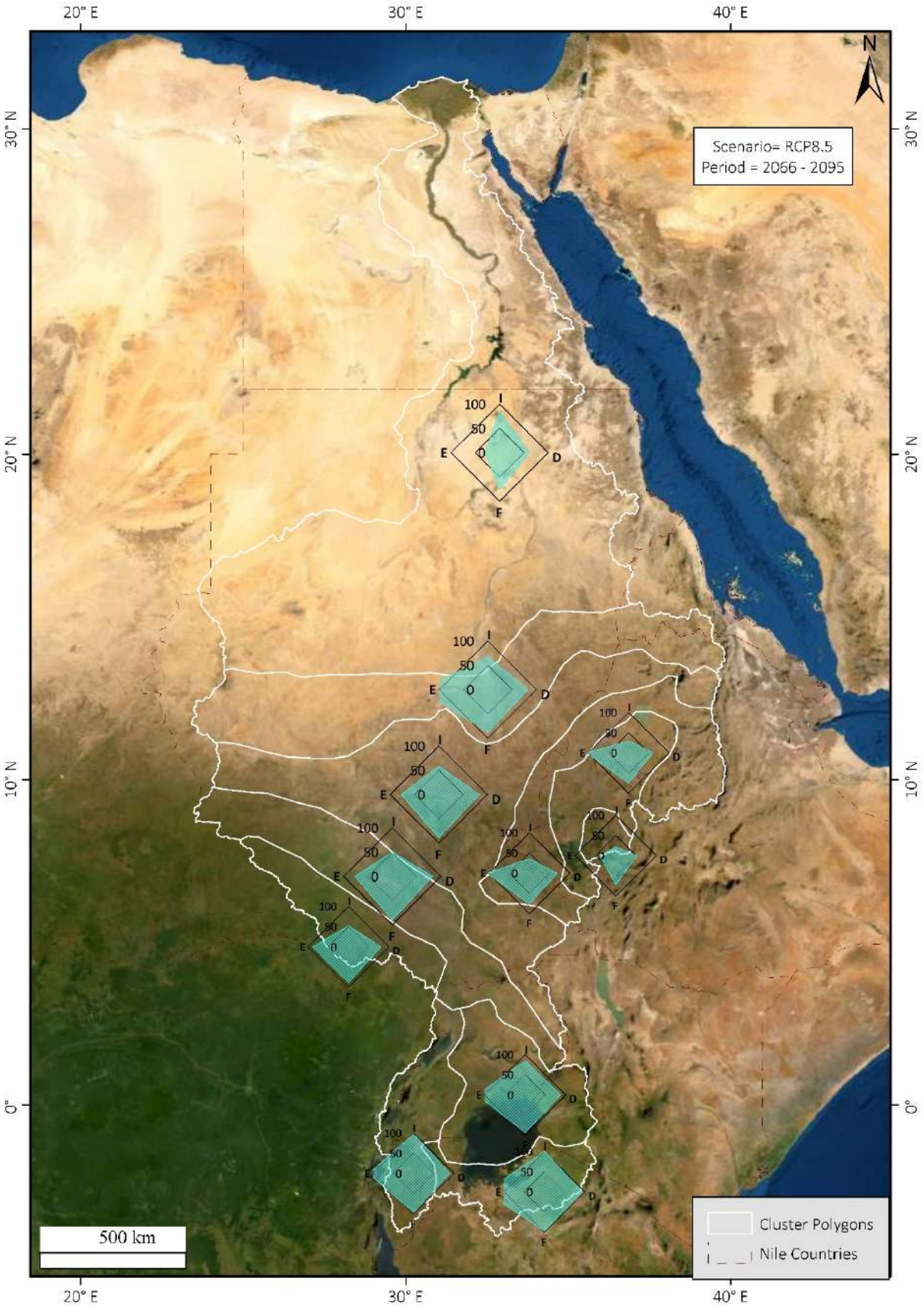

Figure 68: Cluster map (Model = SMHI_RCA4MOHC_HadGEM2, RCP scenario = 8.5, period = 2066-2095).

12 ANNEX – PMP GRID MAPS

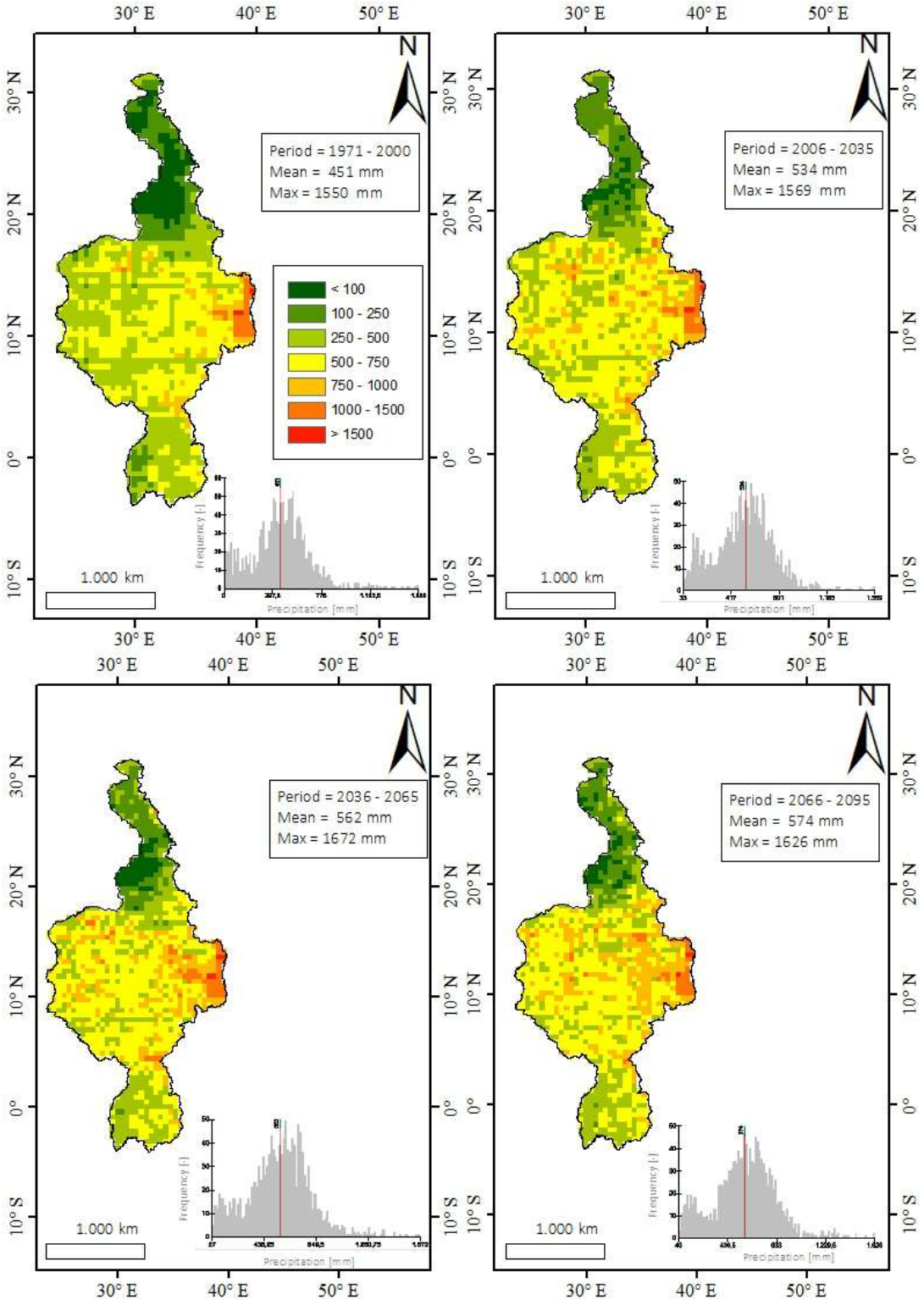

Figure 69: PMP grid map (Model = BCCR_WRF331NCC_NorESM1_M, RCP scenario = 4.5, Duration = 1 day).

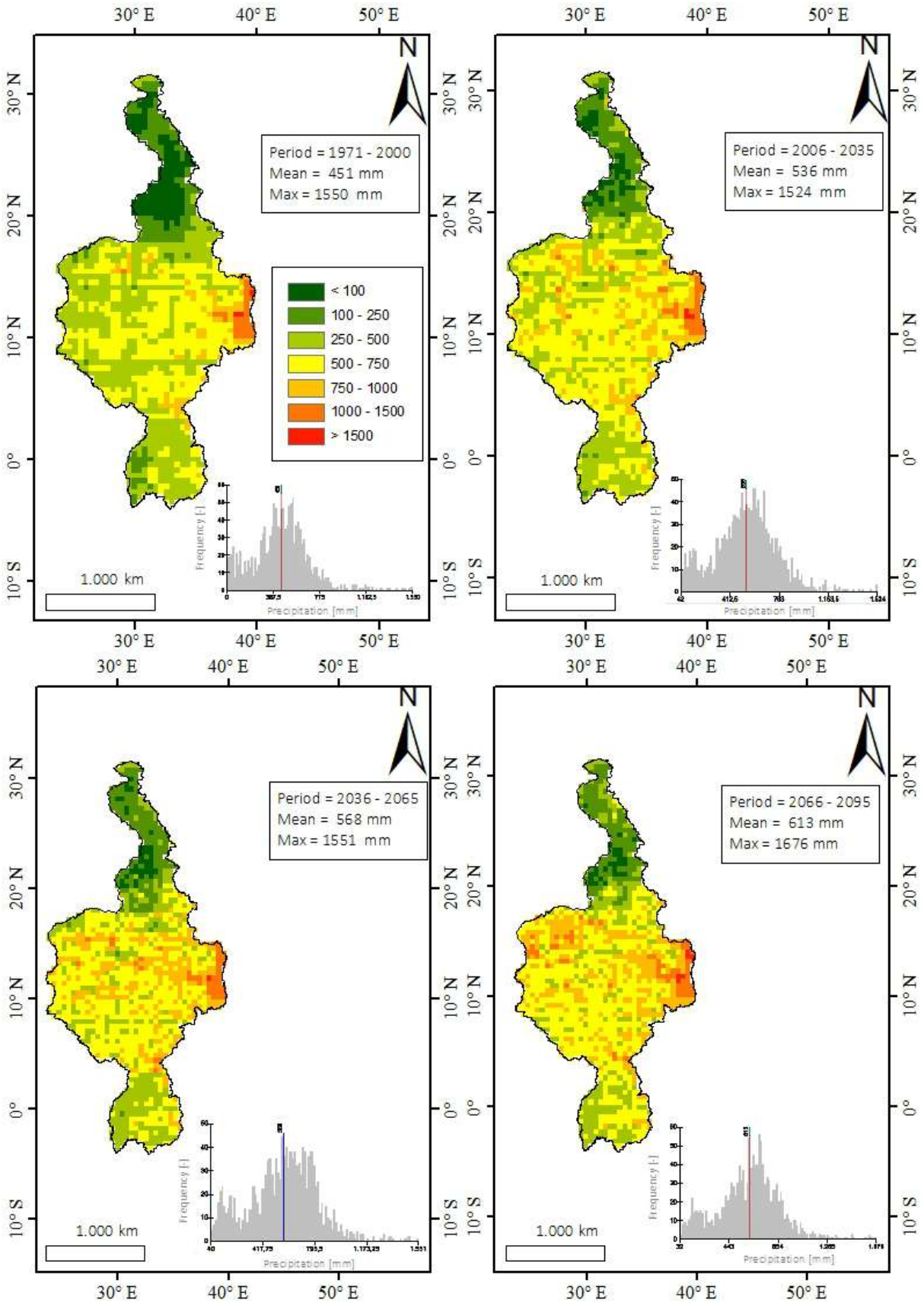

Figure 70: PMP grid map (Model No. = BCCR_WRF331NCC_NorESM1_M , RCP scenario = 8.5, Duration = 1 day).

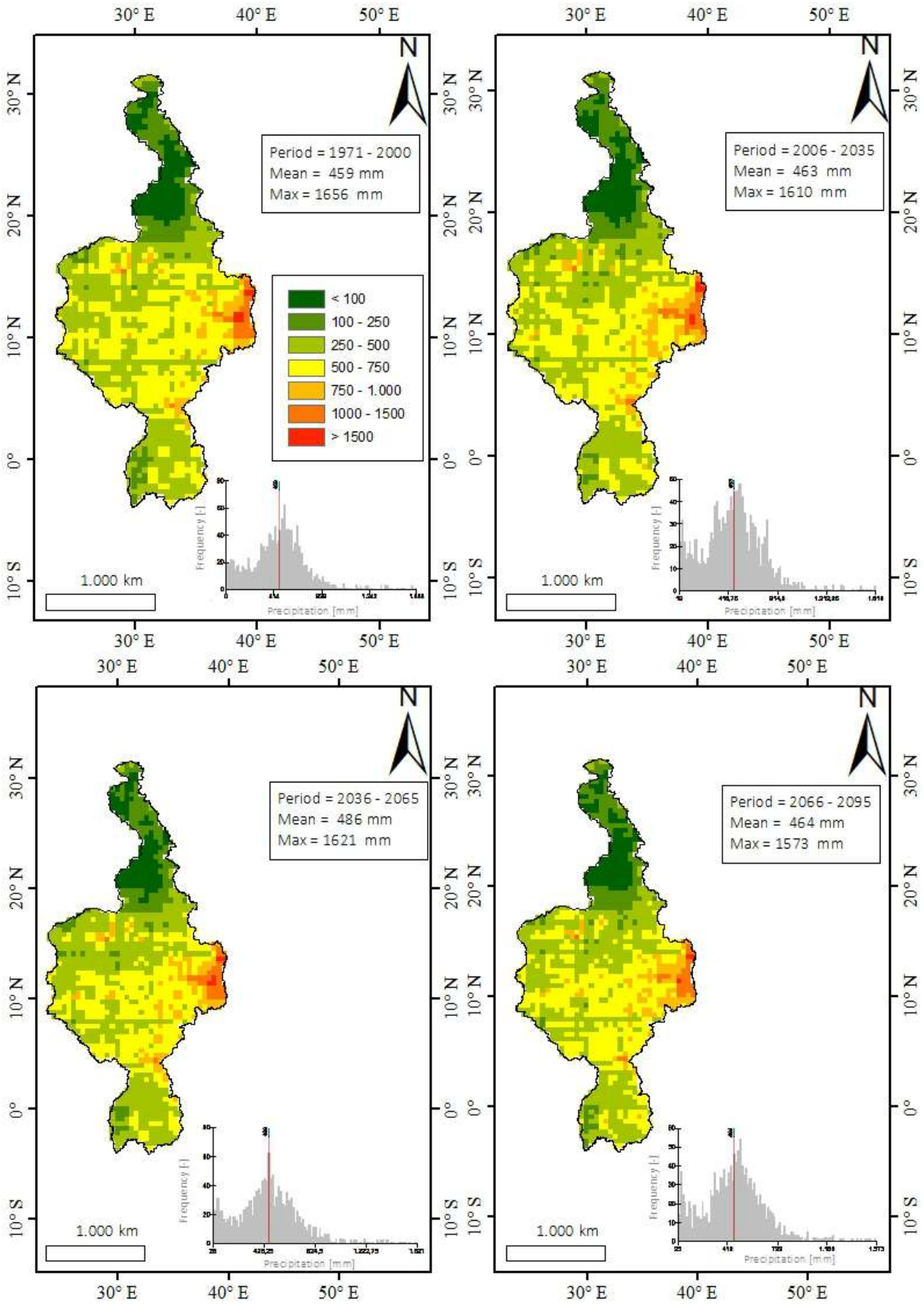

Figure 71: PMP grid map (Model = SMHI_RCA4MOHC_HadGEM2, RCP scenario = 4.5, Duration = 1 day).

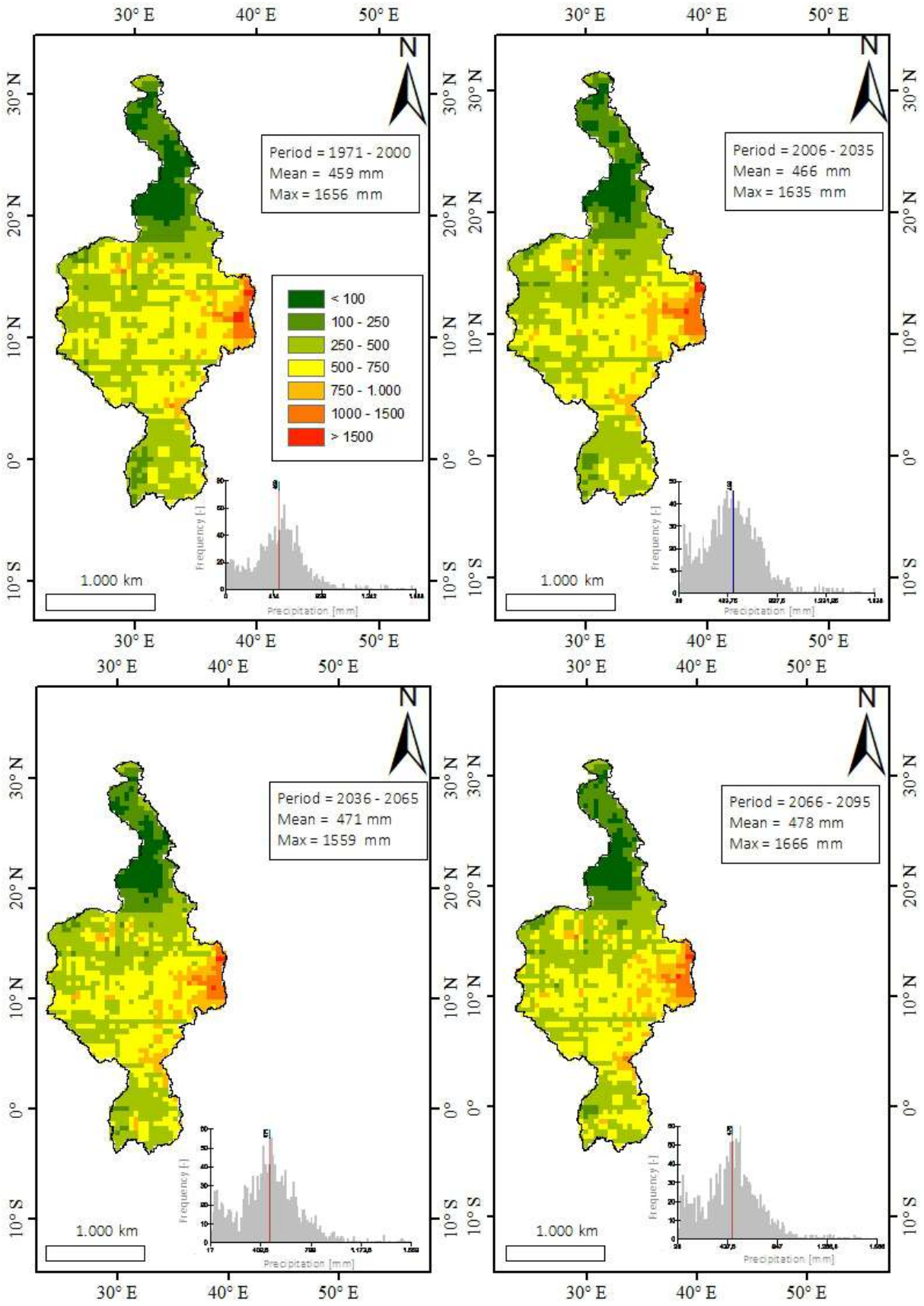

Figure 72: PMP grid map (Model No. = SMHI_RCA4MOHC_HadGEM2, RCP scenario = 8.5, Duration = 1 day).

ONE RIVER
ONE PEOPLE
ONE VISION

Nile Basin Initiative Secretariat
P.O. Box 192
Entebbe – Uganda
Tel: +256 414 321 424
+256 414 321 329
+256 417 705 000
Fax: +256 414 320 971
Email: nbisec@nilebasin.org
Website: http://www.nilebasin.org

/Nile Basin Initiative
@nbiweb

Eastern Nile Technical Regional Office
Dessie Road
P.O. Box 27173-1000
Addis Ababa – Ethiopia
Tel: +251 116 461 130/32
Fax: +251 116 459 407
Email: entro@nilebasin.org
Website: http://ensap.nilebasin.org

ENTRO

Nile Equatorial Lakes Subsidiary Action Program Coordination Unit
Kigali City Tower
KCT, KN 2 St, Kigali
P.O. Box 6759, Kigali Rwanda
Tel: +250 788 307 334
Fax: +250 252 580 100
Email: nelsapcu@nilebasin.org
Website: http://nelsap.nilebasin.org

NELSAP-CU